

# Sterile Neutrino in Cosmology

Dissertation for Doctoral Degree

Submitted to the Department of Physics of

Università degli Studi di Napoli  
“Federico II”

Rosa Consiglio

Naples 2016

# Contents

<b>1</b>	<b>An Overview of Neutrino Physics</b>	<b>4</b>
1.1	Neutrino in Elementary Particle Physics . . . . .	5
1.2	The Electroweak Lagrangian . . . . .	6
1.3	Spontaneous Symmetry Breaking: the Higgs Mechanism and Fermion Masses . . . . .	11
<b>2</b>	<b>Massive Neutrinos and New Physics Beyond the Standard Model</b>	<b>19</b>
2.1	Neutrino Masses in the Standard Model and Beyond . . . . .	20
2.2	Neutrino Mixing . . . . .	23
2.2.1	Dirac Mass Term . . . . .	24
2.2.2	Majorana Mass Term . . . . .	27
2.2.3	Dirac-Majorana Mass Term . . . . .	33
2.3	The Seesaw Mechanism . . . . .	37
2.3.1	Quadratic Seesaw . . . . .	40
2.3.2	Linear Seesaw . . . . .	40
2.4	Right-Handed Sterile Neutrinos . . . . .	42
<b>3</b>	<b>Neutrino Flavor Oscillations</b>	<b>45</b>
3.1	Neutrino Oscillations in Vacuum . . . . .	46
3.2	Neutrino Oscillations in Matter . . . . .	52
3.2.1	The MSW effect . . . . .	58
3.3	Neutrino Oscillations Experiments . . . . .	60
3.3.1	Three-Neutrino Mixing . . . . .	62
3.3.2	Extended Neutrino Oscillation Scenarios . . . . .	65

3.4	Density Matrix Formalism and Kinetic Equation for Mixed Neutrinos . . . . .	68
<b>4</b>	<b>Neutrino in Cosmology and Astrophysics</b>	<b>77</b>
4.1	Early Universe . . . . .	77
4.1.1	Sterile Neutrino Thermalization . . . . .	85
4.2	Cosmological Constraints on Sterile Neutrinos . . . . .	87
4.3	Supernovae Environment . . . . .	90
<b>5</b>	<b>The Effective Number of Neutrino Species</b>	<b>96</b>
5.1	From Neutrino Decoupling to Big-Bang Nucleosynthesis . . . . .	97
5.1.1	Neutron Decay . . . . .	100
5.2	The Big Bang Nucleosynthesis and $N_{eff}$ . . . . .	102
5.3	Sterile Neutrino and Primordial Nucleosynthesis . . . . .	105
<b>6</b>	<b>Neutrino Interactions with a Light Pseudoscalar</b>	<b>110</b>
6.1	Active-Sterile Neutrino Interactions . . . . .	110
6.2	Matter Potential in the Sterile Sector . . . . .	114
6.3	The Collision Integrals . . . . .	116
6.4	Collisions in the Sterile Sector . . . . .	122
6.5	Quantum Kinetic Equations for a $\nu_\alpha - \nu_s$ System . . . . .	122
<b>7</b>	<b>Conclusions</b>	<b>128</b>
	<b>Bibliography</b>	<b>131</b>

## Abstract

Sterile neutrino, in addition to providing neutrino mass generation, depending on its mass scale, may have many important cosmological implications. eV sterile neutrinos may explain the dark radiation problem (i.e. additional relativistic density quantified by the effective number of neutrino species) and the experimental data of short baseline experiments, a KeV sterile neutrino may be a warm dark matter candidate and furthermore sterile neutrinos may also provide baryogenesis through leptogenesis. The main way of obtaining a significant abundance of sterile neutrinos is through their mixing and oscillations with the active neutrinos.

Active-sterile neutrino oscillations may have considerable effects in the early universe. One or more than one sterile neutrino may exist avoiding the cosmological constraints only by suppressing the thermalization of sterile neutrinos in the early universe and/or by considering non-standard cosmological theories.

Two different mechanisms to suppress the sterile neutrinos thermalization and their eventual large production have been studied. In particular, the existence of neutrino asymmetries or the introduction of secret interactions among sterile neutrinos. The existence of sterile neutrinos not fully thermalized with the active species in the early universe in principle is compatible with Big-Bang Nucleosynthesis data. It is also compatible with cosmological measurements of the Cosmic Microwave Background and Large-Scale Structures, if the neutrino masses do not exceed 1 eV.

However, the scenarios of secret self-interactions studied so far are not sufficient to reconcile sterile neutrinos with cosmology. The new picture, that we will introduce consists in assuming the same secret interactions with a light pseudoscalar as the source of sterile neutrino production by oscillations (when they involve active species) and, in addition, along with the self-interactions we will also consider interactions between sterile neutrino and pseudoscalar particle in the sterile sector.

## Introduction

The concept of sterile neutrino was introduced in the late 1960s by Pontecorvo in order to discuss neutrino oscillations. This particle is a neutral fermion which does not take part in weak interactions, except those induced by mixing with active neutrinos, and with opposite chirality with respect to the left-handed neutrino that participates in weak interactions.

The postulated existence of right-handed neutrinos is theoretically and experimentally well-motivated. From the theoretical point of view, in fact, any other known fermion has been observed with left and right chirality. Furthermore, right-handed neutrinos can explain in a natural way, through the seesaw mechanism, the observed extremely small masses of the active neutrinos compared with those of charged fermions in the standard model. The seesaw mechanism leaves the masses of singlet neutrinos as free parameters. They could have any value between  $10^{15}$  GeV and less than 1 eV. This allows to choose these parameters so that they can account for certain phenomena and anomalies beyond the Standard Model, such as providing a dark matter candidate or a mechanism for baryogenesis or explaining various short baseline anomalies. In this latter case, the seesaw scale corresponds to the scale of light sterile neutrinos. Although right-handed neutrinos are sterile under weak interactions, they may participate in Yukawa interactions involving the Higgs boson or in interactions involving new physics beyond the standard model.

From the observational point of view, there exist a few anomalies in experimental results that find no explanation in a three-flavor active neutrino pattern with nonzero mixing, even though this scheme successfully accounts for most of the results of oscillation experiments designed to measure solar, atmospheric, accelerator and reactor neutrinos.

The three-neutrino mixing scheme was first challenged in 1995 by the LSND experiment. The observation of a signal of short-baseline  $\bar{\nu}_\mu \rightarrow \bar{\nu}_e$  oscillations, led to assume the existence of one or more squared-mass differences much larger than the solar and atmospheric ones. The results of subsequent experiments have effectively confirmed the LSND observations, thus reviving interest in the possible existence of one or more sterile neutrinos, with mass in the eV scale, that can generate the squared-mass differences observed in short-baseline oscillations.

Active-sterile neutrino oscillations may have considerable effects in the early universe. They may excite additional light particles into equilibrium, thus affecting the expansion rate of the universe. They may generate neutrino-antineutrino asymmetry and distort neutrino energy spectrum. Active-sterile neutrino oscillations after  $\nu_e$  decoupling, may distort neutrino energy spectrum and deplete neutrino number density. In particular  $\nu_e - \nu_s$  oscillations can affect the weak interaction rates of  $\nu_e$  and hence the Big-Bang Nucleosynthesis. The primordial nucleosynthesis outcome indeed depends on the expansion rate of the universe when the universe is still radiation-dominated and therefore it depends on the effective number of neutrino species  $N_{eff}$ . A larger  $N_{eff}$  produces a larger expansion rate of the universe, which in turn leads to an earlier n/p freeze-out, leading to a larger relic neutron abundance, and thus, to a higher production of  $^4\text{He}$ . Since nucleosynthesis of light elements is based on the rate of weak reactions, the neutron lifetime  $\tau_n$  is another relevant parameter, whose accurate estimate becomes fundamental.

Unlike the BBN, probes of the late-time inhomogeneities of the universe, such as the CMB anisotropies and the LSS distribution, are not sensitive to the flavor content of the neutrino sector but only to its contribution to the stress-energy tensor. Additional relativistic energy density, due to a thermal population of light sterile neutrinos, affects the CMB anisotropies primarily for its effects on the age around matter-radiation equality. A rest mass significantly below the temperature of the thermal population around matter-radiation equality would alter the equality redshift. As for large scale structures, if massive neutrinos have not yet become nonrelativistic at the time of radiation/matter equality, this transition will be delayed causing suppression of the LSS matter power spectrum on small scales.

A fully thermalized population of sterile neutrinos appears to be in conflict with current BBN data and other cosmological observables. In order to relieve this tension, different mechanisms to suppress the sterile neutrino thermalization and their eventual large production have been studied. In particular, the existence of neutrino asymmetries or the introduction of secret interactions among sterile neutrinos. Several models of secret self-interactions have been proposed. None of these models seems to be able to provide sterile

neutrinos with the appropriate interactions to evade all the cosmological constraints and respond to the problem of the observed anomalies. This leads to the conclusion that the scenarios of secret self-interactions studied so far are not sufficient to reconcile sterile neutrinos with cosmology. This motivates the construction of an improved model, which consists in assuming the same secret interactions with a light pseudoscalar as the source of sterile neutrino production by oscillations with the active species and in addition introducing, along with the self-interactions  $\nu_s - \nu_s$ , further interactions in the sterile sector  $\nu_s - \phi$ .

This thesis is organized as follows. Chapter 1 provides an overview of neutrino physics, where the basics of the Standard Model of the elementary particles are presented. Chapter 2 introduces the problem of neutrino masses within the context of the Standard Model and beyond. The discussion on neutrino mass is aimed at introducing the related neutrino properties, such as mixing and oscillations, magnetic moments and decays, as well as the nature itself of neutrinos as Dirac or Majorana particles and the existence of a right-handed component. In Chapter 3 the plane-wave derivation of the neutrino oscillation probability is reviewed with the main phenomenological aspects of neutrino oscillations in vacuum and in matter, in particular the anomalies observed in some oscillation experiments. Along with the three-active neutrino oscillations framework, extended schemes comprising one or more sterile neutrinos are also introduced as viable solutions to the observed anomalies. In Chapter 4 the neutrino role during the different stages of the universe is reviewed. Neutrinos play an important role in the evolution of the universe from the very beginnings to the current state. In this chapter, we will present an overview of the consequences and related constraints associated with the presence of sterile species along with the active ones in the early stages of the universe and in supernovae environments. Chapter 5 is focused on the effective number of neutrino species  $N_{eff}$ , since it parameterizes the shape of relic neutrino spectra and their contribution to radiation. In this chapter the case of additional sterile species and their oscillations with active species is discussed for their possible effects on Big Bang nucleosynthesis. An accurate estimate of the neutron lifetime is provided since the neutron decay process affect the n/p ratio at the onset of primordial nucleosynthesis as well as the light elements abundances produced in the standard Big Bang nucleosynthesis.

In Chapter 6 a new model of sterile neutrino production and secret interactions is introduced in order to explore the possibility of reconciling the sterile neutrino with mass in the eV scale with cosmology. In Chapter 7 some conclusions and prospects are drawn.

## An Overview of Neutrino Physics

The existence of neutrinos was postulated in 1930 by W. Pauli to explain the continuous spectrum of  $\beta$ -decay. The assumption that in  $\beta$ -decay together with the electron a neutral penetrating particle, not yet detected in experiments, is produced such that the total released energy is shared between the electron and the new particle was the alternative explanation to assuming that in  $\beta$ -decay the energy is not conserved. This neutral particle (electron antineutrino) was discovered only 26 years later, in 1956, by C.L. Cowan and F. Reines, during an experiment performed at the Savannah River fission reactor, which showed reactions induced by free neutrinos.

The discovery of the parity violation in the  $\beta$ -decay and other processes of weak interactions led to a two-component theory of massless neutrinos, left-handed neutrinos and right-handed antineutrinos. They were included into the  $V - A$  theory of weak interactions in 1958 and into the Standard Model (SM) of electroweak interactions in 1967. This theory was soon confirmed by experiments, which proved that neutrino is a left-handed particle. Since no right-handed neutrino or left-handed antineutrino takes part in the weak interactions, neutrinos were assumed to be massless in the SM. However, as it does not violate any basic symmetry of this model, the SM can be extended by introducing an isospin singlet  $\nu_R$  ( $\bar{\nu}_L$ ) for neutrinos like all other fermions (Bilenky 2010; Z.-Z. Xing et al. 2011). While the SM is a renormalizable theory, it is necessary to go to non-renormalizable theories in order to describe physics beyond the SM. This is usually done assuming the SM as an effective theory.

In the late 1950s Pontecorvo (Pontecorvo 1957; Pontecorvo 1958) suggested the possibility that neutrino flavor eigenstates are a superposition of mass eigenstates and consequently subjected to the phenomenon of oscillations, analogously to  $K^0 - \bar{K}^0$ . Neutrino oscillation is a quantum mechanical



interference effect generated by the different propagation of different mass eigenstates, which are produced and detected coherently because of their very small mass differences. This means that the flavor composition of a state can change with time. Since in the late 1950s only the electron neutrino was known, in order to discuss neutrino oscillations, Pontecorvo introduced the concept of a sterile neutrino (Pontecorvo 1968), that is, a neutral fermion which does not take part in weak interactions, as opposed to the normal left-handed neutrinos that participate in weak interactions, usually called active. Experimental evidence in favor of neutrino oscillation confirmed that neutrinos are massive particles. This has important cosmological consequences as it affects the expansion rate of the universe and also has consequences on the formation of structures in the early universe and their growth on certain length scales (Giunti & Kim 2007; Lesgourgues et al. 2013; Mohapatra & Pal 2004).

## 1.1 Neutrino in Elementary Particle Physics

The electroweak part of the SM Lagrangian, which determines neutrino interactions in the SM, is related to the  $SU(2)_L \times U(1)_Y$  part of the SM of electroweak and strong interactions gauge group  $SU(3)_C \times SU(2)_L \times U(1)_Y$ , where C, L and Y denote colour, left-handed chirality and weak hypercharge. Interactions and number of vector gauge bosons are uniquely determined by the gauge group. The gauge bosons are eight massless gluons that mediate strong interactions, four gauge bosons responsible for electroweak interactions (three massive,  $W^\pm$  and Z, and one corresponding to a massless photon) which are respectively the generators of  $SU(3)_C$ ,  $SU(2)_L$  and of  $U(1)_Y$ .

Since there can be a mixing between the neutral gauge bosons of  $SU(2)_L$  and  $U(1)_Y$ , electromagnetic and weak interactions must be treated together. The symmetry under the color group  $SU(3)_C$  is unbroken and there is no mixing between the  $SU(3)_C$  and  $SU(2)_L \times U(1)_Y$  sectors thus, in the SM, electroweak interactions can be studied separately from strong interactions.

The symmetry group  $SU(2)_L$ , called weak isospin, has three generators which satisfy the angular momentum commutation relations:

$$[I_a, I_b] = i\epsilon_{abc}I_c \quad a, b = 1, 2, 3 \quad (1.1)$$

where  $\epsilon_{abc}$  is the Levi-Civita totally antisymmetric tensor, with  $\epsilon_{123} = 1$ . In the two-dimensional representation of the weak isospin group the generators are  $I_a = \sigma_a/2$ , where  $\sigma_1$ ,  $\sigma_2$  and  $\sigma_3$  are the three Pauli matrices.

The symmetry group  $U(1)_Y$ , called hypercharge, is generated by the hypercharge operator  $Y$ , which is connected to the third component  $I_3$  and the charge operator  $Q$  by the Gell-Mann-Nishijima relation:

$$Q = I_3 + \frac{Y}{2}. \quad (1.2)$$

The above relation implies the unification of weak and electromagnetic interactions and fixes the action of the hypercharge operator on the fermion fields, which is not constrained by the theory, being  $U(1)_Y$  abelian. Local gauge invariance is obtained by introducing three vector gauge boson fields  $A_\mu^a$  ( $a = 1, 2, 3$ ) and one vector gauge boson field  $B_\mu$  associated with the three generators  $I_a$  ( $a = 1, 2, 3$ ) of the group  $SU(2)_L$  and with the generator  $Y$  of the group  $U(1)_Y$ , respectively.

generation	quarks	leptons
1st	u	$\nu_e$
	d	$e^-$
2nd	c	$\nu_\mu$
	s	$\mu^-$
3rd	t	$\nu_\tau$
	b	$\tau^-$

Table 1.1: Generations of quarks and leptons in the SM.

For the three generations of leptons and quarks currently known are defined three generations (in Table 1.1) of left-handed weak isospin doublets. The right-handed components of quarks and leptons are all  $SU(2)_L$  singlets, except for the three neutrinos, assumed to be massless Weyl particles in the SM, hence only the left-handed components take part in weak interactions (see Table 1.2 for the correspondent electroweak quantum numbers).

## 1.2 The Electroweak Lagrangian

The SM Lagrangian density, invariant under the local symmetry group  $SU(2)_L \times U(1)_Y$ , written in terms of the fermion fields, the gauge boson fields and a Higgs doublet  $\Phi(x)$  for the three generations of leptons and quarks, has the form:

			I	$I_3$	Y	Q
$L_{eL} \equiv \begin{pmatrix} \nu_{eL} \\ e_L \end{pmatrix}$	$L_{\tau L} \equiv \begin{pmatrix} \nu_{\mu L} \\ \mu_L \end{pmatrix}$	$L_{\tau L} \equiv \begin{pmatrix} \nu_{\tau L} \\ \tau_L \end{pmatrix}$	1/2	1/2 -1/2	-1	0 -1
$l_{eR} \equiv e_R$	$l_{\mu R} \equiv \mu_R$	$l_{\tau R} \equiv \tau_R$	0	0	-2	-1
$Q_{1L} \equiv \begin{pmatrix} u_L \\ d_L \end{pmatrix}$	$Q_{2L} \equiv \begin{pmatrix} c_L \\ s_L \end{pmatrix}$	$Q_{3L} \equiv \begin{pmatrix} t_L \\ b_L \end{pmatrix}$	1/2	1/2 -1/2	1/3	2/3 -1/3
$q_{uR}^U \equiv u_R$	$q_{cR}^U \equiv c_R$	$q_{tR}^U \equiv t_R$	0	0	4/3	2/3
$q_{dR}^D \equiv d_R$	$q_{sR}^D \equiv s_R$	$q_{bR}^D \equiv b_R$	0	0	-2/3	-1/3

Table 1.2: Eigenvalues of the weak isospin  $I$  and its third component  $I_3$ , of the hypercharge  $Y$ , and of the charge  $Q$  of the fermion doublets and singlets.

$$\begin{aligned}
\mathcal{L} = & i \sum_{\alpha=e,\mu,\tau} \overline{L'_{\alpha L}} \not{D} L'_{\alpha L} + i \sum_{\alpha=1,2,3} \overline{Q'_{\alpha L}} \not{D} Q'_{\alpha L} \\
& + i \sum_{\alpha=e,\mu,\tau} \overline{l'_{\alpha R}} \not{D} l'_{\alpha R} + i \sum_{\alpha=d,s,b} \overline{q'^D_{\alpha R}} \not{D} q'^D_{\alpha R} + i \sum_{\alpha=u,c,t} \overline{q'^U_{\alpha R}} \not{D} q'^U_{\alpha R} \\
& - \frac{1}{4} \vec{F}_{\mu\nu} \cdot \vec{F}^{\mu\nu} - \frac{1}{4} B_{\mu\nu} B^{\mu\nu} + (D_\mu \Phi)^\dagger (D^\mu \Phi) - \mu^2 \Phi^\dagger \Phi - \lambda (\Phi^\dagger \Phi)^2 \\
& - \sum_{\alpha,\beta=e,\mu,\tau} (Y_{\alpha\beta}^n \overline{L'_{\alpha L}} \Phi l'_{\beta R} + Y_{\alpha\beta}^{n*} \overline{l'_{\beta R}} \Phi^\dagger L'_{\alpha L}) \\
& - \sum_{\substack{\alpha=1,2,3 \\ \beta=d,s,b}} (Y_{\alpha\beta}^D \overline{Q'_{\alpha L}} \Phi q'^D_{\beta R} + Y_{\alpha\beta}^{D*} \overline{q'^D_{\beta R}} \Phi^\dagger Q'_{\alpha L}) \\
& - \sum_{\substack{\alpha=1,2,3 \\ \beta=u,c,t}} (Y_{\alpha\beta}^U \overline{Q'_{\alpha L}} (i \sigma_2 \Phi^*) q'^U_{\beta R} + Y_{\alpha\beta}^{U*} \overline{q'^U_{\beta R}} (-i \Phi^T \sigma_2) Q'_{\alpha L})
\end{aligned} \tag{1.3}$$

where the indices  $\alpha, \beta$  run over the three generations of fermions. The primes on the fermion fields are due to the fact that the fields, listed in Table 1.2, in the above equation (1.3) are meant as having no definite masses, but as linear combinations of the fields with definite mass. The Higgs doublet quantum numbers are:

$$\Phi(x) \equiv \begin{pmatrix} \Phi_+(x) \\ \Phi_0(x) \end{pmatrix} \quad I = 1/2 \quad I_3 = \begin{matrix} 1/2 \\ -1/2 \end{matrix} \quad Y = +1 \quad Q = \begin{matrix} 1 \\ 0 \end{matrix} \quad (1.4)$$

and the covariant derivative  $D_\mu$  which contains two independent coupling constants,  $g$  and  $g'$ , associated respectively with the group  $SU(2)_L$  and  $U(1)_Y$ , is defined as:

$$D_\mu \equiv \partial_\mu + i g \vec{A}_\mu \cdot \frac{\vec{\sigma}}{2} + i g' B_\mu \frac{Y}{2} \quad (1.5)$$

The first two lines of equation (1.3) contain the kinetic and electroweak terms for leptons and quarks, the self-couplings of the gauge bosons and the Lagrangian of the Higgs sector which generates the spontaneous symmetry breaking. The last two lines describe the Higgs–fermion Yukawa interactions, with complex couplings  $Y_{\alpha\beta}^l$ ,  $Y_{\alpha\beta}^{lD}$  and  $Y_{\alpha\beta}^{lU}$ , which are responsible for the generation of charged leptons and quark masses and mixing.

The kinetic and self-interacting term for the gauge bosons is expressed by means of the electroweak tensors  $\vec{F}^{\mu\nu} \equiv (F_1^{\mu\nu}, F_2^{\mu\nu}, F_3^{\mu\nu})$  and  $B^{\mu\nu}$ , where

$$F_a^{\mu\nu} \equiv \partial^\mu A_a^\nu - \partial^\nu A_a^\mu - g \sum_{b,c=1}^3 \epsilon_{abc} A_b^\mu A_c^\nu \quad (1.6)$$

$$B^{\mu\nu} \equiv \partial^\mu B^\nu - \partial^\nu B^\mu \quad (1.7)$$

Since the left-handed and right-handed components of the fermion fields have different gauge transformation properties, the introduction of mass terms proportional to  $\bar{f}_L f_R + \bar{f}_R f_L$  in the Lagrangian is forbidden by the gauge symmetry. For charged leptons and quarks the generation of fermion masses in the SM is achieved through spontaneous symmetry breaking via the Higgs mechanism.

As for neutrinos, equation (1.3) shows that in the SM electroweak theory there is no right-handed neutrino state,  $\nu_R$ , which would be a singlet under the weak isospin group of transformations. This implies that, differently from charged leptons and quarks, there are no mass terms that appear as a consequence of symmetry breaking and active neutrinos  $\nu_L$  remain massless in the the SM.

The expansion of the covariant derivatives in the first line of equation (1.3) yields the charged-current (CC) and neutral-current (NC) weak interaction Lagrangian densities,

$$\mathcal{L}_I^{(CC)} = -\frac{g}{2\sqrt{2}}J_W^\mu W_\mu + h.c., \quad (1.8)$$

where the charged current is:

$$\begin{aligned} J_W^\mu &= J_{W,L}^\mu + J_{W,Q}^\mu \\ &= 2 \left( \overline{\nu'_{eL}} \gamma^\mu e'_L + \overline{\nu'_{\mu L}} \gamma^\mu \mu'_L + \overline{\nu'_{\tau L}} \gamma^\mu \tau'_L \right. \\ &\quad \left. + \overline{u'_L} \gamma^\mu d'_L + \overline{c'_L} \gamma^\mu s'_L + \overline{t'_L} \gamma^\mu b'_L \right). \end{aligned} \quad (1.9)$$

The gauge boson field in equation (1.8), defined as  $W^\mu \equiv (A_1^\mu - iA_2^\mu)/\sqrt{2}$ , annihilates a  $W^+$  boson and creates a  $W^-$  boson.

And as for the NC Lagrangian density,

$$\mathcal{L}_I^{(NC)} = -\frac{g}{2 \cos \theta_W} J_Z^\mu Z_\mu + h.c., \quad (1.10)$$

the neutral current is:

$$\begin{aligned} J_Z^\mu &= J_{Z,L}^\mu + J_{Z,Q}^\mu \\ &= 2 \left( g_L^\nu \overline{\nu'_{\alpha L}} \gamma^\mu \nu'_{\alpha L} + g_L^l \overline{l'_{\alpha L}} \gamma^\mu l'_{\alpha L} + g_R^l \overline{l'_{\alpha R}} \gamma^\mu l'_{\alpha R} \right. \\ &\quad \left. + g_L^U \overline{q'_{\alpha L}} \gamma^\mu q'_{\alpha L} + g_R^U \overline{q'_{\alpha R}} \gamma^\mu q'_{\alpha R} + g_L^D \overline{q'_{\alpha L}} \gamma^\mu q'_{\alpha L} + g_R^D \overline{q'_{\alpha R}} \gamma^\mu q'_{\alpha R} \right) \end{aligned} \quad (1.11)$$

The quantum electrodynamic (QED) Lagrangian, which describes the electromagnetic interactions, is obtained as part of the NC Lagrangian, with the electromagnetic field  $A^\mu$  expressed as a linear combination of  $A_3^\mu$  and  $B^\mu$ . The orthogonal one defines the vector boson field  $Z^\mu$  and is given by a rotation in the plane of the  $A_3^\mu$  and  $B^\mu$  fields through the weak mixing angle (or Weinberg angle)  $\theta_W$ ,

$$A^\mu = \sin \theta_W A_3^\mu + \cos \theta_W B^\mu \quad (1.12)$$

$$Z^\mu = \cos \theta_W A_3^\mu - \sin \theta_W B^\mu \quad (1.13)$$

The gauge boson  $A^\mu$ , associated with the electromagnetic potential of the photon, remains massless, since it corresponds to an unbroken U(1) symmetry. The related gauge generator, the electric charge, is given by Q (1.2).

Inserting the expressions of the gauge fields in the NC Lagrangian one finds an important relation, which connects the gauge coupling constants  $g$  and  $g'$  with the weak mixing angle  $\theta_W$  and the elementary electric charge:

$$e = g \sin \theta_W = g' \cos \theta_W \quad \Rightarrow \quad \tan \theta_W = \frac{g'}{g} \quad (1.14)$$

The couplings  $g_A^f$ , with  $f = \nu, l, U, D$  and  $A = L, R$ , are given by the relations:

$$g_L^f = I_3^f - Q^f \sin^2 \theta_W \quad (1.15)$$

$$g_R^f = -Q^f \sin^2 \theta_W \quad (1.16)$$

where  $Q^f$  is the fermion electric charge in units of the elementary electric charge  $e$  and  $I_3^f$  is the third component of the weak isospin of the fermion, the values of which are summarized in Table 1.2.

Since neutrinos are neutral particles, they do not have a coupling to the electromagnetic field. On the other hand, due to the mixing of the gauge fields  $A_3^\mu$  and  $B^\mu$  in the above equations (1.12) and (1.13), the weak NC interactions of charged fermions involve not only their left-handed component, but also the right-handed one, with a strength proportional to the electric charge and to  $\sin^2 \theta_W$ .

Whenever the typical range for energies and momenta carried by the fermions is much smaller than the mass of the gauge fields  $W^\pm$  and  $Z$  ( $\sim 100$ ) GeV, the gauge bosons produced in the trilinear vertex can only propagate as virtual particles. In the low energy limit, the Lagrangian densities  $\mathcal{L}_I^{(CC)}$  and  $\mathcal{L}_I^{(NC)}$  can be written for the effective theory at the tree-level as:

$$\mathcal{L}_{eff}^{(CC)} = -\frac{G_F}{\sqrt{2}} J_W^{\mu\dagger} J_{\mu W} \quad (1.17)$$

$$\mathcal{L}_{eff}^{(NC)} = -2\frac{G_F}{\sqrt{2}} J_Z^{\mu\dagger} J_{\mu Z} \quad (1.18)$$

where,

$$G_F \equiv \frac{\sqrt{2}g^2}{8m_W^2} = 1.166 \times 10^{-5} GeV^{-2} \quad (1.19)$$

is the Fermi constant, with the  $W$  boson mass  $m_W = m_Z \cos \theta_W$ . The gauge boson masses appear to exhibit a custodial symmetry in the relation between

their masses, in the limit of  $U(1)_Y$  coupling  $g'$  going to zero. That is,  $m_W = m_Z$  as  $g \rightarrow 0$ , whereas this relation changes to  $m_W = 0.88m_Z$  in the presence of nonzero  $U(1)_Y$  coupling.

The interaction Lagrangian densities (1.17) and (1.18) can describe a number of purely four-lepton processes, such as the neutron decay process  $n \rightarrow p + e^- + \bar{\nu}_e$ , which was first studied by Fermi, in the low energy limit, via a four-fermion Lagrangian (1.17). The  $\beta$  – *decay* process is particularly important because it affects the neutron to proton ratio n/p at the onset of primordial nucleosynthesis, as we shall see in chapter 4.

### 1.3 Spontaneous Symmetry Breaking: the Higgs Mechanism and Fermion Masses

In quantum field theories with symmetries, the way in which a symmetry manifests itself is determined by the invariance of Lagrangian and vacuum state under the symmetry transformations. In the early 1960s, it was realized, through the work of Nambu and Goldstone, that a Lagrangian may be invariant under a symmetry transformation but the lowest energy state may not be. If the symmetry is global, the spectrum of the theory contains a massless particle known as the Nambu-Goldstone boson. Through the works of Higgs, Kibble, Guralnik, Hagen, Brout and Englert (Higgs, 1964; Guralnik et al., 1964; Englert & Brout, 1964; Kibble 1967) it became also known that when it is a gauge symmetry that is spontaneously broken, there will be no such massless particle as a result. Moreover, the gauge boson corresponding to broken generators gets mass.

In the SM of particle physics, the Higgs mechanism is essentially the generation mechanism of mass for the gauge bosons as well as fermions, through electroweak symmetry breaking. Without the Higgs mechanism all bosons would be massless, while measurements show that the  $W^\pm$ , and  $Z$  bosons actually have relatively large masses ( $m_Z = 91.1876 \pm 0.0021$  GeV and  $m_W = 80.385 \pm 0.015$  GeV).

The simplest description of the mechanism adds to the SM a quantum field, the Higgs field, permeating the entire space. Below some very high temperature, the field causes spontaneous symmetry breaking during interactions. The breaking of symmetry triggers the Higgs mechanism, which causes the bosons moving through the Higgs-field filled space with which they interact, to acquire mass.

The dynamics of the Higgs field is governed by the term in the Lagrangian density:

$$\mathcal{L}_H = (D_\mu \Phi)^\dagger - V(\Phi) = (D_\mu \Phi)^\dagger (D^\mu \Phi) - \mu^2 \Phi^\dagger \Phi - \lambda (\Phi^\dagger \Phi)^2 \quad (1.20)$$

where  $\Phi$  is the Higgs field doublet, defined in equation (1.4), with  $\Phi^+(x)$  a charged complex scalar field and  $\Phi(x)$  is a neutral complex scalar field.

In the above equation (1.20), the coefficient  $\lambda$  of the quartic self-couplings of the Higgs fields, must be positive,  $\lambda > 0$ , in order  $V(\Phi)$  to be bounded from below, whereas  $\mu^2$  is assumed to be negative, in order to realize the spontaneous breaking of the symmetry  $SU(2)_L \times U(1)_Y$  to the gauge symmetry group of electromagnetic interactions,  $U(1)_Q$ , associated with the conservation of the electric charge, which is unbroken.

Neglecting an irrelevant constant  $\propto v^4$  and defining:

$$v \equiv \sqrt{-\frac{\mu^2}{\lambda}} \quad (1.21)$$

the Higgs potential can be written as:

$$V(\Phi) = \lambda \left( \Phi^\dagger \Phi - \frac{v^2}{2} \right)^2 \quad (1.22)$$

which is minimum for  $\Phi^\dagger \Phi = v^2/2$ . In quantum field theory the minimum of the potential corresponds to the vacuum state and the quantized excitations of each field above the vacuum correspond to particle states.

Fermion and vector boson fields (which carry nonzero spin) and charged scalar fields (which have zero spin) must have a zero value in the vacuum state, in order to preserve the invariance under spatial rotation and electric charge conservation. Only neutral scalar fields can have a nonzero value in the ground state. This is called vacuum expectation value or  $vev$ . Evidently the Higgs fields have a nonzero  $vev$ . Since the vacuum state must be electrically neutral, the  $vev$  of the Higgs fields must be due to  $\Phi_0$ :

$$\langle \Phi \rangle = \frac{1}{\sqrt{2}} \begin{pmatrix} 0 \\ v \end{pmatrix} \quad (1.23)$$

In the unitary gauge, the Higgs doublet takes the form:

$$\Phi = \frac{1}{\sqrt{2}} \begin{pmatrix} 0 \\ v + H(x) \end{pmatrix} \quad (1.24)$$



where  $H(x)$  is a real scalar field, which describes the physical Higgs boson, obtained by excitations of the neutral Higgs field above the vacuum. By substitution of (1.24) in the Higgs Lagrangian (1.20) one gets a mass term for the Higgs boson,

$$m_H = \sqrt{2\lambda}v = \sqrt{-2\mu^2}. \quad (1.25)$$

$\mu^2$  is a negative parameter, suitably introduced in the SM, whose value is not connected to other quantities already measured. Thus, the value of the mass of the Higgs boson must be determined experimentally since the SM gives no prediction for it. However, from the experimental value of the Fermi constant  $G_F$  and the mass terms for the W and Z gauge bosons in the Higgs Lagrangian, which yields:

$$m_W = \frac{gv}{2} \quad m_Z = \frac{gv}{2 \cos \theta_W}, \quad (1.26)$$

the resulting value of  $v$  is  $v \sim 246$  GeV.

As for the fermion masses, in the SM they arise as a result of the Higgs mechanism through the presence of Yukawa couplings of the fermion fields with the Higgs doublet. Substituting the Higgs doublet in the unitary gauge (1.24) in the last three lines of equation (1.3), we derive the lepton masses, starting by those of the charged leptons in the Higgs-lepton part of the Lagrangian (1.3),

$$\mathcal{L}_{H,L} = - \sum_{\alpha,\beta=e,\mu,\tau} Y_{\alpha\beta}^n \overline{L'_{\alpha L}} \Phi l'_{\beta R} + h.c., \quad (1.27)$$

which becomes:

$$\mathcal{L}_{H,L} = - \left( \frac{v + H(x)}{\sqrt{2}} \right) \sum_{\alpha,\beta=e,\mu,\tau} Y_{\alpha\beta}^n \overline{l'_{\alpha L}} l'_{\beta R} + h.c. \quad (1.28)$$

where the term proportional to the  $vev$  of the Higgs doublet of the above equation (1.28) provides the mass term for charged leptons, while the term proportional to the Higgs boson field  $H(x)$  provides trilinear couplings between the charged leptons and the Higgs boson.

The matrix  $Y^n$  of Yukawa couplings is a complex  $3 \times 3$  matrix, generally not diagonal in the three-generations space, consequently the fields  $e'$ ,  $\mu'$  and  $\tau'$  do not have definite masses. In order to find the charged lepton fields with

definite mass, it is necessary to diagonalize  $Y^l$ . This can be done through a biunitary transformation:

$$V_L^{l\dagger} Y^l V_R^l = Y^l \quad \text{with} \quad Y_{\alpha\beta}^l = y_\alpha^l \delta_{\alpha\beta}, \quad \alpha, \beta = e, \mu, \tau \quad (1.29)$$

where  $V_L$  and  $V_R$  are appropriate  $3 \times 3$  unitary matrices by which the left-handed and right-handed components of the charged lepton fields with definite masses are defined:

$$V_L^{l\dagger} l'_L = l_L \quad V_R^{l\dagger} l'_R = l_R \quad (1.30)$$

After performing the diagonalization (1.29) the Higgs–lepton term of the Lagrangian takes the form:

$$\mathcal{L}_{H,L} = - \left( \frac{v + H(x)}{\sqrt{2}} \right) \bar{l}_L Y^l l_R + h.c. = - \sum_{\alpha=e,\mu,\tau} \frac{y_\alpha^l v}{\sqrt{2}} \bar{l}_\alpha l_\alpha - \sum_{\alpha=e,\mu,\tau} \frac{y_\alpha^l}{\sqrt{2}} \bar{l}_\alpha l_\alpha H. \quad (1.31)$$

In the above equation (1.31),  $l_\alpha \equiv l_{\alpha L} + l_{\alpha R}$  are the fields of the charged leptons with definite masses given by:

$$m_\alpha = \frac{y_\alpha^l v}{\sqrt{2}} \quad \alpha = e, \mu, \tau \quad (1.32)$$

where the coefficients  $y_\alpha^l$  are unknown parameters of the SM, so that the masses of the charged leptons cannot be predicted and must be obtained from experimental measurements.

Similar reasoning can be applied to the Higgs–quark part of the Lagrangian (1.3) expressed in the unitary gauge,

$$\mathcal{L}_{H,Q} = - \left( \frac{v + H(x)}{\sqrt{2}} \right) \left( \sum_{\alpha,\beta=d,s,b} Y_{\alpha\beta}^{\prime D} \bar{q}'_{\alpha L} q'_{\beta R} + \sum_{\alpha,\beta=u,c,t} Y_{\alpha\beta}^{\prime U} \bar{q}'_{\alpha L} q'_{\beta R} \right) + h.c. \quad (1.33)$$

The terms proportional to  $v$  are mass terms for the quarks. As in the case of the leptons, it is necessary to proceed by diagonalizing the complex matrices of Yukawa couplings  $Y^{\prime D}$  and  $Y^{\prime U}$ , which are in general not diagonal,

in order to find the massive quark fields. Thus, performing the biunitary transformations by means of appropriate  $3 \times 3$  unitary matrices,  $V_L^D$ ,  $V_R^D$ ,  $V_L^U$  and  $V_R^U$ :

$$V_L^{D\dagger} Y'^D V_R^D = Y^D \quad \text{with} \quad Y_{\alpha\beta}^D = y_\alpha^D \delta_{\alpha\beta}, \quad \alpha, \beta = d, s, b \quad (1.34)$$

$$V_L^{U\dagger} Y'^U V_R^U = Y^U \quad \text{with} \quad Y_{\alpha\beta}^U = y_\alpha^U \delta_{\alpha\beta}, \quad \alpha, \beta = u, c, t \quad (1.35)$$

and defining the transformed quark fields as:

$$V_L^{D\dagger} q_L^D = q_L^D \quad V_R^{D\dagger} q_R^D = q_R^D \quad (1.36)$$

$$V_L^{U\dagger} q_L^U = q_L^U \quad V_R^{U\dagger} q_R^U = q_R^U \quad (1.37)$$

the mass term in *mathcal{L}\_{H,Q}* reads:

$$\begin{aligned} \mathcal{L}_{H,Q} &= - \left( \frac{v + H(x)}{\sqrt{2}} \right) \left( \overline{q_L^D} Y^D q_R^D + \overline{q_L^U} Y^U q_R^U \right) + h.c. \\ &= - \sum_{\alpha=d,s,b} \frac{y_\alpha^D v}{\sqrt{2}} \overline{q_\alpha^D} q_\alpha^D - \sum_{\alpha=u,c,t} \frac{y_\alpha^U v}{\sqrt{2}} \overline{q_\alpha^D} q_\alpha^D \\ &\quad - \sum_{\alpha=d,s,b} \frac{y_\alpha^D}{\sqrt{2}} \overline{q_\alpha^D} q_\alpha^D H - \sum_{\alpha=u,c,t} \frac{y_\alpha^U}{\sqrt{2}} \overline{q_\alpha^U} q_\alpha^U H \end{aligned} \quad (1.38)$$

where  $q_\alpha^{D,U} \equiv q_{\alpha L}^{D,U} + q_{\alpha R}^{D,U}$  are the fields of quarks having definite mass, whose masses are given by:

$$m_\alpha = \frac{y_\alpha^D v}{\sqrt{2}} \quad \alpha = d, s, b \quad (1.39)$$

$$m_\alpha = \frac{y_\alpha^U v}{\sqrt{2}} \quad \alpha = u, c, t. \quad (1.40)$$

The coupling constants  $y_\alpha^{D,U}$  are unknown parameters of the SM, as well as those of leptons, therefore the quark masses must be determined by experimental measurements, as they cannot be predicted.

Since all quarks have different masses, D or U quarks cannot be arbitrarily rotated in the hadronic weak charged current:

$$J_{W,Q}^\mu = 2\overline{q_{\alpha L}^U}\gamma^\mu (V^{U\dagger}V_L^D)_{\alpha\beta} q_{\beta L}^D. \quad (1.41)$$

Hence, the quark weak charged current does not depend separately on the matrices  $V_L^U$  and  $V_L^D$ , but only on their product:

$$V^{U\dagger}V_L^D \equiv V. \quad (1.42)$$

The unitary matrix  $V$  (1.42) is the quark mixing matrix, known as Cabibbo–Kobayashi–Maskawa (CKM) matrix (Cabibbo, 1963; Kobayashi & Maskawa, 1973), which englobes the effects of mixing between different generations of quarks. In fact, the quark mixing matrix determines the weak charged-current interactions of quarks through the current (1.41), which must be used in the calculation of weak interaction processes involving quarks, where the initial and final states describe particles with definite masses. This implies that the measurable quantities depend on the elements of the quark mixing matrix  $V$ :

$$V = \begin{pmatrix} c_{12}c_{13} & s_{12}c_{13} & s_{13}e^{-i\delta} \\ -s_{12}c_{23} - c_{12}s_{23}s_{13}e^{i\delta} & c_{12}c_{23} - s_{12}s_{23}s_{13}e^{i\delta} & s_{23}c_{13} \\ s_{12}s_{23} - c_{12}c_{23}s_{13}e^{i\delta} & -c_{12}s_{23} - s_{12}c_{23}s_{13}e^{i\delta} & c_{23}c_{13} \end{pmatrix} \quad (1.43)$$

where,  $c_{ij} = \cos \theta_{ij}$ ,  $s_{ij} = \sin \theta_{ij}$ , with  $0 \leq \theta_{ij} \leq \pi/2$ . The CKM matrix (1.43) depends upon three angles,  $\theta_{12}$ ,  $\theta_{23}$  and  $\theta_{13}$ , and one phase  $\delta$ . The presence of the complex phase  $\delta$  in  $V$  is the only possible source of CP (charge conjugation and parity) violation, therefore, the observed CP violation processes in the hadron phenomenology have been ascribed to a non vanishing value of  $\delta$ .

To a rather good approximation  $\theta_{12}$  is just the Cabibbo angle. It is known experimentally that  $s_{13} \ll s_{23} \ll s_{12} \ll 1$ . As for the magnitudes of all nine CKM elements, they can be most accurately determined by means of a global fit to all available measurements and imposing the SM constraints, such as unitarity and three generations (PDG 2014).

The quark's weak charged current conserves the baryon number (1/3 for the quark and  $-1/3$  for the antiquark), while there are no conserved flavor numbers for quarks. On the other hand, the quark neutral current has the same form whether it is expressed in terms of the quark mass eigenstates or

	$\nu_e, e^-$	$\nu_\mu, \mu^-$	$\nu_\tau, \tau^-$	$\bar{\nu}_e, e^+$	$\bar{\nu}_\mu, \mu^+$	$\bar{\nu}_\tau, \tau^+$
$L_e$	+1			-1		
$L_\mu$		+1			-1	
$L_\tau$			+1			-1

Table 1.3: Flavor lepton numbers.

in terms of the primed fields that appear in the weak charged current. Which means that the weak neutral current is invariant under mixing of the quark fields. As we shall see, this is also the case for the leptonic weak neutral current.

As regards neutrinos, in the SM they have exactly zero mass. This means that no right-handed partner  $\nu_R$  is introduced in the SM in addition to the left-handed component, hence they cannot couple to the Higgs boson and get mass.

Defining the neutrino field as:

$$\nu_L \equiv \begin{pmatrix} \nu_{eL} \\ \nu_{\mu L} \\ \nu_{\tau L} \end{pmatrix} = V_L^\dagger \nu'_L \equiv V_L^\dagger \begin{pmatrix} \nu'_{eL} \\ \nu'_{\mu L} \\ \nu'_{\tau L} \end{pmatrix}, \quad (1.44)$$

the leptonic weak charged current, in terms of the massless neutrino fields  $\nu_{eL}, \nu_{\mu L}, \nu_{\tau L}$  and the charged lepton fields with definite mass, takes the form:

$$J_{W,L}^\mu = 2 \sum_{\alpha=e,\mu,\tau} \bar{\nu}_{\alpha L} \gamma^\mu l_{\alpha L}. \quad (1.45)$$

In the weak charged current (1.45), the neutrino fields  $\nu_{eL}, \nu_{\mu L}, \nu_{\tau L}$  are called flavor neutrino fields because each of them only couples with the charged lepton field of the corresponding flavor. As a matter of fact, in the SM the flavor neutrino fields are also mass eigenstates, being any linear combination of massless fields still a massless field. In theories beyond the SM, where neutrinos are massive, the neutrino mixing makes the flavor neutrino fields distinguished from the mass eigenstates. As a consequence of the fact that the leptonic current  $J_{W,L}^\mu$  connects each charged lepton with the neutrino of the corresponding flavor, the flavor lepton number for each neutrino,  $L_e, L_\mu, L_\tau$  (see Table 1.3) as well as the total lepton number  $L = L_e + L_\mu + L_\tau$ , are conserved quantities in the SM related with the invariance of the electroweak Lagrangian under global  $U(1)$  gauge transformations. Indeed,

the nonconservation of the lepton numbers  $L_e, L_\mu, L_\tau, L$  plays an important role in the physics of neutrinos beyond the SM.

As regards the weak neutral current of the lepton fields, in the second last line of equation (1.45), because of the unitarity of the matrices  $V_L^l$  and  $V_R^l$ , the expression of the weak neutral current in terms of the unprimed lepton fields with definite masses is the same as that in terms of the primed lepton fields.

## Massive Neutrinos and New Physics Beyond the Standard Model

As it has been shown in the previous Chapter 1.3, the SM predicts massless neutrinos, making them essentially different from all other fermions which have masses. Many scenarios of physics beyond the SM are concerned with the aspect of masslessness of neutrinos, which appears in some way as an artifact in the SM. In fact, there is no fundamental reason why one cannot introduce a right handed field  $\nu_R$  that could have paired with the  $\nu_L$  through the Higgs mechanism and produce a mass term for neutrinos the same way as any other fermion. Comparing neutrino masslessness with that of the photon in the SM, it becomes apparent that differently from the photon, which is massless because of a conserved gauge symmetry that governs the dynamics of the electromagnetic interaction, the masslessness of neutrinos is not based on any symmetry principle.

Interestingly, so far there is no experimental evidence of significant deviations from the SM, except neutrino oscillation observations, which have shown that neutrinos are massive and mixed and pointed out the SM as an effective theory of the yet unknown theory beyond the SM. Since neutrinos are certainly massive, neutrino mass must be included in a realistic model of particle interactions. Then, another question that arises is whether the inclusion of quantum gravity effects into the standard model could explain neutrino masses.

What is the mechanism by which neutrinos gain tiny masses and how they are mixed are quite challenging questions. The assumption that the answer must be found in theories beyond the SM, designates the neutrino as the main hint of a new physics beyond the SM. The justification of the widespread opinion that the SM is not the ultimate theory of the elementary particles physics but just a low-energy effective theory lies in various unsatis-

factory aspects of the SM. For instance, the large number of parameters, the unexplained existence of three generations and moreover the gravitational interactions are not included. As regards the origin of the small neutrino mass, this can find a possible explanation, beyond the SM perspective, in the hypothesis that neutrino masses are a low-energy manifestation of physics beyond the SM and their smallness is due to a suppression generated by a new high-energy scale, possibly related to the unification of forces. This can be achieved, for example, with the seesaw mechanism.

## 2.1 Neutrino Masses in the Standard Model and Beyond

Neutrino mass is the basis for many of the static properties that the neutrino may acquire, such as mixing and oscillations, magnetic moments, decays and the nature itself of neutrinos as Dirac or Majorana particles.

In the SM only one helicity state of neutrino per generation exists, therefore, neutrinos cannot have a Dirac mass, which requires both the helicity states, unless one adds three right-handed neutrino fields. Clearly in the SM the  $\nu_R$  is not introduced because things are arranged so as to predict massless neutrinos. If one is looking for a different outcome, one may arrange things in some other way. The only extension of the SM that is needed to define a Dirac neutrino mass is the introduction of a right-handed component  $\nu_{\alpha R}$  for each flavor  $\alpha = e, \mu, \tau$ . As long as no suitable right-handed partner is introduced it is impossible to add a renormalizable mass term to the SM.

Alternatively, neutrinos may have another type of mass term, named Majorana mass term, of the form  $\nu_L^T C^\dagger \nu_L$ , where  $C$  is the Lorentz charge conjugation matrix. Although this form requires that particles have just one helicity state and uses the opposite helicity state of the antiparticle, this neutrino mass term is not gauge invariant and breaks lepton number by two units, since it transforms as an  $SU(2)_L$  triplet, being  $\nu_L$  part of the  $SU(2)_L$  doublet with lepton number  $+1$ . However, the SM Lagrangian has exact lepton number symmetry even after symmetry breaking, so that such terms can never arise in perturbation theory. Neutrinos are therefore massless to all orders in perturbation theory.

The SM is renormalizable because the ultraviolet divergences of the model are controlled by gauge symmetries, so that counterterms exist to cancel all infinities. The problem of divergences that increase when going to higher loops in gauge theories, spoiling their predictive power, was solved in 1971 by 't Hooft ('t Hooft 1971), who showed that renormalizability requires that the gauge boson mass is generated by the Higgs mechanism and all terms



in the Lagrangian have mass dimensions not greater than four. A further requirement is the absence of triangle anomalies. In fact, it has been shown that if a theory involves chiral interactions (i.e., interactions involving  $\gamma_5$  currents) of fermions, triangular one-loop graphs in general destroy the current conservation which holds at the tree level (Adler 1969; Bell & Jackiw 1967). This is called the axial anomaly. Gauge invariance means that the currents corresponding to gauge symmetries must be conserved to all orders in perturbation theory. Therefore, the constraint of anomaly cancellation must be imposed on gauge theories in order to preserve the theory renormalizability.

One may consider then the possibility that a neutrino mass can be induced by non-perturbative effects in the SM. The lepton number current conservation is effectively broken non-perturbatively through the anomaly. However, since the anomaly contribution to the baryon number current non-conservation has also an identical form, the  $B - L$  current is conserved to all orders in the gauge couplings. This means that non-perturbative effects from the gauge sector cannot induce  $B - L$  violation. Therefore, if the neutrino mass term violates also  $B - L$ , then neutrino masses remain zero even in the presence of non-perturbative effects. In other words, the renormalizable SM Lagrangian has an accidental  $B - L$  symmetry, which would be violated by two units introducing a Majorana mass term for neutrinos. Hence, the symmetry prevents mass terms not only at tree level but also to all orders in perturbation theory. Moreover, since the symmetry  $B - L$  is non-anomalous (unlike  $B$  and  $L$  separately), Majorana mass terms do not arise even at the non-perturbative level. This means that the renormalizable SM predicts  $m_\nu = 0$  to all orders in perturbation theory, and beyond. That is, since the SM is a renormalizable theory, even its quantum corrections are insensitive to the physics beyond the SM. Thus, the standard model gauge group  $SU(2)_L \times U(1)_Y$  fixes only the gauge bosons of the model, not the fermions and Higgs contents. These are chosen arbitrarily in such a way that the neutrinos are massless to all orders in perturbation theory, and even after non-perturbative effects are considered.

On the other hand, one might also wonder whether the inclusion of quantum gravity effects into the SM might explain neutrino masses. As long as we treat gravity in perturbation theory, all gravity couplings respect  $B - L$  symmetry. However, once non-perturbative gravitational effects like black holes and worm holes are included, there is no guarantee that global symmetries will be respected in the low energy theory. This implies that the effective low energy Lagrangian for the SM in the presence of black holes or worm holes must contain baryon and lepton number violating terms. In the context of the SM, the only terms of this kind that can be constructed are non-renormalizable terms of the form  $\psi_L \phi \psi_L \phi / M_{Pl}$ , where  $\psi_L$  is the lepton dou-

blet,  $\phi$  is the Higgs doublet, and  $M_{Pl}$  is the Planck mass,  $M_{Pl} = l/\sqrt{G_N}$  (with  $G_N$  the Newton gravitational constant). After the gauge symmetry breaking, they lead to neutrino masses that are at most of order  $v^2/M_{Pl} \sim 10^{-5}$  eV (Barbieri et al. 1980; Akhmedov et al. 1992), that is, at least three orders of magnitude lower than required to solve the atmospheric neutrino problem.

In this picture, two theoretical questions become crucial. Firstly, how one can extend the standard model to find models with massive neutrinos and secondly how one can understand the smallness of the neutrino masses compared to the masses of the charged fermions. In fact, though the charged fermion masses vary widely, the smallness of the neutrino mass remains puzzling even within a single family. Consider for instance the electron mass,  $m_e = 0.511$  MeV, and the current masses for  $u$  and  $d$  quarks that are in the range (5 – 10) MeV. Evidently they vary within about an order of magnitude, whereas  $\nu_e$  is at least five orders lighter. Similarly, in the second generation, we find  $m_\mu = 105$  MeV,  $m_s \simeq 150$  MeV,  $m_c \simeq 1500$  MeV, that are again within about an order of magnitude, while  $m_{\nu_\mu}$  is at least three orders lighter than  $m_\mu$ . Beside these two fundamental issues, another important question, concerning neutrino mass, is whether the massive neutrinos are Dirac particles or Majorana particles. Namely, neutrinos could be their own antiparticles since they have no electric charge. As pointed out in (Babu & Mohapatra 1989), by including right-handed neutrinos, assumed to be Majorana particles, the anomaly cancellation implies charge quantization regardless of the number of generations. This could be used as an argument for neutrinos being both massive as well as Majorana type, given that Majorana nature of neutrinos might also help us understand the smallness of neutrino masses through the seesaw mechanism. As Majorana particles, neutrinos must not carry additive quantum numbers, local or global. Then, the total lepton number symmetry must be broken. Or more precisely, the symmetry that has to be broken is  $B - L$ , which is the only true global symmetry of the SM in presence of neutrino mixing. Then one should look for processes violating  $B - L$ , such as the neutrinoless double  $\beta$ -decay. If  $B - L$  is violated spontaneously, the Goldstone theorem states the existence of a massless pseudoscalar particle, called Majoron, being the breaking of  $B - L$  symmetry related to neutrinos with Majorana masses.

Another issue related to mass is that of stability. Massless neutrinos cannot decay, but if neutrinos have mass, they should be unstable since there would be no symmetry to prevent their decay, except for the lightest neutrino. This latter, being the lightest fermion, would be stable. The decays of the heavier neutrinos could instead have significant effects on the cosmological observables.

The above considerations lead to go beyond the standard model to ex-

plain the observed evidences for neutrino masses. This does not necessarily mean going beyond the gauge group of the standard model, which fixes only the gauge bosons of the model. Even using the same gauge group, extra fermions or Higgs bosons can be introduced so that the model predicts massive neutrinos. One of the peculiarities of the SM is that it contains left and right chiral projections of all fermions except the neutrinos, which looks artificial. In models with enlarged fermion sector, right-handed neutral fields  $\nu_R$  corresponding to each charged lepton  $L$  are added. Like the other right-handed fields, they are assumed to be  $SU(2)_L$  singlets. The definition of electric charge in equation (1.2) implies that they also have  $Y = 0$ . Although they have no interaction with the gauge bosons, they affect the model non-trivially because of their other properties. Simple models of this type (see Mohapatra & Pal 2004) show one of the major consequences of generic neutrino mass terms, that is, neutrino mixing. A consequence of neutrino mixing is that the flavor lepton numbers,  $L_e, L_\mu, L_\tau$ , are no more good global symmetries, even at the classical level, because any mass eigenstate is a mixture of  $\nu_e, \nu_\mu, \nu_\tau$ . At the classical level, the only global symmetry remaining in the leptonic sector is the total lepton number  $L$ . This feature would give rise to various flavor violating processes in any model with neutrino mixing. Moreover, this kind of models also provide no answer to the question about the lightness of neutrinos.

## 2.2 Neutrino Mixing

In theories beyond the SM in which neutrinos are massive, flavor neutrino fields are, in general, not mass eigenstates. This phenomenon is called neutrino mixing. The treatment of neutrino mixing is analogous to that of quark mixing in the case of Dirac neutrinos and follows a similar procedure in the case of Majorana neutrinos. We will conveniently use the notations  $V$  and  $U$ , respectively, for the quark and neutrino mixing matrices:

$$\nu_L = U \nu_{iL} \equiv \begin{pmatrix} \nu_{eL} \\ \nu_{\mu L} \\ \nu_{\tau L} \end{pmatrix} = \begin{pmatrix} U_{e1} & U_{e2} & U_{e3} \\ U_{\mu 1} & U_{\mu 2} & U_{\mu 3} \\ U_{\tau 1} & U_{\tau 2} & U_{\tau 3} \end{pmatrix} \begin{pmatrix} \nu_{1L} \\ \nu_{2L} \\ \nu_{3L} \end{pmatrix} \quad (2.1)$$

In the case of Dirac neutrinos, all properties of the quark mixing matrix  $V$  (1.43) can be extended to the lepton mixing matrix  $U$ . Namely, the matrix  $U$ , which relates neutrino flavor eigenstates and mass eigenstates fields, essentially depends on three mixing angles  $\theta_{12}, \theta_{13}$  and  $\theta_{23}$  and one CP-violating phase  $\delta$ . In the case of Majorana neutrinos there will be two additional phases, called Majorana phases.  $\nu_i$  is the (Dirac or Majorana) neutrino field

with mass  $m_i$ .

By convention, the quark mixing matrix  $V$  connects weak isospin  $I_3 = 1/2$  quarks on the left to  $I_3 = -1/2$  quarks on the right, whereas the lepton mixing matrix  $U$  connects  $I_3 = -1/2$  charged leptons on the left to  $I_3 = 1/2$  neutrinos on the right.

The mixing among neutrino mass eigenstates as they travel through space is a quantum mechanical phenomenon. A coherent admixture of unequal mass eigenstates is possible in quantum mechanics, where the energy non-conservation problem is addressed by the uncertainty principle. This leads to the phenomenon of neutrino oscillations.

The mechanism of generation of the neutrino mass term is still a matter of hypothesis, as well as the nature of neutrinos with definite masses as Dirac or Majorana particles. The neutrino mass term determines neutrino masses and mixture and neutrinos nature (Dirac and Majorana) and also the possibility of the existence of sterile neutrinos. Hence we will consider possible neutrino mass terms using the fact that a mass term of any spin- $1/2$  field is a sum of Lorentz-invariant products of left-handed and right-handed components of the field.

### 2.2.1 Dirac Mass Term

In order to introduce a Dirac mass term for neutrinos using the same Higgs mechanism that gives masses to quarks and charged leptons, the only extension of the SM required is to add three right-handed neutrino fields  $\nu_{\alpha R}$  with  $\alpha = e, \mu, \tau$ . Since the presence of right-handed neutrino fields does not affect the cancellation of quantum anomalies, unlike the other elementary fermion fields, the number of right-handed neutrino fields is not constrained by the theory. Such fields are sterile, in the sense that they are singlet under the whole gauge group and have no electroweak interactions as well as strong interactions with all other particles.

With the assumption of an additional sterile component to each flavor, the Higgs-lepton Yukawa Lagrangian (1.27) takes the form:

$$\mathcal{L}_{H,L} = - \sum_{\alpha,\beta=e,\mu,\tau} Y_{\alpha\beta}^l \overline{L'_{\alpha L}} \Phi l'_{\beta R} - \sum_{\alpha,\beta=e,\mu,\tau} Y_{\alpha\beta}^{\nu} \overline{L'_{\alpha L}} (i\sigma_2 \Phi^*) \nu'_{\beta R} + h.c., \quad (2.2)$$

where  $Y^{\nu}$  is the matrix of neutrino Yukawa couplings.

In the unitary gauge the Higgs-lepton Yukawa Lagrangian after spontaneous symmetry breaking becomes:

$$\mathcal{L}_{H,L} = - \left( \frac{v + H(x)}{\sqrt{2}} \right) [\overline{l}'_L Y^\mu l'_R + \overline{\nu}'_L Y^\nu \nu'_R] + h.c. \quad (2.3)$$

with the chiral charged lepton  $l'_L$  and the new right-handed neutrino  $\nu'_R$  defined in a similar way as the left-handed neutrino array in (1.44).

The mass terms are obtained by diagonalization through biunitary transformations of the matrices  $Y^\mu$ , as defined in (1.29), and  $Y^\nu$ :

$$V_L^{\nu\dagger} Y^\nu V_R^\nu \quad \text{with} \quad Y_{kj}^\nu = y_k^\nu \delta_{kj}, \quad k, j = 1, 2, 3 \quad (2.4)$$

where  $y_k^\nu$  are real and positive.

Transforming the neutrino fields in the same way as those of the charged leptons (1.30),

$$V_L^{\nu\dagger} \nu'_L = \nu_L \quad V_R^{\nu\dagger} \nu'_R = \nu_R, \quad (2.5)$$

the diagonalized Higgs-lepton Yukawa Lagrangian finally takes the form:

$$\mathcal{L}_{H,L} = - \left( \frac{v + H(x)}{\sqrt{2}} \right) \left[ \sum_{\alpha=e,\mu,\tau} y_\alpha^l \overline{l}_{\alpha L} l_{\alpha R} + \sum_{k=1,2,3} y_k^\nu \overline{\nu}_{kL} \nu_{kR} \right] + h.c. \quad (2.6)$$

The above equation provides the neutrino masses:

$$m_k = \frac{y_k^\nu v}{\sqrt{2}}. \quad (2.7)$$

The neutrino masses (2.7) are proportional to the Higgs  $vev$   $v$ , just as the masses of charged leptons and quarks, but neutrino masses are much smaller than those of charged leptons and quarks. The Higgs mechanism used in the SM, provides no explanation of the very small values of the eigenvalues  $y_k^\nu$  of the Higgs-neutrino Yukawa coupling matrix that are needed, as it leaves the value of the Yukawa couplings with the Higgs of all particles an open question.

The neutrino fields  $\nu_{kL}$  and  $\nu_{kR}$  form the Dirac bispinor  $\nu_k \equiv \nu_{kL} + \nu_{kR}$ . Such neutrino fields with Latin indices denote mass eigenstates, while flavor neutrino fields are labeled by Greek indices. Note that the flavor neutrino fields are useful only when the effects of neutrino masses are neglected, i.e. in the SM limit. When neutrino masses are taken into account the flavor

neutrino fields do not have a definite mass and are not independent, being coupled by the mass terms, therefore, in that case it is much more convenient to work with the independent massive neutrino fields.

Defining the unitary matrix:

$$U = V_L^{\dagger} V_L^{\nu}, \quad (2.8)$$

where  $U$  is the mixing matrix in the lepton sector that appears in equation (2.1), named Pontecorvo–Maki–Nakagawa–Sakata (PMNS) matrix, the leptonic weak charged current can be written in terms of flavor and mass eigenstates as well:

$$J_{W,L}^{\mu} = 2 \overline{\nu_{\alpha L}} \gamma^{\mu} l_{\alpha L} = 2 \nu_{kL} \gamma^{\mu} U_{k\beta}^{\dagger} l_{\beta L}, \quad (2.9)$$

whereas even for massive neutrinos the neutral current interactions remain unchanged.

Although the flavor lepton numbers are conserved in weak interactions, in general they are violated by the neutrino part of the Higgs–lepton Yukawa Lagrangian in equation (2.6). In fact, if the latter is rewritten as:

$$\mathcal{L}_{H,L} = - \left( \frac{v + H(x)}{\sqrt{2}} \right) \sum_{\alpha=e,\mu,\tau} \left[ y_{\alpha}^l \overline{l_{\alpha L}} l_{\alpha R} + \sum_{k=1,2,3} y_k^{\nu} \overline{\nu_{\alpha L}} U_{k\alpha} \nu_{kR} \right] + h.c., \quad (2.10)$$

the first term in (2.10) is invariant under the global  $U(1)$  gauge transformations:

$$l_{\alpha L,R} \rightarrow e^{i\phi_{\alpha}} l_{\alpha L,R} \quad \alpha = e, \mu, \tau \quad (2.11)$$

as well as the weak charged-current  $J_{W,L}^{\mu}$ , but this is not the case for the neutrino term in (2.10). There is no transformation that can be made on the right-handed neutrino fields  $\nu_{kR}$  leaving simultaneously invariant the neutrino part of the Higgs–lepton Yukawa Lagrangian in (2.10) and the kinetic part of the neutrino Lagrangian (see Giunti & Kim 2007).

Therefore, for massive Dirac neutrinos, the flavor lepton numbers are not conserved, which leads to the interesting phenomenon of neutrino oscillations. The only exceptions are the cases where the mixing matrix  $U$  is unity, that

is, there is no mixing, or the Yukawa couplings  $y_k^\nu$  are all equal. The latter case implies neutrino mass degeneracy, which is experimentally ruled out. In both cases the flavor lepton numbers are conserved and neutrinos do not oscillate. Since the Lagrangian is invariant under the global  $U(1)$  gauge transformations corresponding to the choice  $\phi_\alpha = \phi$  for all  $\alpha$ , for massive Dirac neutrinos the only remaining symmetry is the one associated with total lepton number.

Note that the right-handed components  $\nu_{kR}$  of the massive Dirac neutrino fields represent sterile degrees of freedom with respect to weak interactions. The mixing of the left-handed neutrino fields is independent of the right-handed neutrino fields, so that the active and sterile degrees of freedom remain decoupled in the presence of Dirac mixing and oscillations between active and sterile states is not possible. On the other hand, although weak interactions do not involve both left and right components of these fields, the mass term can couple right-handed with the ordinary neutrinos and generate a complicated mixing between active and sterile degrees of freedom.

The reason why the mixing is always applied to the neutrinos, whereas the charged leptons are treated as particles with definite mass, is that the three charged leptons are characterized by their mass. The flavor of a charged lepton is identified by measuring its mass. The mass determines its kinematic properties and its decay modes, which can be measured directly through long-range electromagnetic interactions. Hence, charged leptons with a definite flavor are, by definition, particles with definite mass. Conversely, neutrinos can be detected only indirectly by identifying the charged particles produced in weak interactions and the flavor of a neutrino created or destroyed in a weak charged current process is the flavor of the associated charged lepton. Therefore, flavor neutrinos need not have a definite mass and the mixing connotes them as a superpositions of neutrinos with definite masses.

The Dirac neutrino mixing matrix  $U$  can be written using the same convenient parameterization used for quarks, given in equation (1.43), in terms of three angles and one complex phase  $\delta$ . A nonzero value for  $\delta$  implies CP violation in the leptonic sector.

### 2.2.2 Majorana Mass Term

The description of a massive fermion requires a four-component spinor, solution of the Dirac equation:

$$(i\gamma^\mu \partial_\mu - m) \psi = 0. \tag{2.12}$$

With the free field  $\psi$  expressed in terms of the Weyl components of definite chirality  $\psi_L$  and  $\psi_R$ ,

$$\psi = \psi_L + \psi_R, \quad (2.13)$$

the above equation (2.12) reads:

$$i\gamma^\mu \partial_\mu \psi_L = m\psi_R \quad (2.14)$$

$$i\gamma^\mu \partial_\mu \psi_R = m\psi_L. \quad (2.15)$$

Since space-time evolutions of the chiral fields are coupled by the mass  $m$ , for a massless neutrino there is no need to introduce both chiral components. Indeed, in the SM only the left-handed neutrino field is considered. However, a two-component spinor can be sufficient for the description of a massive fermion if one assumes that  $\psi_R$  and  $\psi_L$  are not independent and the relation connecting them is such that the two equations (2.14) and (2.15) are two ways of writing the same equation for one independent field, say  $\psi_L$ . The field with such properties was introduced in 1937 by Ettore Majorana (Majorana 1937).

Using the defining properties of the charge conjugation matrix  $\mathcal{C}$  and its action on a spinor field:

$$\psi(x) \xrightarrow{\mathcal{C}} \psi^C(x) = \xi_C \mathcal{C} \bar{\psi}^T(x) = i\xi_C \gamma^2 \gamma^0 \bar{\psi}^T(x) \quad (2.16)$$

$$\bar{\psi}(x) \xrightarrow{\mathcal{C}} \bar{\psi}^C(x) = -\xi_C^* \psi^T(x) \mathcal{C}^\dagger, \quad (2.17)$$

with  $\xi_C$  an arbitrary phase factor such that  $|\xi_C|^2 = 1$ .

The field defined as:

$$\psi_L^C = \mathcal{C} \bar{\psi}_L^T \quad (2.18)$$

provides the Majorana relation between  $\psi_R$  and  $\psi_L$ :

$$\psi_R = \xi_C \mathcal{C} \bar{\psi}_L^T \quad (2.19)$$

and behaves as a right-handed field. In fact, using  $P_L \mathcal{C} = \mathcal{C} P_L$ , it follows that:



$$P_L (\mathcal{C}\overline{\psi}_L^T) = \mathcal{C} (\overline{\psi}_L P_L)^T = \mathcal{C} [(P_R \psi_L)^\dagger \gamma^0]^T = 0 \quad (2.20)$$

where,

$$P_L \equiv \frac{(1 - \gamma_5)}{2} \quad P_R \equiv \frac{(1 + \gamma_5)}{2} \quad (2.21)$$

are the left-handed and right-handed projectors, respectively.

The Majorana field can thus be written as:

$$\psi = \psi_L + \mathcal{C}\overline{\psi}_L^T = \psi_L + \psi_L^C. \quad (2.22)$$

The Majorana condition,

$$\psi = \psi^C, \quad (2.23)$$

implies the equality of particle and antiparticle. Hence, the two independent components Majorana field only describes neutral fermions, such as neutrinos.

Note that Dirac and Majorana descriptions of neutrino field lead to different phenomenological consequences only if neutrinos are massive. In the massless Majorana theory, the left-handed and right-handed chiral fields, related by equation (2.19), obey the same decoupled Weyl equations, obtained from (2.14) and (2.15) in the case  $m = 0$ , which hold for the independent left-handed and right-handed chiral components of Dirac neutrino field. Furthermore, since only the left-handed chiral component of the neutrino field takes part in weak interactions and obeys the same Weyl equation in both the Dirac and Majorana descriptions, the right-handed chiral component is irrelevant and Dirac and Majorana theories are physically equivalent. This means that measuring some effect due to the neutrino mass appears as the only way to distinguish a Dirac from a Majorana neutrino. Moreover, the mass effect must not be of kinematic nature, such as neutrino oscillations, because the kinematic effects of Dirac and Majorana masses are the same. An appropriate way to identify neutrinos as Majorana particles is the observation of neutrinoless double  $\beta$ -decay.

Evidently, the neutrino mass term and its form play an important role. A Majorana mass can be generated by a Lagrangian mass term with only a chiral fermion field. As neutrinos are produced left-handed through weak

interactions, we consider the left-handed chiral field  $\nu_L$ . Chirality and Lorentz invariance impose that any mass term combines the adjoint of a spinor of definite chirality with a spinor of opposite chirality so that a proper Majorana mass term can then be written as:

$$\mathcal{L}_{mass}^M = -\frac{1}{2}m\overline{\nu_L^C}\nu_L + h.c. \quad (2.24)$$

Using the above mass term, the full free Majorana Lagrangian, comprising the kinetic terms for the neutrino chiral fields, is given by:

$$\mathcal{L}^M = \frac{1}{2} \left[ \overline{\nu_L} i \overleftrightarrow{\not{\partial}} \nu_L + \overline{\nu_L^C} i \overleftrightarrow{\not{\partial}} \nu_L^C - m \left( \overline{\nu_L^C} \nu_L + \overline{\nu_L} \nu_L^C \right) \right] \quad (2.25)$$

where, the factor  $1/2$  avoids a double counting of degrees of freedom due to the fact that  $\nu_L^C$  and  $\overline{\nu_L}$  are not independent, as shown by equation (2.18).

Defining the Majorana field as:

$$\nu \equiv \nu_L + \nu_L^C \quad (2.26)$$

such that the Majorana condition (2.23) is satisfied, the Majorana Lagrangian (2.25) takes the form:

$$\mathcal{L}^M = \frac{1}{2} \overline{\nu} \left( i \overleftrightarrow{\not{\partial}} - m \nu_L^C \right) \nu \quad (2.27)$$

Using the anticommutation property of the fermion field and the explicit expression for  $\mathcal{C}$ , the Lagrangian (2.25) can be expressed in terms of the only independent field  $\nu_L$ :

$$\mathcal{L}^M = \overline{\nu_L} i \overleftrightarrow{\not{\partial}} \nu_L - \frac{m}{2} \left( -\nu_L^T \mathcal{C}^\dagger \nu_L + \overline{\nu_L} \mathcal{C} \overline{\nu_L}^T \right). \quad (2.28)$$

This expression for the Majorana Lagrangian is more convenient because the kinetic term has the same form as that of a massless neutrino in the SM and is the same as the Dirac Lagrangian. As for the mass term, this takes a completely different form and represents a physical effect beyond the SM. As already mentioned, if massive neutrinos are Dirac particles, the total lepton number associated with the global  $U(1)$  gauge transformations is conserved. In the case of massive Majorana neutrinos, this residual symmetry, whose conserved charge counts the number of leptons minus anti-leptons summed

over the flavor, is lost because the Majorana mass term in eqn (2.24) is not invariant under the global  $U(1)$  gauge transformation  $\nu_L \rightarrow e^{i\phi}\nu_L$ .

For small neutrino masses one can treat the Majorana mass term as a perturbation of the massless Lagrangian. Its effect at first order is to generate observable processes where  $\Delta L = \pm 2$ . This is precisely the case of neutrinoless double  $\beta$ -decay.

Although the Majorana mass term in (2.25) involves only the neutrino left-handed chiral field  $\nu_L$  that is present in the SM, the SM neutrinos cannot have Majorana masses, because  $\nu_L$  has third component  $I_3 = 1/2$  and hypercharge  $Y = -1$ , hence  $\overline{\nu_L^C}\nu_L$  has  $I_3 = 1$  and  $Y = -2$ . Such a term behaves as a weak isospin triplet, then it cannot be obtained by spontaneous symmetry breaking from a gauge-invariant Yukawa term involving a single Higgs doublet. Since the SM does not contain any weak isospin triplet with  $Y = 2$ , it is not possible to have a renormalizable Lagrangian term which can generate a Majorana neutrino mass. By using two Higgs doublets, whose product contains a weak-isospin triplet, one can construct the mass dimension-5 coupling term:

$$\mathcal{L}_5 = \frac{g}{\mathcal{M}} (L_L^T \sigma_2 \Phi) C^\dagger (\Phi^T \sigma_2 L_L) + h.c., \quad (2.29)$$

where  $g$  is a dimensionless coupling coefficient,  $\mathcal{M}$  is a mass scale,  $L_L$  is the one-generation SM lepton doublet and  $\Phi$  is the Higgs doublet.

The Lagrangian term  $\mathcal{L}_5$  is not renormalizable because it contains a product of fields with energy dimension five. Therefore it should not be allowed in the framework of the SM. However, with a view to consider the SM as a low-energy effective theory which is the product of the symmetry breaking of a high-energy unified theory, it is plausible an additional effective low-energy Lagrangian term such as  $\mathcal{L}_5$  which respects the SM symmetries, though not renormalizable. The high-energy theory will be some more fundamental and renormalizable theory that contains new heavy degrees of freedom which only manifest as asymptotic states (real particles) at energies of the order of  $\mathcal{M}$  or higher, while at low energies, they can contribute to physical processes as virtual particles and mediate new interaction terms among the SM degrees of freedom.

Note that a dimension-5 effective operator similar to  $\mathcal{L}_5$  cannot be written for quarks, because it would generate a quark Majorana mass term that is forbidden for charged particles. As for (2.29), spontaneous symmetry breaking provides the Majorana mass term for  $\nu_L$ :

$$\mathcal{L}_{mass}^M = \frac{1}{2} \frac{g v^2}{\mathcal{M}} \nu_L^T \mathcal{C}^\dagger \nu_L + h.c., \quad (2.30)$$

which provides the Majorana mass:

$$m = \frac{g v^2}{\mathcal{M}}. \quad (2.31)$$

Since the generated neutrino Majorana mass in (2.31) is proportional to the ratio  $v^2/M$ , where  $v$  is the scale of the electroweak symmetry breaking, it sets the scale of the Dirac fermion masses  $m_D$  generated through the Higgs mechanism. Hence, equation (2.31) can be written as:

$$m \propto \frac{m_D^2}{\mathcal{M}}. \quad (2.32)$$

$m_D$  is a typical Dirac mass, which could be of order of the mass of the charged lepton or quark of the same generation. The relation in equation (2.32) has the same structure of the relation that one obtains through the seesaw mechanism that will be briefly discussed in section 2.3. As suggested by the name *seesaw* the heavier the mass  $\mathcal{M}$ , the lighter is the neutrino mass  $m$ .

The relation in equation (2.32) can explain the observed smallness of neutrino masses. For example, taking  $m_D \sim v \sim 10^2$  GeV and  $\mathcal{M} \sim 10^{15}$  GeV, which is a plausible grand unification scale, then  $m \sim 10^{-2}$  eV, which is a plausible scale for the neutrino mass, according to the experimental data.

The Lagrangian term (2.29) can be straightforwardly generalized to the case of three generations of neutrinos:

$$\mathcal{L}_5 = \frac{1}{\mathcal{M}} \sum_{\alpha,\beta} g_{\alpha\beta} (L_{\alpha L}^{\prime T} \sigma_2 \Phi) \mathcal{C}^\dagger (\Phi^T \sigma_2 L'_{\beta L}) + h.c., \quad (2.33)$$

where  $g$  is a symmetric  $3 \times 3$  matrix of coupling constants. The neutrino Majorana mass term that arise after the electroweak symmetry breaking has the form:

$$\mathcal{L}_{mass}^M = \frac{1}{2} \frac{v^2}{\mathcal{M}} \sum_{\alpha,\beta} g_{\alpha\beta} \nu_{\alpha L}^{\prime T} \mathcal{C}^\dagger \nu'_{\beta L} + h.c., \quad (2.34)$$

which leads to the following Majorana mass matrix:

$$M_{\alpha\beta}^L = \frac{v^2}{\mathcal{M}} g_{\alpha\beta}. \quad (2.35)$$

Since the scale of the Majorana neutrino masses is set by the small ratio  $v^2/M$ , the strong suppression of neutrino masses with respect to the electroweak scale finds a natural explanation in this framework.

### 2.2.3 Dirac-Majorana Mass Term

From the discussion in the previous sections of this chapter it follows that the existence of the chiral field  $\nu_L$  is well established, given that it enters in the charged-current weak interactions Lagrangian. This is not the case for the chiral field  $\nu_R$ , whose existence is anyhow allowed by the symmetries of the SM.

If there existed only  $\nu_L$ , the neutrino Lagrangian would contain only the Majorana mass term:

$$\mathcal{L}_{mass}^L = \frac{1}{2} \sum_{\alpha,\beta} \nu_{\alpha L}^{\prime T} \mathcal{C}^\dagger M_{\alpha\beta}^L \nu'_{\beta L} + h.c. \quad (2.36)$$

and neutrinos would be Majorana particles.

Assuming that in addition to the three known active left-handed neutrino fields  $\nu'_{\alpha L}$ , with  $\alpha = e, \mu, \tau$ , there also exist  $N_s$  sterile right-handed neutrino fields  $\nu_{sR}$ , with  $s = s_1, \dots, s_{N_s}$  (the right-handed neutrino fields are unprimed, because these fields do not take part in weak interactions, whereas the active left-handed neutrino fields need to be redefined in order to diagonalize the leptonic weak charged current), then the neutrino Lagrangian must contain the Majorana mass term for such fields:

$$\mathcal{L}_{mass}^R = \frac{1}{2} \sum_{s,s'} \nu_{sR}^T \mathcal{C}^\dagger M_{ss'}^R \nu_{s'R} + h.c. \quad (2.37)$$

If  $\nu_{sR}$  exists, the neutrino Lagrangian can also contain the Dirac mass term:

$$\mathcal{L}_{mass}^D = - \sum_s \sum_\alpha \bar{\nu}_{sR} M_{s\alpha}^D \nu'_{\alpha L} + h.c., \quad (2.38)$$

which would imply that neutrinos are Dirac particles.

The most general mass term, where left-handed active flavor fields and right-handed sterile fields enter, has thus the form:

$$\mathcal{L}_{mass}^{D+M} = \mathcal{L}_{mass}^L + \mathcal{L}_{mass}^R + \mathcal{L}_{mass}^D. \quad (2.39)$$

The Dirac–Majorana mass term (2.39) contains three complex mass matrices  $M^L$ ,  $M^R$  and  $M^D$ . In particular, The Majorana mass matrices  $M^L$  and  $M^R$  are symmetric. The left-handed Majorana mass matrix  $M^L$  is a  $3 \times 3$  square matrix, the right-handed Majorana mass matrix  $M^R$  is a  $N_s \times N_s$  square matrix, and the Dirac mass matrix  $M^D$  is a  $N_s \times 3$  rectangular matrix.

The above mass term is not invariant under the global gauge transformations. Thus, in the theory with the Dirac–Majorana mass term the lepton number  $L$  is not conserved. This means that the fields of neutrinos with definite masses are expected to be Majorana fields.

The neutrino fields with definite masses are given by the diagonalization of the Dirac–Majorana mass term. For this purpose it is convenient to define the column matrix of  $N = 3 + N_s$  left-handed fields:

$$N'_L \equiv \begin{pmatrix} \nu'_L \\ \nu'_R \end{pmatrix}, \quad (2.40)$$

where  $\nu'_L$  is the column matrix defined in equation (1.44) and  $\nu'_R$  is the column matrix of charge-conjugated right-handed sterile neutrinos:

$$\nu'_R \equiv \begin{pmatrix} \nu_{s_1 R}^C \\ \vdots \\ \nu_{s_{N_s} R}^C \end{pmatrix}. \quad (2.41)$$

Thereby the Dirac–Majorana mass term (2.39) can be written in compact form:

$$\mathcal{L}_{mass}^{D+M} = \frac{1}{2} N'^T_L C^\dagger M^{D+M} N'_L + h.c. \quad (2.42)$$

where

$$M^{D+M} \equiv \begin{pmatrix} M^L & M^{D^T} \\ M^D & M^R \end{pmatrix} \quad (2.43)$$

is a symmetric  $N \times N$  mass matrix.

Writing the left-handed flavor fields as unitary linear combinations of the left-handed components of  $N$  fields with definite mass:

$$N'_L \equiv V'_L n_L \quad \text{with} \quad n_L = \begin{pmatrix} \nu_{1L} \\ \vdots \\ \nu_{NL} \end{pmatrix}, \quad (2.44)$$

where  $V'_L$  is the unitary matrix which diagonalizes the mass matrix  $M^{D+M}$ :

$$(V'_L)^T M^{D+M} V'_L = M \quad \text{with} \quad M_{kj} = m_k \delta_{kj}, \quad k, j = 1, \dots, N. \quad (2.45)$$

The Dirac–Majorana mass term now can be written in terms of the massive left-handed fields as:

$$\begin{aligned} \mathcal{L}_{mass}^{D+M} &= \frac{1}{2} n_L^T \mathcal{C}^\dagger M n_L + h.c. = \frac{1}{2} \sum_{k=1}^N m_k \nu_{kL}^T \mathcal{C}^\dagger \nu_{kL} + h.c. \\ &= -\frac{1}{2} \overline{n_L^C} M n_L + h.c. = -\frac{1}{2} \sum_{k=1}^N m_k \overline{\nu_{kL}^C} \nu_{kL} + h.c., \end{aligned} \quad (2.46)$$

where  $m_k$  are real and positive Majorana masses, corresponding to the Majorana neutrino fields:

$$n = \begin{pmatrix} \nu_1 \\ \vdots \\ \nu_N \end{pmatrix}, \quad (2.47)$$

with  $\nu_k$  such that the Majorana condition is satisfied:

$$\nu_k = \nu_{kL} + \nu_{kL}^C \quad \nu_k^C = \nu_k. \quad (2.48)$$

In order to examine the relevant consequences for weak interactions of the mixing of active and sterile neutrino fields in equation (2.44), consider the leptonic charged current written in terms of massive fields:

$$J_{W,L}^\mu = 2 \overline{n_L} U^\dagger \gamma^\mu l_L, \quad (2.49)$$

where the mixing matrix  $U$  is the product of the  $3 \times 3$  unitary matrix  $V_L^l$  that diagonalizes the charged lepton mass matrix and the  $N \times N$  unitary matrix  $V'_L$  that diagonalizes the Dirac–Majorana mass matrix,

$$U_{\alpha k} = \sum_{\beta=e,\mu,\tau} \left( V_L^{l\dagger} \right)_{\alpha\beta} (V_L^\nu)_{\beta k}. \quad (2.50)$$

The mixing matrix  $U$  (2.50) is a  $3 \times N$  matrix not unitary, since  $UU^\dagger = 1$  but  $U^\dagger U \neq 1$ .

Despite the formal analogy between the expression of the leptonic charged current in equation (2.49) and those for the Dirac case and for the mixing of three Majorana neutrinos, the Dirac-Majorana case under consideration is very different, because the mixing matrix is a  $3 \times N$  matrix which connects the three active flavor neutrinos to  $N$  massive neutrinos.

The mixing of active and sterile neutrinos is given by:

$$\nu_{\alpha L} = \sum_{k=1}^N U_{\alpha k} \nu_{kL} \quad \alpha = e, \mu, \tau \quad (2.51)$$

$$\nu_{sR}^C = \sum_{k=1}^N (V_L^\nu)_{sk} \nu_{kL} \quad s = s_1, \dots, s_{N_s}. \quad (2.52)$$

Since active and sterile neutrino fields are linear combinations of the same massive neutrino fields, oscillations between active and sterile states become possible. This is also signaled by the non-unitarity of the mixing matrix  $U$  which implies that the total probability of active flavors is not conserved.

The above mixing relations can be written in the compact matrix form:

$$N_L = \mathcal{U} n_L, \quad (2.53)$$

where

$$N_L \equiv \begin{pmatrix} \nu_L \\ \nu_R^C \end{pmatrix}, \quad \mathcal{U} \equiv \begin{pmatrix} U \\ V_L^\nu L|_{N_s \times N} \end{pmatrix} = \begin{pmatrix} V_L^{l\dagger} V_L^\nu|_{3 \times N} \\ V_L^\nu|_{N_s \times N} \end{pmatrix} \quad (2.54)$$

The matrices  $V_L^\nu|_{3 \times N}$  and  $V_L^\nu|_{N_s \times N}$  are obtained by taking the first three rows and the remaining  $N_s$  rows of  $V_L^\nu$ . The matrix  $\mathcal{U}$  so defined is a  $N \times N$  unitary matrix.

As regards the neutrino neutral current,

$$J_{Z,\nu}^\mu = \bar{n}_L \gamma^\mu U^\dagger U n_L, \quad (2.55)$$

as a consequence of the non-unitarity of  $U$  the GIM mechanism does not



work, meaning that in the general Dirac–Majorana case it is possible to have neutral current transitions among different massive neutrinos.

## 2.3 The Seesaw Mechanism

The seesaw mechanism was introduced at the end of the seventies (Gell-Mann et al. 1979; Yanagida 1980; Mohapatra & Senjanovic 1980) to explain the extremely small masses of neutrinos compared with those of charged fermions in the SM. Even if there was still no solid evidence for neutrino masses at that time, there were extensions of the SM that led to nonzero masses for neutrinos.

There are various types of extensions of the SM. The simplest version, type 1, assumes two or more additional right-handed sterile neutrino fields and the existence of a very large mass scale. This allows to identify the mass scale with the postulated scale of grand unification.

The seesaw mechanism is a viable mechanism of neutrino mass generation, based on the Dirac-Majorana mass term. This is achieved by adding right-handed neutrinos and have these couple to left-handed neutrinos with a Dirac mass term. The right-handed neutrinos have to be sterile with respect to any of the SM interactions. Being neutral, the right-handed neutrinos can act as their own anti-particles, and have a Majorana mass term. Like any other Dirac mass in the SM, the neutrino Dirac mass is expected to be generated through the Higgs mechanism and therefore cannot be predicted. The Majorana mass for the right-handed neutrinos instead is not generated through the Higgs mechanism and consequently is expected to be tied to some energy scale of new physics beyond the SM. This implies that any process involving right-handed neutrinos will be suppressed at low energies. The correction related to these suppressed processes gives the left-handed neutrinos a mass that is inversely proportional to the right-handed Majorana mass.

The introduction of heavy right-handed neutrinos can then explain both the small mass of the left-handed neutrinos and the absence of the right-handed neutrinos in observations. However, because of the uncertainty in the Dirac neutrino masses, the right-handed neutrino masses can have any value. For instance, the heavy sterile right-handed neutrinos have been studied as a possible candidate for a dark matter WIMP (Murayama 2007). Right-handed neutrinos with masses in the range  $(0.1 - 1.0)$  keV have been studied (Dodelson & Widrow 1993), leading to warm dark matter and a structure formation scenario alternative to both the standard hot and cold dark matter scenarios. Light neutrinos are, in general, disfavored as an explanation for

dark matter, because they are too hot, that is, their kinetic energy is large compared to their mass, while formation of structures similar to the galaxies seemingly requires cold dark matter.

They can also have a mass in the LHC energy range. An example is provided by the Left–Right symmetric theory that originally led to the seesaw mechanism. A TeV scale  $L - R$  symmetric theory could have significant signatures at LHC, with a possible discovery of  $\nu_R$  and observation of parity restoration as well as the Majorana nature of neutrinos. If the scale of parity restoration is in the few TeV region, Type I seesaw connects neutrino mass to the scale of parity restoration, leading to a rich LHC phenomenology and a number of lepton flavor violating processes (Senjanovic 2010). Right-handed neutrinos can also have masses near the GUT scale, linking the right-handed neutrinos to grand unified theories (Senjanovic 2011).

The mass terms mix neutrinos of different generations through the PMNS matrix, which is the neutrino analogue of the CKM quark mixing matrix. Although the quark mixing is almost minimal, the fact that some neutrino mixing angles are large and even nearly maximal, was soon realized to be compatible with a unified picture of quark and lepton masses within GUTs. The symmetry group at  $M_{GUT}$  could be either (SUSY)  $SU(5)$  or  $SO(10)$  or a larger group (Altarelli 2007 and references therein). According to the seesaw mechanism, light neutrino masses are small because neutrinos are Majorana particles with masses inversely proportional to the large scale of lepton number violation, which is close to  $10^{14} - 10^{15}$  GeV not far from  $M_{GUT}$ , so that neutrino masses fit well in the SUSY GUT picture.

Large neutrino mixings and possible complex phases that break CP invariance could potentially create a surplus of leptons over anti-leptons in the early universe, a process known as leptogenesis. This asymmetry at a later stage could be converted in an excess of baryons over anti-baryons (baryogenesis via leptogenesis), and explain the matter-antimatter asymmetry in the universe. In  $SU(5)$  models the heavy Majorana neutrino masses are not constrained by low energy physics as light neutrino masses and mixings. Successful leptogenesis is possible, but it depends on the choice of the heavy Majorana neutrino masses. In  $SO(10)$  models the implications of large neutrino mixings are much more stringent because of the connection between Dirac neutrino and up-quark mass matrices. The requirement of large neutrino mixings then determines the relative magnitude of the heavy Majorana neutrino masses in terms of the known quark mass hierarchy. This leads to predictions for neutrino mixings and masses, CP violation in neutrino oscillations and neutrinoless double  $\beta$ -decay. In models where the CP asymmetry is determined by the mass hierarchy of light and heavy Majorana neutrinos, the observed baryon asymmetry is obtained without any fine tuning of pa-

rameters, if  $B - L$  is broken at the unification scale  $M_{GUT}$  and the generated baryon asymmetry does not depend on the flavor mixing of the light neutrinos. The predicted order of magnitude of the baryon asymmetry is also in accord with observation (Buchmüller & Plümacher 1996; Buchmüller 2002). In fact, in unified theories with right-handed neutrinos  $B - L$  is spontaneously broken. In theories where  $B - L$  is a spontaneously broken local symmetry, out of equilibrium decays with CP and  $L$  violation of heavy right-handed neutrinos can produce a  $B - L$  asymmetry, then converted near the weak scale by instantons into an amount of  $B$  asymmetry compatible with observations (Buchmüller et al. 2005).

In order to expose the main idea of the seesaw mechanism, consider the Dirac-Majorana mass matrix, in equation (2.43), with  $M^L = 0$ :

$$M^{D+M} = \begin{pmatrix} 0 & M^{D^T} \\ M^D & M^R \end{pmatrix} \quad (2.56)$$

and the elements of the right-handed Majorana mass matrix  $M^R$  much larger than the elements of the Dirac mass matrix  $M^D$ . The physical justifications of such assumptions are that the left-handed Majorana mass matrix  $M^L$  is forbidden by the SM symmetries and  $M^R$  is generated by new physics beyond the SM. In fact, the right-handed Majorana mass term breaks conservation of the lepton number therefore it is assumed that the lepton number is violated at a scale which is much larger than the electroweak scale.

If all the eigenvalues of  $M^R$  are much larger than all the elements of  $M^D$ , the mass matrix can be diagonalized by blocks, up to corrections of the order  $(M^R)^{-1}M^D$ :

$$W^T M^{D+M} W \simeq \begin{pmatrix} M_{light} & \\ & M_{heavy} \end{pmatrix} \simeq \begin{pmatrix} -M^{D^T} (M^R)^{-1} M^D & \\ & M^R \end{pmatrix} \quad (2.57)$$

with

$$W \simeq \begin{pmatrix} 1 - \frac{1}{2} M^{D^T} (M^R M^{R^\dagger})^{-1} M^D & [(M^R)^{-1} M^D]^\dagger \\ - (M^R)^{-1} M^D & 1 - \frac{1}{2} (M^R)^{-1} M^D M^{D^T} (M^{R^\dagger})^{-1} \end{pmatrix}. \quad (2.58)$$

The heavy masses are given by the eigenvalues of the  $N_s \times N_s$  mass matrix

$M_{heavy} \simeq M^R$ , whereas the light masses are given by the eigenvalues of the light  $3 \times 3$  mass matrix  $M_{light}$  whose elements are suppressed, with respect to the elements of the Dirac mass matrix  $M^D$ , by the small matrix factor  $M^{D^T} (M^R)^{-1}$ . However, the values of the light neutrino masses and their relative sizes can vary over wide ranges, depending on the values of the elements of  $M^D$  and  $M^R$ .

The two possibilities often considered in literature are those which follow (Bludman et al. 1992).

### 2.3.1 Quadratic Seesaw

In the case:

$$M^R = \mathcal{M}I \quad (2.59)$$

where  $I$  is the  $N_s$ -dimensional identity matrix and  $M$  is the high-energy scale of new physics beyond the SM at which the total lepton number is violated.

The light mass matrix is:

$$M_{light} \simeq -\frac{M^{D^T} M^D}{\mathcal{M}} \quad (2.60)$$

and the light neutrino masses are given by:

$$m_k = \frac{(m_k^D)^2}{\mathcal{M}} \quad k = 1, 2, 3. \quad (2.61)$$

$(m_k^D)^2$  are the three eigenvalues of the  $3 \times 3$  matrix  $M^{D^T} M^D$  which are expected to be of order of the charged lepton or around the up quark masses, being  $M^D$  generated by the SM Higgs mechanism.

The large energy scale  $\mathcal{M}$  in equation (2.60) suppresses the light neutrino masses with respect to the masses of the charged leptons and quarks. The reason why the case under consideration is called quadratic seesaw is that the light neutrino masses  $m_k$  scale as the squares of the masses  $m_k^D$ :

$$m_1 : m_2 : m_3 = (m_1^D)^2 : (m_2^D)^2 : (m_3^D)^2 \quad (2.62)$$

### 2.3.2 Linear Seesaw

Consider  $N_s = 3$ . In this case it is possible to have:

$$M^R = \frac{\mathcal{M}}{\mathcal{M}^D} M^D, \quad (2.63)$$

where  $\mathcal{M}^D$  is the scale of the elements of  $M^D$ ,  $\mathcal{M} \gg \mathcal{M}^D$  is the high-energy scale of new physics beyond the SM at which the total lepton number is violated and  $M^D$  is the energy scale of the SM electroweak symmetry breaking, i.e.  $M^D \sim 10^2$  GeV, since  $M^D$  is generated by the SM Higgs mechanism.

Equation (2.57) leads to:

$$M_{light} \simeq -\frac{\mathcal{M}^D}{\mathcal{M}} M^D. \quad (2.64)$$

The light neutrino masses are given by:

$$m_k = \frac{\mathcal{M}^D}{\mathcal{M}} m_k^D \quad k = 1, 2, 3 \quad (2.65)$$

where  $m_k^D$  are the eigenvalues of  $M^D$ .

The light neutrino masses are suppressed by the small ratio  $\mathcal{M}^D/\mathcal{M}$  with respect to the masses  $m_k^D$ , which are expected to be of order of the charged lepton or around the up quark masses.

The above considered case is called linear seesaw because of the proportionality of the light neutrino masses  $m_k$  to the masses  $m_k^D$ :

$$m_1 : m_2 : m_3 = m_1^D : m_2^D : m_3^D. \quad (2.66)$$

In conclusion, if the seesaw mechanism is realized in nature then, neutrinos are expected to be Majorana particles, with masses much smaller than lepton and quark masses, and heavy Majorana particles, namely the seesaw partners of neutrinos, are also expected to exist.

The standard seesaw mechanism presented in this section, due to the lepton-Higgs-right-handed neutrinos interaction, is called type I seesaw mechanism. Models with interactions of lepton pairs and Higgs pair with triplet heavy scalar boson  $\Delta$  are called type II and models with an interaction of lepton-Higgs pairs with heavy Majorana triplet fermion  $\sigma_R$  are called type III seesaw models.

## 2.4 Right-Handed Sterile Neutrinos

A sterile right-handed neutrino is an  $SU(2)$  singlet which is sterile under weak interactions except those induced by mixing with active neutrinos. It may participate in Yukawa interactions involving the Higgs boson or in interactions involving new physics beyond the SM. Many extensions of the standard model introduce a right-chiral sterile  $\nu_R$ , with its left-chiral CP conjugate  $\nu_L^C$ . As it will be shown in Chapter 3, the three-flavor active neutrino pattern with nonzero mixing successfully accounts for most of the results of oscillation experiments designed to measure solar, atmospheric, accelerator and reactor neutrinos. On the other hand, there also exist a few anomalies in experimental results that find no explanation in such a framework. Additional sterile neutrinos might be required for explaining all experimental data through neutrino oscillations. These sterile species, predicted by many theoretical models beyond the SM, are neutral leptons gravitationally interacting which have no weak interactions as well as strong and electromagnetic interactions, as all neutrino fields.

The three-neutrino mixing scheme was first challenged in 1995 by the LSND (Neutrino Liquid Scintillator) experiment (Athanasopoulos et al. 1995; Athanasopoulos et al. 1998; Aguilar et al. 2001). The observation of a signal of short-baseline  $\bar{\nu}_\mu \rightarrow \bar{\nu}_e$  oscillations, led to assume the existence of one or more squared-mass differences much larger than  $\Delta_{SOL}^2$  and  $\Delta_{ATM}^2$ . The first results of the MiniBooNE experiment, designed to check the LSND signal, did not find any signal compatible with that of LSND in neutrino mode, but the results in antineutrino mode have effectively confirmed the LSND observations. This has revived interest in the possible existence of one or more neutrinos, with mass in the  $eV$  scale, that can generate the squared-mass differences observed in short-baseline oscillations. The additional massive neutrinos, which in the flavor basis correspond to sterile neutrinos, do not contribute to the number of active neutrinos determined by LEP experiments through the measurement of the invisible width of the Z boson,  $N_a = 2.9840 \pm 0.0082$  (Schael et al. 2006).

For sterile neutrinos to have a relevant role in neutrino oscillations, as suggested by LSND and MiniBooNE, or for most astrophysical and cosmological implications, it is necessary a non-negligible mixing between active and sterile states of the same chirality. This does not occur in the pure Majorana, pure Dirac, or very high energy seesaw limits, but only for the pseudo-Dirac and active-sterile cases. The pseudo-Dirac case is in fact excluded, unless  $M^L, M^R \lesssim 10^{-9}$  eV, because this would imply significant oscillations of solar neutrinos into sterile states, which is not observed. Significant active-sterile mixing requires that at least some Dirac masses ( $M^D$ )

and some Majorana masses ( $M^R$  and/or  $M^L$ ) are simultaneously very small but non-zero. One possibility is that some new symmetry forbids all of the mass terms at the perturbative level, but allows, for instance  $M^R \sim 1$  eV and  $M^D \sim 0.1$  eV due to higher-dimensional operators.

Assuming that sterile neutrino has mass around eV and mixing around 0.1, then its contribution to the active neutrino masses is expected to be of order  $M^{D^2}/M^R \sim 0.1$  eV, so that active-sterile mixing can lead to induced contribution to the neutrino mass matrix (Smirnov & Zukanovich 2006). If sterile neutrino is assumed having mass around keV and mixing around  $10^{-4}$ , then its contribution to the active neutrino masses is of order  $M^{D^2}/M_R \sim 10^{-5}$  eV, and completely negligible.

An example of a theory with sterile neutrinos and the seesaw mechanism is the SO(10) grand unified theory (GUT), in which a sterile neutrino is the SU(5)-singlet member of the 16-dimensional spinor representation for each SM generation. Similarly, sterile neutrinos appear naturally as the spinor component of the corresponding chiral superfields in supersymmetric SO(10) GUTs.

As regards low energy seesaw, consider the most general renormalizable Lagrangian:

$$\mathcal{L}_\nu \supset \mathcal{L}_{SM} - \frac{M_{ij}^R}{2} N_i N_j - y^{\alpha i} L_\alpha N_i H + h.c., \quad (2.67)$$

where  $\mathcal{L}_{SM}$  is the SM Lagrangian without gauge singlet fermions,  $y^{\alpha i}$  are the neutrino Yukawa couplings and  $M_{ij}^R$  are the entries of the right-handed neutrino Majorana mass matrix. The above equation (2.67) is expressed in the weak basis where the Majorana mass matrix for the right-handed neutrinos is diagonal.

The seesaw formula leaves the mass of singlet neutrinos as a free parameter. This allows to choose these parameters so that they can account for certain phenomena and anomalies beyond the SM, such as providing a dark matter candidate or a mechanism for baryogenesis or explaining various short baseline anomalies. In this latter case, the seesaw scale corresponds to the scale of light sterile neutrinos. Considering in particular this eV-scale seesaw, non-oscillation experiments sensitive to the low energy seesaw include searches for double  $\beta$ -decay and cosmological bounds on the number of relativistic particle species in the early universe as well as on the fraction of hot dark matter. It is also possible a partial cancellation, that is, the contribution to neutrinoless double  $\beta$ -decay of a light sterile neutrino, which generates an active neutrino via seesaw, may cancel the contribution to double  $\beta$ -decay from this active state. Assuming that no other mechanisms that can lead to

double beta decay is realized in nature, the observation of a finite lifetime for neutrinoless double  $\beta$ -decay would rule out equation (2.67), unless at least one of the right-handed neutrino mass parameters is above a few tens of MeV.

It has been showed (Donini et al. 2011) that minimal models based on the  $3 + 1$  scheme are ruled out, even though in principle there would be sufficient parameters to fit two mass splittings and two mixing angles. The most minimal working model is the  $3 + 2$  model, which contains one massless neutrino, four massive states, four angles and 2 CP phases. The simplified case with degenerate eigenvalues of  $M^R$  and in the CP conserving limit, i.e.,  $M_1 = M_2 = M$  and no phases, leads to reduce the number of extra parameters, with respect to the standard three-neutrino scenario, to just one extra mass, the common Majorana mass,  $M$ . This model in fact reduces to the standard three neutrino scenario in the two limits:  $M \rightarrow 0$ , when the four eigenstates degenerate into two Dirac pairs, and the opposite  $M \rightarrow \infty$ , when the two heavier states decouple. The fit to neutrino data will be good for  $M$  below the quasi-Dirac limit,  $M \leq M_{QD}$  (with  $M_{QD}$  the scale where the two massive neutrinos become Pseudo-Dirac particles) and also for  $M$  above the seesaw limit  $M \geq M_{SS}$  (with  $M_{SS}$  the scale where the mass of the active neutrinos is given by the seesaw formula). The value of  $M_{QD}$  is fixed by solar data to be very small whereas the seesaw limit is mostly determined by long-baseline data. However, due to cancellations of the probabilities related to the existence of two almost degenerate heavy states, the degenerate case does not provide a sufficiently good fit to the anomalies than the standard three neutrino scenario. A different situation is found dropping the degenerate limit. In this case the heavy-light mixings depend on the light masses and mixings, but also on the two heavy masses, and on a new complex angle (Abazajian et al. 2012 and references therein).



## Neutrino Flavor Oscillations

The neutrino flavor oscillations are a quantum mechanical phenomenon. Neutrinos are produced through charged-current weak interactions as flavor states. The charged current can produce any neutrino in conjunction with a charged lepton. The neutrino beam produced is a linear superposition of different mass eigenstates. As the beam propagates, different components of this beam have different velocities and evolve differently, so that the probability of finding different eigenstates in the beam varies with time. In other words, during the time  $t$ , different mass-components of the coherent neutrino state acquire different phases. The oscillations are generated by the interference of the different massive neutrinos, which are produced and detected coherently because of the very small mass differences. This consequence of neutrino mixing, named neutrino oscillation, was first suggested by Pontecorvo (Pontecorvo 1957). If differences among neutrino masses are exceedingly small so that energy and momentum resolutions are not sufficient to distinguish among neutrino mass eigenstates, the effect of interference, i.e. the oscillations, can be observed. Whereas if the resolution of energy and momentum measurements of all particles involved in the process were high enough to allow the inference of the mass of the produced neutrino, no oscillations would be observed.

Since in the late 1950s only one active neutrino was known, the electron neutrino, in order to discuss neutrino oscillations, Pontecorvo introduced the concept of sterile neutrino. In particular, in 1967 Pontecorvo predicted the Solar Neutrino Problem as a consequence of  $\nu_e \rightarrow \nu_\mu$  (or  $\nu_e \rightarrow \nu_{sterile}$ ) transitions even before the first measurement of the solar electron neutrino flux in the Homestake experiment. The positive evidence of neutrino oscillations gives essentially two parameters: the mass difference squared  $\Delta m^2$  and mixing angle  $\theta$ . A great deal of evidence for neutrino oscillations has been

collected by many experiments covering a wide range of neutrino energies and with different detector technologies. The standard theory of neutrino flavor oscillations successfully accounts for the results of terrestrial and Solar neutrino experiments. In fact, nearly all the mixing parameters are precisely measured, except for the sign of the atmospheric mass-squared difference and eventual CP violating phases.

In this chapter the plane-wave derivation of the neutrino oscillation probability is reviewed with the main phenomenological aspects of neutrino oscillations in vacuum and in matter. The derivation of a general expression for the probability of neutrino oscillations is obtained by using the fact that neutrinos in oscillation experiments are ultra-relativistic, since their masses are smaller than about one eV and only neutrinos with energy larger than about 100 keV can be detected (via nuclei conversions or elastic scattering on electrons).

### 3.1 Neutrino Oscillations in Vacuum

In this section, the mathematical formulation of the neutrino propagation through the vacuum is exposed including the sterile degrees of freedom. In the standard theory of neutrino oscillations (Eliezer & Swift 1976; Fritzsche & Minkowski; Bilenky & Pontecorvo 1976; Bilenky & Pontecorvo 1978) a neutrino with flavor  $\alpha$  and momentum  $\vec{p}$ , created in a charged-current weak interaction process from a charged lepton  $l_\alpha$  or together with a charged antilepton  $\bar{l}_\alpha$ , is not in general a physical particle but rather a superposition of the physical fields  $\nu_k$  with different masses  $m_k$ , described by the *ket* state:

$$|\nu_\alpha\rangle = \sum_{k=1}^N \mathcal{U}_{\alpha k}^* |\nu_k\rangle \quad \alpha = e, \mu, \tau, s_1, \dots, s_{N_s}, \quad (3.1)$$

where  $\mathcal{U}$  is the  $N \times N$  (with  $N = 3 + N_s$ ) square mixing matrix defined in the previous chapter.

We consider a finite normalization volume  $V$  in order to have orthonormal massive neutrino states:

$$\langle \nu_k | \nu_j \rangle = \delta_{kj}. \quad (3.2)$$

The unitarity of the mixing matrix implies that also the flavor states are orthonormal:

$$\langle \nu_\alpha | \nu_\beta \rangle = \delta_{\alpha\beta}. \quad (3.3)$$

Since the massive neutrino states  $|\nu_k\rangle$  are eigenstates of the Hamiltonian,

$$\mathcal{H} |\nu_k\rangle = E_k |\nu_k\rangle, \quad (3.4)$$

a generic massive neutrino state produced at  $t = 0$  evolves in time as a plane wave:

$$|\nu_k(t)\rangle = e^{-iE_k t} |\nu_k\rangle. \quad (3.5)$$

A flavor state  $|\nu_\alpha\rangle$ , which describes a neutrino created with a definite flavor  $\alpha$  at time  $t = 0$ , from equations (3.1) and (3.5) evolves in time as:

$$|\nu_\alpha(t)\rangle = \sum_{k=1}^N \mathcal{U}_{\alpha k}^* e^{-iE_k t} |\nu_k\rangle. \quad (3.6)$$

Using the unitarity of the matrix  $\mathcal{U}$ ,  $\mathcal{U}^\dagger \mathcal{U} = \mathbf{1}$ , the massive states can be expressed in terms of flavor states,

$$|\nu_k\rangle = \sum_{\beta} \mathcal{U}_{\beta k} |\nu_\beta\rangle, \quad (3.7)$$

and substituting equation (3.7) into (3.6) we obtain:

$$|\nu_\alpha(t)\rangle = \sum_{\beta} \left( \sum_{k=1}^N \mathcal{U}_{\alpha k}^* e^{-iE_k t} \mathcal{U}_{\beta k} \right) |\nu_\beta\rangle, \quad (3.8)$$

which means that the superposition of massive neutrino states  $|\nu_\alpha(t)\rangle$ , that at  $t = 0$  is the pure flavor state in equation (3.1), becomes a superposition of different flavor states at  $t > 0$  (if the mixing matrix  $\mathcal{U}$  is not diagonal, that is, neutrinos are mixed).

Note that if the number of massive neutrinos is greater than three, the additional neutrinos in the flavor basis are sterile, then they interact with ordinary matter only gravitationally or through interactions beyond those in the SM. Eventual transitions of active flavor neutrinos into sterile ones can be observed only through the disappearance of active neutrinos.

As at this stage we mean to focus on the evolution of active neutrino flavor states, in what follows the Greek indices will be assumed to label only the three active neutrinos and the mixing matrix  $\mathcal{U}$  is replaced by the restriction to active states  $U$ , introduced in the previous chapter.

The coefficient of  $|\nu_\beta\rangle$  in equation (3.8) provides the amplitude of  $\nu_\alpha \rightarrow \nu_\beta$  transitions as a function of time:

$$\mathcal{A}_{\nu_\alpha \rightarrow \nu_\beta}(t) \equiv \langle \nu_\beta | \nu_\alpha(t) \rangle = \sum_{k=1}^N U_{\alpha k}^* U_{\beta k} e^{-iE_k t}. \quad (3.9)$$

This expression gives the probability of detecting a flavor  $\beta$  in a measurement of neutrino flavor at time  $t > 0$ , in an originally  $\nu_\alpha$  beam:

$$P_{\nu_\alpha \rightarrow \nu_\beta}(t) = |\mathcal{A}_{\nu_\alpha \rightarrow \nu_\beta}(t)|^2 = \sum_{k=1}^N U_{\alpha k}^* U_{\beta k} U_{\alpha j} U_{\beta j}^* e^{-i(E_k - E_j)t}. \quad (3.10)$$

For ultra-relativistic neutrinos, the dispersion relation can be approximated as:

$$E_k = \sqrt{|\vec{p}|^2 + m_k^2} \simeq |\vec{p}| + \frac{m_k^2}{2|\vec{p}|}. \quad (3.11)$$

Substituting this expression into (3.10), the transition probability can be written as:

$$P_{\nu_\alpha \rightarrow \nu_\beta}(t) = |\mathcal{A}_{\nu_\alpha \rightarrow \nu_\beta}(t)|^2 = \sum_{k=1}^N U_{\alpha k}^* U_{\beta k} U_{\alpha j} U_{\beta j}^* e^{-i \frac{\Delta m_{kj}^2}{2|\vec{p}|} t}, \quad (3.12)$$

where  $\Delta m_{kj}^2 \equiv m_k^2 - m_j^2$  is the squared-mass difference.

Since in neutrino oscillation experiments the time dependence of the flavor transition probability cannot be followed, whereas the distance  $L$  between the source of the neutrino beam and the detector is a measured quantity, the time dependence is usually replaced with the variable  $L/c$ . For ultra-relativistic neutrinos this means that, in natural units, it is possible to approximate  $t = L$ , so that equation (3.12) becomes:

$$P_{\nu_\alpha \rightarrow \nu_\beta}(L) = \sum_{k=1}^N U_{\alpha k}^* U_{\beta k} U_{\alpha j} U_{\beta j}^* e^{-i \frac{\Delta m_{kj}^2}{2|\vec{p}|} L}. \quad (3.13)$$

The above equation (3.13) shows that the source-detector distance  $L$  and the neutrino energy  $E \simeq |\vec{p}|$  are the experiment-dependent quantities which determine the phases of neutrino oscillations, along with the squared-mass differences  $\Delta m_{kj}^2$ , which are physical constants:

$$\phi_{kj} = \frac{\Delta m_{kj}^2}{2|\vec{p}|} L. \quad (3.14)$$

The amplitude of the oscillations is specified by the elements of the mixing matrix  $U$ , which are constants that can be measured in neutrino oscillation experiments as well as the squared-mass differences. Measurements of neutrino oscillations yield precise information only on the values of the squared-mass differences  $\Delta m_{kj}^2$ , but not on the absolute values of neutrino masses, except a lower bound on  $m_k^2$  or  $m_j^2$ , that must be larger than  $|\Delta m_{kj}^2|$ .

The oscillation probability (3.13) depends on the elements of the mixing matrix  $U$  through the quartic products,  $U_{\alpha k}^* U_{\beta k} U_{\alpha j} U_{\beta j}^*$ , which is independent of the chosen parameterization and rephasing, and this is also the case for Majorana mixing matrices. This rephasing invariance means that the Majorana phases cannot be measured in neutrino oscillation experiments. This is true for any number of generations, so that neutrino oscillations are in general independent of the Majorana phases, which are always factorized in a diagonal matrix on the right of the mixing matrix. Then, eventual CP and T violations in neutrino oscillations can only depend on the Dirac phases.

Taking into account that  $\sum_{k=1, \dots, N} = \sum_{k>j} + \sum_{j>k} + \sum_{k=j}$ , equation (3.13) can be written as:

$$P_{\nu_\alpha \rightarrow \nu_\beta}(L) = \sum_{k=1}^N |U_{\alpha k}|^2 |U_{\beta k}|^2 + 2Re \left[ \sum_{k>j} U_{\alpha k}^* U_{\beta k} U_{\alpha j} U_{\beta j}^* e^{-i \frac{\Delta m_{kj}^2}{2|\vec{p}|} L} \right], \quad (3.15)$$

and using again the unitarity of the mixing matrix  $U$ , the above expression takes the form:

$$\begin{aligned} P_{\nu_\alpha \rightarrow \nu_\beta}(L) = & \delta_{\alpha\beta} - 4 \sum_{k>j} Re [U_{\alpha k}^* U_{\beta k} U_{\alpha j} U_{\beta j}^*] \sin^2 \left( \frac{\Delta m_{kj}^2}{4|\vec{p}|} L \right) \\ & + 2 \sum_{k>j} Im [U_{\alpha k}^* U_{\beta k} U_{\alpha j} U_{\beta j}^*] \sin \left( \frac{\Delta m_{kj}^2}{2|\vec{p}|} L \right). \end{aligned} \quad (3.16)$$

The oscillation probabilities of the channels with  $\alpha \neq \beta$  so far considered are called *transition probabilities*. The oscillation probabilities of the channels with  $\alpha = \beta$  are usually called *survival probabilities* and are given by:

$$P_{\nu_\alpha \rightarrow \nu_\alpha}(L) = 1 - 4 \sum_{k>j} |U_{\alpha k}|^2 |U_{\beta k}|^2 \sin^2 \left( \frac{\Delta m_{kj}^2}{4|\vec{p}|} L \right). \quad (3.17)$$

The transition probability can be conveniently written in terms of the oscillation length,  $L_{kj}^{osc} = 4\pi|\vec{p}|/\Delta m_{kj}^2$ , which measures the distance at which the phase generated by  $\Delta m_{kj}^2$  becomes equal to  $2\pi$ ,

$$P_{\nu_\alpha \rightarrow \nu_\beta}(L) = \sum_{k=1}^N |U_{\alpha k}|^2 |U_{\beta k}|^2 + 2Re \left[ \sum_{k>j} U_{\alpha k}^* U_{\beta k} U_{\alpha j} U_{\beta j}^* e^{-i \frac{2\pi L}{L_{kj}^{osc}}} \right]. \quad (3.18)$$

The oscillating term in the transition probability stems from the interference of the different massive neutrino components of the state (3.6), meaning that its existence depends on the coherence of the massive neutrino components. If different massive neutrinos were produced or detected in an incoherent way, the probability of  $\nu_\alpha \rightarrow \nu_\beta$  would be reduced to the constant term in equation (3.18). The incoherent average of the oscillation probability over the energy resolution of the detector or over the uncertainty of the distance L can also lead to an effectively constant measurable probability which has the same value as the incoherent transition probability. In fact, if the neutrino production-detection distance L has uncertainty much larger than the oscillation lengths  $L_{kj}^{osc}$ , the transition probability (3.18) should be averaged over distances larger than  $L_{kj}^{osc}$  and thus the second term of the r.h.s. of equation (3.18) cancels out, leading to:

$$\langle P_{\nu_\alpha \rightarrow \nu_\beta}(L) \rangle = \sum_{k=1}^N |U_{\alpha k}|^2 |U_{\beta k}|^2. \quad (3.19)$$

An analogous treatment applied to antineutrinos, produced by weak charged current via positive charged lepton transitions  $\bar{l}_\alpha \rightarrow \nu_\alpha$ , pair creation  $l_\alpha \bar{\nu}_\alpha$ , and neutrino-antineutrino pair creation  $\nu_\alpha \bar{\nu}_\alpha$  mediated by weak neutral current, leads to the antineutrino oscillation probability:

$$P_{\nu_\alpha \rightarrow \nu_\beta}(L) = \delta_{\alpha\beta} - 4 \sum_{k>j} Re [U_{\alpha k}^* U_{\beta k} U_{\alpha j} U_{\beta j}^*] \sin^2 \left( \frac{\Delta m_{kj}^2}{4|\vec{p}|} L \right) - 2 \sum_{k>j} Im [U_{\alpha k}^* U_{\beta k} U_{\alpha j} U_{\beta j}^*] \sin \left( \frac{\Delta m_{kj}^2}{2|\vec{p}|} L \right), \quad (3.20)$$

which differs from the neutrino oscillation probability in (3.16) only in the sign of the terms that depend on the imaginary parts of the quartic products

of the mixing matrix elements.

Note that as long as the theory of neutrino oscillations is formulated in the framework of a local quantum field theory, such as the SM and its extensions comprising neutrino masses, the CPT is a symmetry of the oscillation probabilities. This means:

$$P_{\nu_\alpha \rightarrow \nu_\beta}(L) = P_{\bar{\nu}_\beta \rightarrow \bar{\nu}_\alpha}(L). \quad (3.21)$$

As for the CP transformation, this interchanges neutrinos with negative helicity and antineutrinos with positive helicity, transforming the  $\nu_\alpha \rightarrow \nu_\beta$  channel into the  $\bar{\nu}_\alpha \rightarrow \bar{\nu}_\beta$  channel. Since the mixing matrix is, in general, complex and leads to violations of the CP symmetry, such violations can be detected in neutrino oscillation experiments by measuring the CP asymmetry:

$$P_{\nu_\alpha \rightarrow \nu_\beta}(L) - P_{\bar{\nu}_\alpha \rightarrow \bar{\nu}_\beta}(L) = 4 \sum_{k>j} \text{Im} [U_{\alpha k}^* U_{\beta k} U_{\alpha j} U_{\beta j}^*] \sin \left( \frac{\Delta m_{kj}^2}{2|\vec{p}|} L \right). \quad (3.22)$$

The above expression confirms that a CP asymmetry can be measured only in the transitions between different flavors, since for  $\alpha = \beta$  the imaginary parts in equation (3.22) vanish  $\text{Im} [U_{\alpha k}^* U_{\alpha k} U_{\alpha j} U_{\alpha j}^*] = 0$  for any  $k, j$ .

Sterile neutrinos cannot be detected in the standard weak processes. However the unitarity relation,

$$\sum_{\beta} P_{\nu_\alpha \rightarrow \nu_\beta}(t) = \sum_{\beta, k, j} U_{\alpha k}^* U_{\beta k} U_{\alpha j} U_{\beta j}^* e^{-i(E_k - E_j)t} = \sum_k |U_{\alpha k}|^2 = 1, \quad (3.23)$$

can provide information about transitions into sterile states. In fact, equation (3.23) yields:

$$\sum_{\beta=e, \mu, \tau} P_{\nu_\alpha \rightarrow \nu_\beta}(t) = 1 - \sum_{s=s_1, \dots, s_{N_s}} P_{\nu_\alpha \rightarrow \nu_s}(t). \quad (3.24)$$

The left-handed part of this relation is the total transition probability of a flavor neutrino  $\nu_\alpha$  into all possible flavor active neutrinos. This probability can be measured if neutrinos are detected at some distance from the source by the observation of a NC process. If the probability  $\sum_{\beta=e, \mu, \tau} P_{\nu_\alpha \rightarrow \nu_\beta}$  should be less than one this would be a proof of the transition of an active neutrino into sterile states.

## 3.2 Neutrino Oscillations in Matter

In the previous section, it has been shown that for the propagation of massive neutrinos in vacuum, the flavor content of the neutrino beam is determined by the neutrino mass-squared differences  $\Delta m_{kj}^2$  and the elements of the neutrino mixing matrix  $U_{\alpha k}$ . As was first shown by Wolfenstein (Wolfenstein 1978), in the context of neutrino propagation in a medium with constant matter density, the patterns of neutrino oscillations can be significantly affected by the medium. If neutrinos travel through a material medium rather than through the vacuum, along with their masses and mixing also the coherent scattering of neutrinos in matter must be taken into account. In other words, due to the coherent forward elastic scattering with the particles in the medium (electrons and nucleons), neutrinos propagating in matter are subject to a matter-induced potential. This potential, which is equivalent to an index of refraction, modifies the mixing of neutrinos.

In the vacuum, a physical eigenstate can have components of  $\nu_e$ ,  $\nu_\mu$ ,  $\nu_\tau$  and other possible states. When such a state travels through a medium, the modulation of its  $\nu_e$  component is different from the same modulation in the vacuum. This leads to changes in the oscillation probabilities compared to their values in the vacuum. Interactions modify the effective mass of a particle traveling through a medium. Since  $\nu_e$  has different interactions with respect to the other neutrinos, the modification is different for  $\nu_e$  than for the other flavor neutrinos. The reason is that typically the medium comprises electrons but no muons or taus. Thus, if a  $\nu_e$  beam goes through matter, it experiences both charged and neutral current interactions with the electrons. But a  $\nu_\mu$  as well as a  $\nu_\tau$  can interact with the electron only via the neutral current, so that their interaction is different in magnitude than that of the  $\nu_e$ .

In 1985 Mikheev and Smirnov (Mikheev & Smirnov 1985) showed that it is possible to have resonant flavor transitions when neutrinos propagate in a medium with varying density and the existence of a region along their path in which the effective mixing angle passes through the maximal mixing value of  $\pi/4$ . The so-called Mikheev-Smirnov-Wolfenstein (MSW) mechanism, derived from the above-mentioned studies, can explain the flavor conversion of solar neutrinos during their propagation out of the Sun, even in the case of a small vacuum mixing angle. Today it is known that the vacuum mixing angle relevant for solar neutrino oscillations is large but not maximal and that the flavor transitions of solar neutrinos occur through the MSW effect.

Neutrinos in matter are affected not only by coherent forward elastic scattering, but also by incoherent scatterings with the particles in the medium, although in most situations the amount of these incoherent scatterings is



sufficiently small to be neglected.

Let us compute the effect of the coherent forward elastic scattering with the particles in the medium, which does not change the state of the matter, by determining the potential experienced by a neutrino propagating in a homogeneous and isotropic medium. We consider first elastic scattering through charged current interactions. The CC interactions can only involve  $\nu_e$  through the process of elastic scattering on electrons, since there are no  $\mu$ s or  $\tau$ s in the background at the ordinary temperatures of interest. Assuming that the medium consists of a gas of unpolarized electrons, the effective CC Hamiltonian, corresponding to the effective low-energy CC weak interaction Lagrangian (1.17), after a Fierz transformation is given by:

$$\mathcal{H}_{eff}^{CC}(x) = \frac{G_F}{\sqrt{2}} [\bar{\nu}_e(x)\gamma^\mu (1 - \gamma_5) \nu_e(x)] [\bar{e}(x)\gamma_\mu (1 - \gamma_5) e(x)]. \quad (3.25)$$

A gas of unpolarized electrons is described by the density matrix:

$$\rho_e = \int \frac{d^3p_e}{(2\pi)^3} \frac{1}{2E_e} f(E_e) \frac{1}{2} \sum_{h_e=\pm 1} |e^-(p_e, h_e)\rangle \langle e^-(p_e, h_e)|, \quad (3.26)$$

where the function  $f(E_e)$  is the statistical distribution of the electron energy  $E_e$ , which also depends on the temperature of the electron background;  $h_e$  denotes the helicity states and the normalization condition is assumed to be  $\| |e^-(p_e, h_e)\rangle \|^2 = 2E_e$ .

The effective potential induced by the charged current interactions,  $V^{CC}$ , is obtained by averaging (3.25) over the background particle distribution and multiplying by their number density:

$$\begin{aligned} \overline{\mathcal{H}_{eff}^{CC}}(x) &\equiv Tr [\rho_e \mathcal{H}_{eff}^{CC}(x)] = \frac{G_F}{\sqrt{2}} \bar{\nu}_e(x)\gamma^\mu (1 - \gamma_5) \nu_e(x) \int \frac{d^3p_e}{(2\pi)^3} \frac{1}{2E_e} f(E_e) \\ &\times \frac{1}{2} \sum_{h_e=\pm 1} \langle e^-(p_e, h_e) | \bar{e}(x)\gamma_\mu (1 - \gamma_5) e(x) | e^-(p_e, h_e) \rangle. \end{aligned} \quad (3.27)$$

Four-momenta and helicities of the electron states before and after the scattering are identical, because the interaction must leave the medium unchanged in order to contribute coherently to the neutrino potential.

Using ordinary properties of Dirac spinors and gamma matrix traces,

$$\begin{aligned} & \sum_{h_e=\pm 1} \langle e^-(p_e, h_e) | \bar{e}(x) \gamma_\mu (1 - \gamma_5) e(x) | e^-(p_e, h_e) \rangle \\ &= Tr \left[ (\not{p}_e + m_e) \gamma_\mu (1 - \gamma_5) \right] = 4 p_{e\mu}, \end{aligned} \quad (3.28)$$

and the isotropy of the electron background,

$$\int \frac{d^3 p}{(2\pi)^3} f(E_e) \frac{p_{e\mu}}{E_e} = n_e \delta_{0\mu}, \quad (3.29)$$

equation (3.27) becomes:

$$\overline{\mathcal{H}}_{eff}^{CC}(x) = V_{CC} \overline{\nu_{eL}}(x) \gamma^0 \nu_{eL}(x), \quad (3.30)$$

with

$$V_{CC} = \sqrt{2} G_F n_e \quad (3.31)$$

the charged-current effective potential, where:

$$n_e = Tr [\rho_e] = \int \frac{d^3 p_e}{(2\pi)^3} f(E_e), \quad (3.32)$$

is the electron number density.

Similarly, the neutral-current potential of neutrinos propagating in a medium with number density  $n_f$  of fermions  $f$ , can be calculated starting from the effective low-energy NC weak interaction Lagrangian (1.18) and the corresponding NC effective Hamiltonian:

$$\mathcal{H}_{eff}^{NC}(x) = \frac{G_F}{\sqrt{2}} \sum_{e,\mu,\tau} [\overline{\nu_\alpha}(x) \gamma^\mu (1 - \gamma_5) \nu_\alpha(x)] \sum_f \left[ \bar{f}(x) \gamma_\mu (g_V^f - g_A^f \gamma_5) f(x) \right], \quad (3.33)$$

which yields the following NC effective potential, for any flavor neutrino  $\nu_\alpha$ , induced by coherent interactions with fermions  $f$ :

$$V_{NC}^f = \sqrt{2} G_F g_V^f n_f, \quad (3.34)$$

where,  $g_V^f \equiv g_L^f + g_R^f$ .

The total NC effective potential in a typical astrophysical environment, such as the Sun, where the only fermions present are electrons, protons and neutrons, is:

$$V_{NC} = \sum_f V_{NC}^f = \sqrt{2} G_F [g_V^e n_e + g_V^p n_p + g_V^n n_n], \quad (3.35)$$

where,

$$g_V^e = -\frac{1}{2} + 2 \sin^2 \theta_W, \quad (3.36)$$

$$g_V^p = 2 g_V^U + g_V^D = \frac{1}{2} - 2 \sin^2 \theta_W = -g_V^e \quad (3.37)$$

$$g_V^n = g_V^U + 2 g_V^D = -\frac{1}{2}. \quad (3.38)$$

From electrical neutrality it follows that the number density of protons and electrons are equal, so that the NC potentials of protons and electrons cancel each other and only neutrons contribute,

$$V_{NC} = -\frac{1}{2} \sqrt{2} G_F n_n. \quad (3.39)$$

For neutrino wavelength large compared to the typical background inter-particle distance, neutrinos propagation in a medium can be described by introducing a neutrino index of refraction  $n_{(\nu)}$ :

$$n_{(\nu)} = \frac{p_{Med}}{p}, \quad (3.40)$$

where  $p_{Med}$  and  $p$  are the linear momenta in medium and vacuum, respectively, for a given energy  $E = \sqrt{p^2 + m_\nu^2}$ . For relativistic neutrinos  $p_{Med} = p - V_{CC} - V_{NC}$ , which leads to:

$$n_{(\nu)} - 1 = -\frac{1}{p} (V_{CC} + V_{NC}). \quad (3.41)$$

Using the expressions of  $V_{CC}$  for electron neutrinos, and  $V_{NC}$  experienced by all active neutrinos, the effective potential for a generic flavor neutrino can be written as:

$$V_\alpha = V_{CC}\delta_{e\alpha} + V_{NC} = G_F \sqrt{2} \left( n_e \delta_{e\alpha} - \frac{n_n}{2} \right). \quad (3.42)$$

The above potentials  $V_\alpha$  are very small as  $G_F \sqrt{2} \simeq 7.63 \times 10^{-14}$  eV  $cm^3/N_A$ , with  $N_A$  the Avogadro number.

Considering an ultra-relativistic left-handed flavor neutrino with momentum  $\vec{p}$ , described in equation (3.1). The total Hamiltonian in matter is

$$\mathcal{H} = \mathcal{H}_0 + \mathcal{H}_I, \quad (3.43)$$

where  $\mathcal{H}_0$  is the free Hamiltonian, such that:

$$\mathcal{H}_0 |\nu_k\rangle = E_k |\nu_k\rangle \quad \text{with} \quad E_k = \sqrt{|\vec{p}|^2 m_k^2}, \quad (3.44)$$

and  $\mathcal{H}_I$  is the interaction Hamiltonian, which is instead diagonal in the flavor basis:

$$\mathcal{H}_I |\nu_\alpha\rangle = V_\alpha |\nu_\alpha\rangle. \quad (3.45)$$

The evolution of a neutrino, which is initially in the flavor state  $\alpha$ , in the Schrödinger picture is given by:

$$i \frac{d}{dt} |\nu_\alpha(t)\rangle = \mathcal{H} |\nu_\alpha(t)\rangle \quad \text{with} \quad |\nu_\alpha(0)\rangle = |\nu_\alpha\rangle. \quad (3.46)$$

The transition probability for a neutrino born at  $t = 0$  with flavor  $\alpha$  to be found in a flavor state  $\beta$  after a time  $t$  is:

$$P_{\nu_\alpha \rightarrow \nu_\beta} = |\mathcal{A}_{\nu_\alpha \rightarrow \nu_\beta}(t)|^2 \equiv |\langle \nu_\beta | \nu_\alpha(t) \rangle|^2. \quad (3.47)$$

The time evolution equation for the amplitude  $\mathcal{A}_{\nu_\alpha \rightarrow \nu_\beta}(t)$ , analogous to (3.46), can be also written in terms of the distance  $L$  from the source:

$$i \frac{d}{dL} \mathcal{A}_{\nu_\alpha \rightarrow \nu_\beta}(L) = \sum_\rho \left( \sum_k U_{\beta k} E_k U_{\beta k}^\dagger + \delta_{\beta\rho} V_\rho \right) \quad (3.48)$$

Taking into account that the typical energies of neutrinos are much larger

than their masses, the evolution equation in space (3.48) can be written in the relativistic limit (3.11) as:

$$i \frac{d}{dL} \mathcal{A}_{\nu_\alpha \rightarrow \nu_\beta}(L) = \left( |\vec{p}| + \frac{m_1^2}{2|\vec{p}|} + V_{NC} \right) \mathcal{A}_{\nu_\alpha \rightarrow \nu_\beta}(L) + \sum_\rho \left( \sum_k U_{\beta k} \frac{\Delta m_{k1}^2}{2|\vec{p}|} U_{\beta k}^\dagger \delta_{\beta\rho} \delta_{\beta e} V_{CC} \right) \mathcal{A}_{\nu_\alpha \rightarrow \nu_\rho}(L), \quad (3.49)$$

where  $m_1$  is the smallest mass eigenvalue. The term in the first line of equation (3.49) is irrelevant for the flavor transitions, since it generates a phase common to all flavor that can be eliminated by a local the phase shift, leading to:

$$i \frac{d}{dL} \mathcal{A}_{\nu_\alpha \rightarrow \nu_\beta}(L) = \sum_\rho \left( \sum_k U_{\beta k} \frac{\Delta m_{k1}^2}{2|\vec{p}|} U_{\beta k}^\dagger \delta_{\beta\rho} \delta_{\beta e} V_{CC} \right) \mathcal{A}_{\nu_\alpha \rightarrow \nu_\rho}(L). \quad (3.50)$$

The above equation (3.50) shows that neutrino oscillations, both in vacuum and in matter, depend on the differences of the squared neutrino masses and not on the absolute value of neutrino masses.

In matrix form equation (3.50) reads:

$$i \frac{d}{dL} \mathcal{A}_{\nu_\alpha \rightarrow \nu_\beta}(L) = (\mathcal{H}_F)_\beta^\rho \mathcal{A}_{\nu_\alpha \rightarrow \nu_\rho}(L), \quad (3.51)$$

where the effective Hamiltonian matrix  $\mathcal{H}_F$  in the flavor basis has the form:

$$\mathcal{H}_F = \frac{1}{2|\vec{p}|} (U \mathbb{M}^2 U^\dagger + \mathbb{A}), \quad (3.52)$$

with,

$$\mathbb{M}^2 = \begin{pmatrix} 0 & 0 & 0 \\ 0 & \Delta m_{21}^2 & 0 \\ 0 & 0 & \Delta m_{31}^2 \end{pmatrix}, \quad \mathbb{A} = \begin{pmatrix} 2|\vec{p}| V_{CC} & 0 & 0 \\ 0 & 0 & 0 \\ 0 & 0 & 0 \end{pmatrix} \quad (3.53)$$

Note that on the basis of the above evolution equation (3.51), it can be shown that the Majorana phases in the mixing matrix do not affect the effective Hamiltonian  $\mathcal{H}_F$  and hence neutrino oscillations in matter (Langacker et al.

1987), as well as it occurs in vacuum. In fact, the unitary  $3 \times 3$  mixing matrix of Majorana neutrinos, dependent on three mixing angles and three physical CP-violating phases, can be written as a product  $U = U^D D^M$  of a unitary matrix  $U^D$ , with three mixing angles and one phase, analogously to the mixing matrix of Dirac neutrinos, and a diagonal unitary matrix  $D^M$  with two independent phases. The diagonal matrix of Majorana phases  $D^M$  on the right of the mixing matrix  $U$  cancels in the product  $U M^2 U^\dagger$ . This means that the Dirac or Majorana nature of neutrinos cannot be determined in neutrino oscillations in vacuum as in matter.

### 3.2.1 The MSW effect

The above discussion is referred to the case of three-neutrino mixing, for the sake of simplicity in what follows we consider the case of two neutrino mixing. Namely, the mixing between an electron neutrino and a  $\nu_\mu$  or  $\nu_\tau$ . If one wants to consider the mixing with a sterile neutrino  $\nu_e - \nu_s$ , one needs to replace  $V_{CC} \rightarrow V_{CC} + V_{NC}$ , which corresponds to the replacement  $N_e \rightarrow N_e - N_n/2$ , since sterile states have no weak currents interactions and the resonant condition is expected to involve both electron and neutron number densities.

Since  $\nu_\mu$  and  $\nu_\tau$  have the same matter-induced potential, the two cases of mixing  $\nu_e \rightarrow \nu_\mu$  and  $\nu_e \rightarrow \nu_\tau$  are equivalent. For definiteness we consider the  $\nu_e$  and  $\nu_\mu$  bi-dimensional space, and two corresponding mass eigenstates  $\nu_1$  and  $\nu_2$ . In this case  $\mathcal{H}_F$  reduces to the following  $2 \times 2$  hermitian matrix:

$$\begin{aligned} \mathcal{H}_F = & \frac{1}{4|\vec{p}|} (\Delta m^2 + 2|\vec{p}|V_{CC}) \mathbb{1} \\ & + \frac{1}{4|\vec{p}|} \begin{pmatrix} -\Delta m^2 \cos 2\theta + 2|\vec{p}|V_{CC} & \Delta m^2 \sin 2\theta \\ \Delta m^2 \sin 2\theta & \Delta m^2 \cos 2\theta - 2|\vec{p}|V_{CC} \end{pmatrix}, \end{aligned} \quad (3.54)$$

where  $\Delta m^2 \equiv m_2^2 - m_1^2$  and  $\theta$  is the mixing angle:

$$\begin{aligned} |\nu_e\rangle &= \cos \theta |\nu_1\rangle + \sin \theta |\nu_2\rangle \\ |\nu_\mu\rangle &= -\sin \theta |\nu_1\rangle + \cos \theta |\nu_2\rangle. \end{aligned} \quad (3.55)$$

Neglecting the term proportional to the identity operator in the first line of equation (3.54), the second term can be diagonalized by the orthogonal transformation:

$$U_M^T \mathcal{H}_F U_M \quad (3.56)$$

with

$$\mathcal{H}_F = \frac{1}{4|\vec{p}|} \text{diag}(-\Delta m_M^2, \Delta m_M^2), \quad (3.57)$$

the in-medium effective Hamiltonian matrix in the mass basis and

$$U_M = \begin{pmatrix} \cos \theta_M & \sin \theta_M \\ -\sin \theta_M & \cos \theta_M \end{pmatrix}, \quad (3.58)$$

the unitary matrix which represents the effective mixing matrix in matter.

The in-medium effective mixing angle  $\theta_M$  is given by:

$$\tan 2\theta_M = \frac{\tan 2\theta}{1 - \frac{2|\vec{p}|V_{CC}}{\Delta m^2 \cos 2\theta}}, \quad (3.59)$$

whereas the effective squared-mass difference is

$$\Delta m_M^2 = \sqrt{(\Delta m^2 \cos 2\theta - 2|\vec{p}|V_{CC})^2 + (\Delta m^2 \sin 2\theta)^2}. \quad (3.60)$$

The interesting phenomenon, discovered by Mikheev and Smirnov is that the evolution equation shows a resonance when

$$\Delta m^2 \cos 2\theta = 2|\vec{p}|V_{CC}. \quad (3.61)$$

Inserting the expression of  $V_{CC}$  (3.31) in the above equation (3.61) provides the electron number density corresponding to the resonance:

$$n_e^R = \frac{\Delta m^2 \cos 2\theta}{2\sqrt{2}G_F|\vec{p}|}. \quad (3.62)$$

At the resonance the effective mixing angle is maximal,  $\theta_M = \pi/4$ , which means that the transitions from one flavor to the other may even be total if the resonance region is wide enough. This mechanism, called MSW effect, plays a significant role in astrophysical environments, such as the Sun and type II supernovae, where the matter density radial profile can provide the proper condition for a resonant conversion.

When the resonance condition is satisfied, the oscillation length in matter can also be significantly different from the oscillation length in vacuum:

$$L_M^{osc} = \frac{L^{osc}}{\sin 2\theta} \quad (3.63)$$

### 3.3 Neutrino Oscillations Experiments

Neutrino flavor oscillation experiments can be classified in two types. The *appearance experiments* measure transitions between different neutrino flavors in which the final flavor to be observed is absent in the original beam. In this case the background can be very small and the experiment can be sensitive to rather small values of the mixing angle. These experiments look for enhancement of the flux of a specific flavor, when the distance  $L$  is far from any integer multiple of all the  $L_{kj}^{osc}$ , which means that a positive detection requires:

$$P_{\alpha\beta}(L) > 0. \quad (3.64)$$

The *disappearance experiments* measure the depletion of neutrinos of a particular flavor. This is performed considering the survival probability of a neutrino flavor by means of comparison between the number of interactions in the detector and the expected one:

$$P_{\alpha\alpha}(L) < 1. \quad (3.65)$$

Taking into account that the number of detected events has statistical fluctuations, even in the absence of oscillations, a small depletion is very difficult to detect, meaning that small values of the mixing angle are difficult to measure through this kind of experiments. The appearance experiments might seem much simpler than those of disappearance, as the observation of even a single event would provide evidence of neutrino oscillation, whereas a disappearance experiment requires the observation of a significant deviation of a certain probability from unity. However this is not the case because an appearance experiment can only search for a specific channel, say a  $\nu_\mu$  oscillating to a  $\nu_e$ . If  $\nu_\mu$  mixes very little with  $\nu_e$  but very strongly with some other state, the  $\nu_\mu \rightarrow \nu_e$  appearance experiment would be somewhat negative. While in a disappearance experiment on a  $\nu_e$  beam, observable effects are independent of whether the  $\nu_e$  oscillates to  $\nu_\mu$  or  $\nu_\tau$ , or to anything else.

As previously mentioned, many models of neutrino mass predict right-handed neutrinos which do not have interactions mediated by the gauge bosons of the SM. Suppose that the  $\nu_e$ , for example, mixes significantly with



one of these sterile neutrinos. In this case an appearance experiment would be useless, since the cross section for the production of a charged lepton must be extremely small if a sterile neutrino is involved, whereas a disappearance experiment can still register a depletion in the probability of a  $\nu_e$  beam. This means that an appearance experiment measures oscillations  $\nu_\alpha \rightarrow \nu_\beta$  specifically for active neutrinos, whereas a disappearance experiment is sensitive to  $\nu_\alpha \rightarrow \nu_x$  oscillations where  $\nu_x$  can be any flavor state, including the sterile ones.

Let us briefly review the experiments of neutrino oscillations which have primarily proven that neutrinos have small masses and that the flavor neutrinos  $\nu_e, \nu_\mu, \nu_\tau$  are “mixed particles”.

Neutrino oscillations experiments started in the late 1960s with the Homestake solar neutrino radiochemical experiment by Davis and Bahcall (Davis 1964; Davis et al. 1968). In this experiment, the observed rate of solar  $\nu_e$  was found to be significantly smaller than the rate predicted by the Standard Solar Model (SSM). This discrepancy was called the solar neutrino problem. The second solar neutrino experiment Kamiokande, performed in the eighties, was a direct-counting experiment for which it was used a large water-Cherenkov detector. The solar neutrino rate measured by the Kamiokande experiment was lower than the rate predicted by the SSM, confirming the previous experimental results (Fukuda et al. 1996).

In the Homestake and Kamiokande experiments the flux of high-energy solar neutrinos is about  $10^{-4}$  of the total solar neutrino flux and its predicted value strongly depends on the model. In the nineties, the new radiochemical solar neutrino experiments SAGE and GALLEX searched for neutrinos from all reactions of the proton-proton and CNO cycles, including low-energy neutrinos from the reaction  $pp \rightarrow de^+ \nu_e$ . This reaction gives the largest contribution to the flux of the solar neutrinos and the flux of the  $p-p$  neutrinos can be predicted in a practically model-independent way. The event rates measured in the SAGE and GALLEX experiments were about two times smaller than the predicted rates (Hampel et al. 1999; Abdurashito et al. 1999). These experiments provided evidence in favor of the disappearance of solar  $\nu_e$  on the path from the central region of the sun, where solar neutrinos are produced, to the earth, whereas no indications in favor of neutrino oscillations were found in the eighties and nineties in numerous reactor and accelerator short baseline experiments.

In 1998 in the water-Cherenkov Super-Kamiokande experiment a significant up-down asymmetry of the high-energy atmospheric muon neutrino events was observed. To be specific, this experiment found out that the number of up-going high-energy muon neutrinos passing through the earth is

about two times smaller than the number of the down-going muon neutrinos coming directly from the atmosphere (Fukuda et al. 1998).

Previous indications in favor of a disappearance of solar  $\nu_e$  became model-independent evidence in 2002 when the solar neutrino experiment SNO detected solar neutrinos through the observation of CC and NC reactions (Ahmad et al. 2002). It was shown that the flux of the solar  $\nu_e$  is approximately three times smaller than the flux of  $\nu_e$ ,  $\nu_\mu$  and  $\nu_\tau$ . In the same year in the KamLAND reactor neutrino experiment it was found that the number of reactor  $\bar{\nu}_e$  events at the average distance of  $\sim 170$  km from the reactors is about 0.6 of the number of the expected events (Eguchi et al. 2003). Subsequently it was also observed a significant distortion of the  $\bar{\nu}_e$  spectrum in the experiment. The SNO and Super-Kamiokande results have found confirmation in another solar neutrino experiment based on time and energy dependent rates, Borexino (Bellini, et al. 2010). Neutrino oscillations have been observed also in the accelerator long-baseline experiments K2K (Abe, et al. 2014) and MINOS (Adamson et al. 2011), which confirmed the results obtained in the atmospheric Super-Kamiokande experiment.

The accelerator short-baseline LSND experiment, projected to look for evidence of neutrino oscillations, produced results at odds with the SM expectation, when considered in the context of the observations in solar and atmospheric neutrino oscillation experiments. The observed anomaly could be explained through the existence of an additional sterile neutrino (Athanasopoulos et al. 1985). The KARMEN and MiniBooNE experiments have partially confirmed the LSND appearance result (Church et al. 2002; Conrad et al. 2013). The most favored allowed region for the mass-squared difference appears to be the band from  $0.2 - 2.0 eV^2$ , although a region around  $7 eV^2$  might also be possible.

### 3.3.1 Three-Neutrino Mixing

Solar and atmospheric neutrino experiments have shown that neutrinos oscillate with two different squared-mass differences,  $\Delta m_{SOL}^2$  and  $\Delta m_{ATM}^2$ , respectively. This has found confirmation in the results of the independent measurements performed in terrestrial KamLAND and K2K experiments. The possibility of two independent squared-mass differences can be realized in three-neutrino mixing schemes. Although in the case of three-neutrino mixing there are three squared-mass differences only two of them are independent, since  $\Delta m_{32}^2 + \Delta m_{21}^2 - \Delta m_{31}^2 = 0$ , meaning that the observed hierarchy:

$$\Delta m_{SOL}^2 \ll \Delta m_{ATM}^2, \quad (3.66)$$

can be arranged in the two types of three-neutrino mixing schemes, named normal and inverted hierarchy. Although the absolute neutrino mass scale is not known, we have information on the squared-mass differences from experiments. It is then possible to express the neutrino masses as functions of only one unknown parameter, representing the absolute mass scale, which is conveniently chosen as the value of the lightest mass, that is  $m_1$  in the normal scheme and  $m_3$  in the inverted scheme. In particular, in the normal scheme we have:

$$m_2^2 = m_1^2 + \Delta m_{21}^2 = m_1^2 + \Delta m_{SOL}^2 \quad (3.67)$$

and

$$m_3^2 = m_1^2 + \Delta m_{31}^2 = m_1^2 + \Delta m_{ATM}^2 \quad (3.68)$$

whereas in the inverted scheme:

$$m_1^2 = m_3^2 - \Delta m_{31}^2 = m_3^2 + \Delta m_{ATM}^2 \quad (3.69)$$

and

$$m_2^2 = m_1^2 + \Delta m_{21}^2 = m_3^2 + \Delta m_{ATM}^2 + \Delta m_{SOL}^2. \quad (3.70)$$

Following the global analysis and notations in (Gonzalez-Garcia et al. 2015) we summarize the main results of neutrino oscillations experiments. Disappearance of solar  $\nu_e$ s and long baseline reactor  $\bar{\nu}_e$ s proceeds mainly via oscillations with wavelength  $\propto E/\Delta m_{21}^2$  (with  $\Delta m_{21}^2 > 0$  by convention) and amplitudes controlled by  $\theta_{12}$ . Disappearance of atmospheric and LBL accelerator  $\nu_\mu$ s instead proceeds mainly via oscillations with wavelength  $\propto E/|\Delta m_{31}^2| \ll E/\Delta m_{21}^2$  and amplitudes controlled by  $\theta_{23}$ . The angle  $\theta_{13}$  controls the amplitude of oscillations involving  $\nu_e$  flavor with  $E/|\Delta m_{31}^2|$  wavelengths. Given the observed hierarchy between the solar and atmospheric wavelengths there are two possible non-equivalent orderings for the mass eigenvalues,

$$\Delta m_{21}^2 \ll \Delta m_{32}^2 \simeq \Delta m_{31}^2 > 0, \quad (3.71)$$

which corresponds to the so-called Normal Hierarchy (NH), and

$$\Delta m_{21}^2 \ll -(\Delta m_{31}^2 \simeq \Delta m_{32}^2 > 0), \quad (3.72)$$

which in the above form corresponds to the opposite choice of the sign, labeled as Inverted Hierarchy (NH).

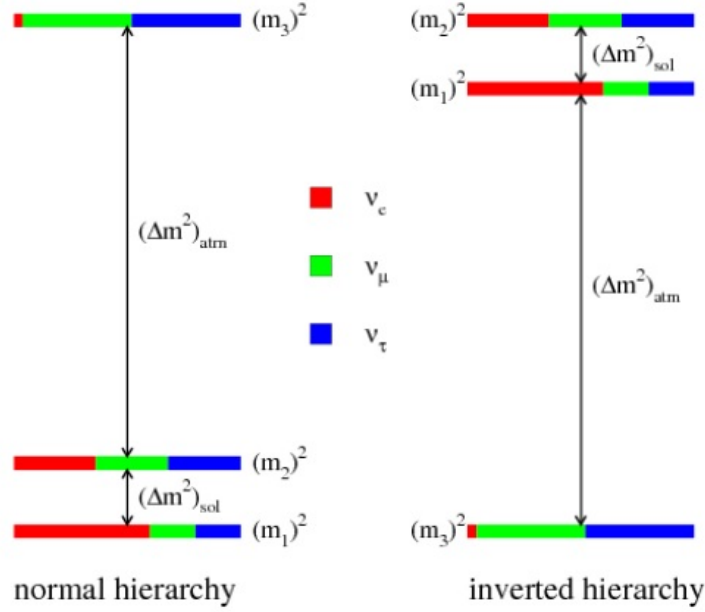


Figure 3.1: Normal and Inverted Hierarchy.

The three-neutrino oscillation analysis of the available data involves six parameters: 2 mass differences (one of which can be positive or negative), 3 mixing angles, and the CP phase  $\delta_{CP}$ . The determination of these parameters requires a global analysis of the data. In Table 3.1 we recollect the main results (see Gonzalez-Garcia et al. 2015 and references therein for a detailed survey), the corresponding best fit values and the derived ranges for the six parameters at the  $1\sigma$  ( $3\sigma$ ) level. The results in the table are shown for three scenarios: Normal or Inverted Hierarchy and with no assumption of the order. In the first and second columns the hierarchy of the neutrino mass states is known “a priori” to be Normal or Inverted, respectively. In the third column no assumptions is made on the mass hierarchy. For this third case only the  $3\sigma$  intervals are given. In this case the range of  $\Delta m_{3l}^2$ , where  $l = 1$  for NH and  $l = 2$  for IH, is composed of two disconnected intervals, one containing the absolute minimum (IH) and the other the secondary local minimum (NH).

	Normal Hierarchy		Inverted Hierarchy		Any Hierarchy
	bfp $\pm 1\sigma$	$3\sigma$ range	bfp $\pm 1\sigma$	$3\sigma$ range	$3\sigma$ range
$\theta_{12}/^\circ$	$33.438^{+0.78}_{-0.75}$	$31.29 \rightarrow 35.91$	$33.438^{+0.78}_{-0.75}$	$31.29 \rightarrow 35.91$	$31.29 \rightarrow 35.91$
$\theta_{23}/^\circ$	$42.3^{+3.0}_{-1.6}$	$38.2 \rightarrow 53.34$	$49.5^{+1.5}_{-2.2}$	$38.6 \rightarrow 53.3$	$38.3 \rightarrow 53.3$
$\theta_{13}/^\circ$	$8.50^{+0.20}_{-0.21}$	$7.85 \rightarrow 9.10$	$8.51^{+0.20}_{-0.21}$	$7.87 \rightarrow 9.11$	$7.87 \rightarrow 9.11$
$\delta_{CP}/^\circ$	$306^{+39}_{-70}$	$0 \rightarrow 360$	$254^{+63}_{-62}$	$0 \rightarrow 360$	$0 \rightarrow 360$
$\frac{\Delta m_{21}^2}{10^{-5}eV^2}$	$7.50^{+0.19}_{-0.17}$	$7.02 \rightarrow 7.09$	$7.50^{+0.19}_{-0.17}$	$7.02 \rightarrow 7.09$	$7.02 \rightarrow 7.09$
$\frac{\Delta m_{3l}^2}{10^{-3}eV^2}$	$2.457^{+0.0479}_{-0.047}$	$2.317 \rightarrow 2.607$	$2.449^{+0.0479}_{-0.047}$	$-2.590 \rightarrow -2.307$	$\left[ \begin{array}{l} +2.325 \rightarrow +2.599 \\ -2.590 \rightarrow -2.307 \end{array} \right]$

Table 3.1: Three-flavor oscillations parameters from the fit to global data in (Gonzalez-Garcia et al. 2015). The values in the first and second column are obtained assuming NH and IH, i.e., relative to the respective local minimum, whereas in the third column no ordering is assumed. Note that  $\Delta m_{3l}^2 \equiv \Delta m_{31}^2 > 0$  for NH and  $\Delta m_{3l}^2 \equiv \Delta m_{32}^2 < 0$  for IH.

All the data from oscillation experiments presented above can be consistently interpreted within a three-flavor active neutrinos scheme with non zero mixing. However, as already mentioned, in addition to these data, several anomalies at short baselines (SBL) have been observed which cannot be explained in the framework of 3  $\nu$  oscillations. Such results could be interpreted as oscillations involving an O(eV) mass sterile state, assuming that neutrino oscillations may account for all the experimental data. This issue will be discussed in Section 3.3.2.

### 3.3.2 Extended Neutrino Oscillation Scenarios

Although the three-flavor neutrino oscillations is a phenomenologically well established framework, the anomalies observed in LSND, MiniBooNE, Gallium solar neutrino experiments, and some reactor experiments (Achkar et al. 1995) cannot be explained within that context. The possible existence of additional sterile neutrinos with masses at the eV scale has provided a viable solution to the observed anomalies as ascribable to oscillations between active and sterile neutrinos. In the following we will give a brief overview of the anomalies observed in neutrino experiments and the extended schemes, comprising four or more light neutrinos, that could explain them. A more detailed review of this subject can be found in (Kopp et al. 2013; Conrad et al. 2013; Abazajian et al. 2012). The observed anomalies can be summarized

as follows:

- evidence in the LSND experiment for  $\bar{\nu}_\mu \rightarrow \bar{\nu}_e$  transitions with  $E/L \sim 1 \text{ eV}^2$ , where E and L are the neutrino energy and the distance between source and detector, respectively;
- the MiniBooNE experiment searched for the same effect. The result is the observation of a yet unexplained event excess in the low-energy region of the electron neutrino and anti-neutrino event spectra. No significant excess is found at higher neutrino energies. Interpreting the data in terms of oscillations, the parameter values obtained are consistent with those from LSND;
- an event rate lower than expected in radioactive source experiments at the Gallium solar neutrino experiments SAGE and GALLEX (“Gallium anomaly”). Possible explanation of the observed effect is the hypothesis of  $\nu_e$  disappearance due to oscillations with  $\Delta m^2 \gtrsim 1 \text{ eV}^2$  (Giunti & Laveder 2011);
- observations in SBL ( $L \lesssim 100 \text{ m}$ ) reactor experiments are not in agreement with calculations of the neutrino flux emitted by nuclear reactors (Mueller et al. 2011) which predict a neutrino rate a few percent higher than observed. A decreased rate at those distances can be explained by assuming  $\bar{\nu}_e$  disappearance due to oscillations with  $\Delta m^2 \sim 1 \text{ eV}^2$  (“reactor anomaly”).

Note that one important reason for tension in the global data including the LSND results is the non-observation of  $\nu_\mu$  disappearance at the eV-scale, which is a generic prediction related to a possible explanation of the LSND signal in terms of sterile neutrino oscillations. However, even if the LSND signal is discarded, indications for the existence of sterile neutrinos from the reactor and Gallium anomalies remain. Such indications are related to  $\bar{\nu}_e$  disappearance and do not require  $\nu_\mu$  disappearance.

Here we resume the results of a global analysis (Kopp et al. 2013; Gonzalez-Garcia et al. 2015) of those data under the hypothesis of additional neutrino species at the eV scale. A 3+1 mass scheme requires the introduction of a neutrino state,  $\nu_4$ , with a mass-squared difference  $\Delta m_{41}^2$  much larger than  $|\Delta m_{31}^2|$ . In this case the oscillation probabilities for experiments surveying the range  $E/L \sim 1 \text{ eV}^2$  are given by:

$$P_{\alpha\alpha} = 1 - \sin^2 2\theta_{\alpha\alpha} \sin^2 \left( \frac{\Delta m_{41}^2 L}{4E} \right) \quad (3.73)$$

$$P_{\mu e} = \sin^2 2\theta_{\mu e} \sin^2 \left( \frac{\Delta m_{41}^2 L}{4E} \right), \quad (3.74)$$

with  $E \simeq |\vec{p}|$  and the effective mixing angles defined as:

$$\sin^2 2\theta_{\alpha\alpha} \equiv 4 |U_{\alpha 4}|^2 (1 - |U_{\alpha 4}|^2) \quad (3.75)$$

$$\sin^2 2\theta_{\mu e} \equiv 4 |U_{\mu 4}|^2 |U_{e 4}|^2, \quad (3.76)$$

where  $\alpha = e, \mu$  and  $U_{\alpha 4}$  are the elements of the mixing matrix describing the mixing of the 4th neutrino mass state with the electron and muon flavor.

There is no CP violation in 3+1 SBL oscillations and the same relations hold for both neutrinos and antineutrinos. Neglecting quadratic terms in the mixing matrix elements yields the following relation between the effective amplitudes relevant for appearance and disappearance probabilities:

$$4 \sin^2 2\theta_{\mu e} \approx \sin^2 2\theta_{ee} \sin^2 2\theta_{\mu\mu}. \quad (3.77)$$

The tension in the global data and equation (3.77) makes it difficult to obtain a good fit to all available data, hence first is considered the global data including SBL anomalies related to  $\bar{\nu}_e$  and  $\nu_e$  disappearance (reactor and Gallium anomalies), ignoring the  $\nu_\mu \rightarrow \nu_e$  and  $\bar{\nu}_\mu \rightarrow \bar{\nu}_e$  appearance anomalies (LSND and MiniBooNE). In this case, the SBL phenomenology is determined by the two parameters  $\Delta m_{41}^2$  and  $U_{e4}$  for which a consistent region not in conflict with any other data is found. The best fit point occurs at  $\sin^2 2\theta_{ee} = 0.09$  and  $\Delta m_{41}^2 = 1.78 \text{ eV}^2$ , while the no-oscillation hypothesis for the eV-scale is excluded at 3.1  $\sigma$ .

Consider now the question whether the hints for  $\nu_e$  disappearance can be reconciled with the appearance hints from LSND and MiniBooNE. Given the relation in equation (3.77) between those appearance signals to disappearance in the  $\nu_e$  and  $\nu_\mu$  channels, since so far no positive signal has been observed in  $\nu_\mu$  disappearance, several experiments set bounds on the relevant mixing parameter  $U_{\mu 4}$ . The combined limits on  $\nu_\mu$  and  $\nu_e$  mixing with the eV-scale mass state  $\nu_4$  lead to a tension between appearance signals and disappearance data in the 3+1 scheme. This seems to indicate that extending the standard model by adding one sterile neutrino state with a mass at the eV scale (3+1) could be not sufficient to well describe all data. This leads to consider whether any improvement could be achieved by introducing more

neutrino states at the eV scale, namely, adding two states with eV scale mass splittings,  $\nu_4$  and  $\nu_5$ , that can be arranged so that  $\Delta m_{41}^2$  and  $\Delta m_{51}^2$  are both positive (“3+2”) or one of them is negative (“1+3+1”). The new interesting feature in such 5-neutrino schemes is CP violation at the  $E/L \sim eV^2$  scale which introduces some freedom in fitting neutrino versus anti-neutrino data from LSND and MiniBooNE together. However, the main prediction from the 4-neutrinos case remains valid also for 5-neutrinos. In fact, a non-zero  $\nu_\mu \rightarrow \nu_e$  appearance at SBL necessarily predicts SBL disappearance for  $\nu_e$  and  $\nu_\mu$ . Thus, the tension between appearance and disappearance data remains significant even in the 5-neutrinos case. The best fit points for the two scenarios are summarized in Table 3.2.

	$\Delta m_{41}^2 [eV^2]$	$ U_{e4} $	$\Delta m_{51}^2 [eV^2]$	$ U_{e5} $
3+1	1.78	0.151		
3+2	0.46	0.108	0.89	0.124

Table 3.2: Best fit points for the 3+1 and 3+2 scenarios from reactor antineutrino data.

### 3.4 Density Matrix Formalism and Kinetic Equation for Mixed Neutrinos

Neutrino interactions with matter play an important role in determining the nucleosynthesis outcome in explosive astrophysical environments such as core-collapse supernovae or mergers of compact objects, as well as in the formation of light nuclei in the early universe. Along with interactions with matter, an important feature is the quantum phenomenon of neutrino flavor oscillations. As neutrinos with different flavors interact differently with matter, any mechanism that alters the flavor of neutrinos after their production can affect the prediction of the matter property and the outcome of the nucleosynthesis. To first order of a perturbation expansion, a modification of the neutrino dispersion relation leads to the effect of resonant neutrino oscillations indicated as a solution of the solar neutrino problem. To second order, neutrinos are scattered, absorbed, or produced by the medium. Therefore, they play an important thermal and dynamical role in certain phases of stellar evolution, in particular in supernovae, and in the early universe. The first-order (or refractive) effects are usually treated on the amplitude level in the form of a Schrödinger equation for the single-particle wave functions for the mixing flavors. While the second-order effects are treated in the form of a kinetic equation, that is, a differential equation for the occupation numbers of



the neutrino field modes that involves a Boltzmann collision integral. These two approaches cannot account for a situation where neutrino oscillations and collisions are both important, as is the case in the early universe and in a supernova core immediately after collapse where the electron neutrinos differently from the other flavors have a large chemical potential. In this case, the action of oscillations and collisions could lead to flavor equilibrium, i.e. to identical chemical potentials for some or all neutrino flavors. In this environment, sterile neutrinos production and possible active-sterile neutrino mixing could also play an important role to be accounted for. A systematic unification of the first- and second-order interaction effects in a single self-consistent equation and the derivation of a general Boltzmann-type collision integral for mixed neutrinos interacting with each other and with a medium is achieved in Refs. (Raffelt et al. 1993; Raffelt & Sigl 1993). This collision integral allows to account for the simultaneous effects of neutrino oscillations in a medium and for the effects of collisions.

The density matrix formalism is the appropriate tool to describe time-dependent vacuum and matter terms, mixed quantum states of neutrinos and possible loss of coherence due to real collisions in the primordial plasma. Unmixed neutrinos are usually studied by means of a kinetic equation for the evolution of particle and antiparticle occupation numbers. In order to generalize this approach for mixed neutrinos in the framework of field theory we consider the momentum expansion of the left-handed massless neutrino field:

$$\psi_L(x) = \int \frac{d^3\mathbf{p}}{(2\pi)^3} \left( a_{\mathbf{p}}(t)u_{\mathbf{p}} + b_{-\mathbf{p}}^\dagger v_{-\mathbf{p}} \right) e^{i\mathbf{p}\cdot\mathbf{x}}, \quad (3.78)$$

where  $a_{\mathbf{p}}$  is the annihilation operator for negative-helicity neutrinos of momentum  $\mathbf{p}$  and  $b_{-\mathbf{p}}^\dagger$  is the creation operator for positive-helicity antineutrinos. The Dirac spinors  $u$  and  $v$ , which refer to massless negative-helicity particles and positive-helicity antiparticles, are taken normalized to unity.

For  $n$  flavors  $a_{\mathbf{p}}$  and  $b_{-\mathbf{p}}^\dagger$  are column vectors of  $n$  particle annihilators  $a_i(\mathbf{p})$  and antiparticle creators  $b_i^\dagger(\mathbf{p})$ , respectively, which satisfy the anticommutation relations  $\{a_i(\mathbf{p}), a_j^\dagger(\mathbf{p}')\} = \{b_i(\mathbf{p}), b_j^\dagger(\mathbf{p}')\} = \delta_{ij} (2\pi)^3 \delta^{(3)}(\mathbf{p} - \mathbf{p}')$ . The only bilinears needed to describe the neutrino ensemble are the slowly-varying density operators  $a_{\mathbf{p}}^\dagger a_{\mathbf{p}'}$  and  $b_{\mathbf{p}}^\dagger b_{\mathbf{p}'}$ , since the other bilinears either violate the lepton number by two units or can be ignored because their expectation values oscillate rapidly around zero. Making the additional assumption of spatial homogeneity, the expectation value of every physical observable con-

structed from the field  $\psi$  is independent of location and contributes only for equal momenta  $\mathbf{p} = \mathbf{p}'$ . Therefore, a homogeneous neutrino ensemble is completely characterized by the dimensionless  $n \times n$  density matrices,  $\rho_{\mathbf{p}}(t)$  and  $\bar{\rho}_{\mathbf{p}}(t)$ , respectively for neutrinos and antineutrinos:

$$\langle a_j(\mathbf{p}) a_i^\dagger(\mathbf{p}') \rangle = (2\pi)^3 \delta^{(3)}(\mathbf{p} - \mathbf{p}') (\rho_{\mathbf{p}})_{ij} \quad (3.79)$$

$$\langle b_i(\mathbf{p}) b_j^\dagger(\mathbf{p}') \rangle = (2\pi)^3 \delta^{(3)}(\mathbf{p} - \mathbf{p}') (\bar{\rho}_{\mathbf{p}})_{ij}, \quad (3.80)$$

where the reversed order of the flavor indices in equation (3.80) guarantees that both density matrices transform in the same way under a unitary transformation in flavor space,  $\psi' = U\psi$ . The diagonal elements of  $\rho_{\mathbf{p}}$  and  $\bar{\rho}_{\mathbf{p}}$  are the ordinary particle and antiparticle occupation numbers, whereas the off-diagonal elements represent correlations between the mixing flavors, hence they vanish for zero mixing. This means that for a homogeneous ensemble of mixed neutrinos these matrices are the appropriate generalization of the occupation numbers and it is sufficient to study the time evolution of  $\rho_{\mathbf{p}}$  and  $\bar{\rho}_{\mathbf{p}}$ , which is given by:

$$i \dot{\rho}_{\mathbf{p}} = [\Omega_{\mathbf{p}}^0, \rho_{\mathbf{p}}] + [\Omega_{\mathbf{p}}^{int}, \rho_{\mathbf{p}}] + \mathbf{C} [\rho_{\mathbf{p}}, \bar{\rho}_{\mathbf{p}}] \quad (3.81)$$

where the first term on the r.h.s. describes oscillations in vacuum:

$$\Omega_{\mathbf{p}}^0 = \frac{M^2}{2|\vec{p}|} \quad (3.82)$$

with  $M$  the neutrino mass matrix, diagonal in the mass basis. An equation analogous to (3.81) can be written for the antineutrino  $\bar{\rho}_{\mathbf{p}}$ , with  $\bar{\Omega}_{\mathbf{p}}^0 = -\Omega_{\mathbf{p}}^0$ .

As for the matter-induced potential term, this is defined as:

$$\Omega_{\mathbf{p}}^{int} = \sqrt{2}G_F \left[ L - \frac{8p}{3m_W^2} E \right] + \sqrt{2}G_F \left[ \rho - \bar{\rho} - \frac{8p}{3m_Z^2} (\mathbf{U} + \bar{\mathbf{U}}) \right] \quad (3.83)$$

$$\bar{\Omega}_{\mathbf{p}}^{int} = \sqrt{2}G_F \left[ L + \frac{8p}{3m_W^2} E \right] + \sqrt{2}G_F \left[ \rho - \bar{\rho} + \frac{8p}{3m_Z^2} (\mathbf{U} + \bar{\mathbf{U}}) \right], \quad (3.84)$$

where the first two terms correspond to the matter potentials felt by neutrinos in a background of charged leptons. Both are diagonal matrices in

the interaction basis, one proportional to the difference  $L$  of number densities of flavor- $k$  leptons and the other to the sum  $E$  of energy densities of charged leptons and antileptons of flavor  $k$ . Since  $L$  is proportional to the asymmetry, the second kind of terms are dominant at high temperatures (in the early universe the number of baryons and antibaryons were almost equal, with present baryon asymmetry fixed by observations to the value  $\eta_B = (n_B - n_{\bar{B}})/n_\gamma \sim 6 \times 10^{-10}$ . Charge neutrality implies that the electron and proton densities should be equal, meaning that the first-order matter effect of the  $L$  term does not dominate at MeV temperatures). The last two terms are the refractive contributions of background neutrinos, caused by neutrino self-interactions, and depend on the the number and energy density of the interacting neutrino type:

$$\rho = \int \frac{d^3\mathbf{p}}{(2\pi)^3} \rho_{\mathbf{p}} \quad \mathbf{U} = \int \frac{d^3\mathbf{p}}{(2\pi)^3} |\mathbf{p}| \rho_{\mathbf{p}}, \quad (3.85)$$

with  $p_0 = |\mathbf{p}|$ , the energy of a neutrino mode. The analogous of the above definitions for antineutrinos only needs the replacement of the density matrix for the antiparticle. These matter terms caused by neutrino self-interactions can have non diagonal elements in the flavor basis, which can lead to unexpected behavior of neutrino transitions in media where the neutrino density is large. In particular, when cosmological flavor asymmetries of neutrinos are considered. The above terms are also quite important in media with high density such as Type-II supernovae.

Note that in equations (3.83) (3.84) the diagonal components of  $L$  and  $E$  vanish in the corresponding entries for sterile neutrino states. Zeroes appear in the last contributions also, whenever either of the two flavor indices in  $\rho_{ij}$  corresponds to a sterile neutrino state.

In general, the backreaction on the medium of neutrinos evolution cannot be neglected. In special cases it is possible, however, to regard the medium as an external heat bath, whose properties remain unaffected by the evolution of the neutrino ensemble, so that the medium may be thought of as absorbing or producing energy and lepton number without changing its temperature or chemical potentials. In equilibrium, neutrinos will take on the same temperature  $T$  while all mixing flavors will be characterized by the same chemical potential  $\mu$ . For a medium of nucleons and charged leptons, this would be  $\mu = \mu_1 + \mu_p - \mu_n$ . Studying the approach to thermal equilibrium, allowing for the violation of individual flavor lepton numbers by neutrino oscillations, it can be assumed that the medium is characterized by chemical potentials for the charged leptons which are identical,  $\mu_1 \equiv \mu_e = \mu_\mu = \mu_\tau$ . This require-

ment does not apply when considering oscillations between an active species  $\nu_\alpha$  and a sterile species  $\nu_s$ ; the role of  $\mu_1$  in this case is played by  $\mu_\alpha$ , without any restriction on the other chemical potentials  $\mu_\beta$ .

The collision integral  $\mathbf{C} [\rho_{\mathbf{p}}, \bar{\rho}_{\mathbf{p}}]$ , in equation (3.81), includes all the allowed neutrino interaction processes. Different types of neutrino interactions will lead to separate contributions to the collision term. Since for the moment we are considering chiral neutrinos involved in weak interaction, such contributions are: charged-current (CC) and effective neutral-current (NC) interactions with a medium and neutral current neutrino self-interactions (S):

$$\mathbf{C} [\rho_{\mathbf{p}}, \bar{\rho}_{\mathbf{p}}] = (\dot{\rho}_{\mathbf{p}})_{CC} + (\dot{\rho}_{\mathbf{p}})_{NC} + (\dot{\rho}_{\mathbf{p}})_S, \quad (3.86)$$

and an analogous equation can be written for the antineutrino collision terms.

The CC term is given by:

$$(\dot{\rho}_{\mathbf{p}})_{CC} = \{\mathcal{P}_p, (1 - \rho_{\mathbf{p}})\} - \{\mathcal{A}_p, \rho_{\mathbf{p}}\}, \quad (3.87)$$

where

$$\mathcal{P}_\Delta = \frac{1}{2} \sum_{k=1}^n \mathcal{P}_k(\Delta) I_k \quad (3.88)$$

$$\mathcal{A}_\Delta = \frac{1}{2} \sum_{k=1}^n \mathcal{A}_k(\Delta) I_k \quad (3.89)$$

with  $I_k$  a projector on the neutrino flavor  $k$ .

The analogous equation for the antineutrino density matrix  $\bar{\rho}_{\mathbf{p}}$  is obtained from that for neutrinos (3.87) by means of the transformation:

$$p \rightarrow -p \quad \rho_{\mathbf{p}} \rightarrow (1 - \bar{\rho}_{\mathbf{p}}). \quad (3.90)$$

An evaluation of  $\mathcal{P}_k(\Delta)$  and  $\mathcal{A}_k(\Delta)$  can be very complicated for a dense and strongly interacting medium, as in a supernova core. However, in a sufficiently dilute medium they can be determined using perturbation theory, treating the medium constituents as free Dirac fields between collisions. For example, in a medium of protons, neutrons, and electrons  $\mathcal{P}_k(\Delta)$  and  $\mathcal{A}_k(\Delta)$  take the explicit form:

$$\begin{aligned} \mathcal{P}_e(p) &= \int \frac{d^3\mathbf{p}'}{(2\pi)^3} \frac{d^3\mathbf{q}}{(2\pi)^3} \frac{d^3\mathbf{q}'}{(2\pi)^3} (2\pi)^4 \delta^{(4)}(p + q - p' - q') \\ &\quad \times \sum_{spins} |\mathcal{M}(q, q', p, p')|^2 n_e(\mathbf{p}') n_p(\mathbf{q}') (1 - n_n(\mathbf{q})) \end{aligned} \quad (3.91)$$

$$\begin{aligned} \mathcal{A}_e(p) &= \int \frac{d^3\mathbf{p}'}{(2\pi)^3} \frac{d^3\mathbf{q}}{(2\pi)^3} \frac{d^3\mathbf{q}'}{(2\pi)^3} (2\pi)^4 \delta^{(4)}(p + q - p' - q') \\ &\quad \times \sum_{spins} |\mathcal{M}(q, q', p, p')|^2 n_n(\mathbf{q}) (1 - n_e(\mathbf{p}')) (1 - n_p(\mathbf{q}')), \end{aligned} \quad (3.92)$$

where  $n_e(\mathbf{p}')$ ,  $n_n(\mathbf{q})$  and  $n_p(\mathbf{q}')$  are the electron, neutron, and proton occupation numbers typically given by the Fermi-Dirac distributions;  $\mathcal{M}$  is the usual weak matrix element for the process  $e(\mathbf{p}') + p(\mathbf{q}') \leftrightarrow n(q) + \nu_e(\mathbf{p})$ . This kind of processes give a negligible contribution in the early universe. Consider now the weak processes that contribute to the NC term, which come from the part of the interaction Hamiltonian which is bilinear in the left-handed neutrino field  $\psi$ . Using the standard  $V - A$  four-fermion interaction and a suitable Fierz transformation they can be written as an effective NC interaction with an external medium. After a lengthy but straightforward calculation, the NC collision term takes the form:

$$\begin{aligned} (\dot{\rho}_{\mathbf{p}})_{NC} &= -i\sqrt{2}G_F \rho_m [G, \rho_{\mathbf{p}}] \\ &\quad \frac{1}{2} \int \frac{d^3\mathbf{p}'}{(2\pi)^3} [W(p', p) (1 - \rho_{\mathbf{p}}) G \rho_{\mathbf{p}'} - W(p, p') \rho_{\mathbf{p}} G (1 - \rho_{\mathbf{p}'}) G \\ &\quad + W(-p', p) (1 - \rho_{\mathbf{p}}) G (1 - \bar{\rho}_{\mathbf{p}}) G - W(p, -p') \rho_{\mathbf{p}} G \bar{\rho}_{\mathbf{p}} + h.c.], \end{aligned} \quad (3.93)$$

where  $\rho_m$  is a kind of baryon or charged-lepton number density of the medium and  $G$  is a hermitian  $n \times n$  matrix of dimensionless coupling constants, which in the flavor basis reads  $G^a = \text{diag}(g_1^a, \dots, g_n^a)$  for each species  $a$  (nucleons and charged leptons); the non-negative transition probabilities  $W(k', k)$  are Wick contractions of medium operators of the form:

$$W(k', k) = 2G_F^2 \mathcal{W}^{\mu\nu}(k' - k) \mathcal{N}_{\mu\nu}(k', k), \quad (3.94)$$

with  $k$  and  $k'$  correspond to neutrino four-momenta with  $k_0, k'_0$  positive or

negative,  $\mathcal{W}^{\mu\nu}$  the tensorial medium structure function and  $\mathcal{N}_{\mu\nu}$  the neutrino tensor written in the ultrarelativistic limit (see Raffelt & Sigl 1993). The first two terms in the integral are due to neutrino scattering off the medium. Both the positive gain term and the negative loss term correspond to scattering processes. The third and fourth expressions in the integral account for pair processes, with the positive term being a gain term from pair creations by the medium, whereas the negative one is a loss term from pair annihilations.

The corresponding equation for  $\bar{\rho}_{\mathbf{p}}$  can be found by applying the crossing operation in equation (3.90) to all neutrinos and antineutrinos appearing in (3.93).

Note that the CC and NC interactions with the medium do not fulfill rigorously the assumption that the medium is not significantly affected by neutrinos. For example, in a supernova core a change of the  $\nu_e$  density due to oscillations into other neutrino flavors will also change the electron and nucleon chemical potentials. However, assuming that the medium components always stay in kinetic equilibrium, the impact of the interaction on the medium will consist of a slow time variation of the temperature and chemical potentials.

As regards neutrino self-interactions, the corresponding effective interaction Hamiltonian is quartic in the neutrino field  $\psi$ . In this case the restriction to the usual  $V - A$  coupling is maintained and allowing for different coupling strengths for different neutrino flavors, but not a local four-fermion coupling, which in the early universe would be a too rough approximation for the resulting refractive terms.

Therefore, including gauge boson propagator effects the neutrino self-interaction term takes the form:

$$\begin{aligned}
(\dot{\rho}_{\mathbf{p}})_N C = & -i [\Omega_{\mathbf{p}}^S, \rho_{\mathbf{p}}] \\
& + G_F^2 \int \frac{d^3 \mathbf{q}}{(2\pi)^3} \frac{d^3 \mathbf{p}'}{(2\pi)^3} \frac{d^3 \mathbf{q}'}{(2\pi)^3} (2\pi)^4 \delta^{(4)}(p + q - p' - q') f_{scatt}(p, q, p') \\
& \times \{ (1 - \rho_{\mathbf{p}}) G_S \rho_{\mathbf{p}'} G_S [(1 - \rho_{\mathbf{q}}) G_S \rho_{\mathbf{q}'} G_S + Tr(\dots)] \\
& - \rho_{\mathbf{p}} G_S (1 - \rho_{\mathbf{p}'} ) G_S [\rho_{\mathbf{q}} G_S (1 - \rho_{\mathbf{q}'} ) G_S + Tr(\dots)] + h.c. \} \\
& + G_F^2 \int \frac{d^3 \mathbf{q}}{(2\pi)^3} \frac{d^3 \mathbf{p}'}{(2\pi)^3} \frac{d^3 \mathbf{q}'}{(2\pi)^3} (2\pi)^4 \delta^{(4)}(p + q - p' - q') f_{pair}(p, q, p') \\
& \times \{ (1 - \rho_{\mathbf{p}}) G_S (1 - \bar{\rho}_{\mathbf{q}}) G_S [\bar{\rho}_{\mathbf{q}'} G_S \rho_{\mathbf{p}'} + Tr(\dots)] \\
& - \rho_{\mathbf{p}} G_S \bar{\rho}_{\mathbf{q}} G_S [(1 - \bar{\rho}_{\mathbf{q}'} ) G_S (1 - \rho_{\mathbf{p}'} ) G_S + Tr(\dots)] \\
& + (1 - \rho_{\mathbf{p}}) G_S \rho_{\mathbf{p}'} G_S [\bar{\rho}_{\mathbf{q}'} G_S (1 - \bar{\rho}_{\mathbf{q}}) G_S + Tr(\dots)] \\
& - \rho_{\mathbf{p}} G_S (1 - \rho_{\mathbf{p}'} ) G_S [(1 - \bar{\rho}_{\mathbf{q}'} ) G_S \bar{\rho}_{\mathbf{q}} G_S + Tr(\dots)] + h.c. \}, \tag{3.95}
\end{aligned}$$

where  $Tr(\dots)$  means the trace of the term in front of it,  $G_S$  is an  $n \times n$  dimensionless hermitian matrix of NC coupling constant,  $f_{scatt}$  and  $f_{pair}$  are non-negative numbers which are functions of the physical four-momenta  $p$ ,  $q$  and  $p'$  and only depend on scattering angles:

$$f_{scatt}(p, q, p') = \frac{p \cdot q p' \cdot (p + q - p')}{p_0 q_0 p'_0 (p + q - p')_0} \tag{3.96}$$

$$f_{pair}(p, q, p') = \frac{p \cdot p' q \cdot (p + q - p')}{p_0 q_0 p'_0 (p + q - p')_0}. \tag{3.97}$$

The first phase space integral in equation (3.95) represents the gain and loss term due to the scattering reaction  $\nu_{\mathbf{p}'} \nu_{\mathbf{q}'} \rightarrow \nu_{\mathbf{p}} \nu_{\mathbf{q}}$  and the inverse reaction, respectively, whereas the second integral describes gain and loss terms due to the pair reaction  $\nu_{\mathbf{p}'} \bar{\nu}_{\mathbf{q}'} \rightarrow \nu_{\mathbf{p}} \bar{\nu}_{\mathbf{q}}$  and its inverse. The first two terms of the second integral can be obtained from the first integral by crossing  $\nu_{\mathbf{p}'}$  and  $\nu_{\mathbf{q}'}$ , and relabeling  $p' \leftrightarrow q$ ,  $p' \leftrightarrow q'$ . The last two terms arise from crossing  $\nu_{\mathbf{q}'}$  and  $\nu_{\mathbf{q}}$  and relabeling  $q' \leftrightarrow q$ ,  $p' \leftrightarrow q'$ .

The antineutrino equation is again obtained by crossing all neutrinos on both sides of the equation, which means by interchanging all the  $\rho$  and  $\bar{\rho}$  and substituting the refractive energy shift  $\Omega_{\mathbf{p}}^S$  with  $-\bar{\Omega}_{\mathbf{p}}^S$ , where  $\Omega_{\mathbf{p}}^S$  is given by:

$$\begin{aligned}
\Omega_{\mathbf{p}}^S = & \sqrt{2} G_F \int \frac{d^3 \mathbf{q}}{(2\pi)^3} \{ G_S (\rho_{\mathbf{q}} - \bar{\rho}_{\mathbf{q}}) G_S + G_S \text{Tr} [(\rho_{\mathbf{q}} - \bar{\rho}_{\mathbf{q}}) G_S] \} \\
& - \frac{8 \sqrt{2} G_F p_0}{3 m_Z^2} \int \frac{d^3 \mathbf{q}}{(2\pi)^3} q_0 G_S (\rho_{\mathbf{q}} + \bar{\rho}_{\mathbf{q}}) G_S.
\end{aligned} \tag{3.98}$$

Differently from the matrix of vacuum frequencies  $\Omega_{\mathbf{p}}^0$ ,  $\Omega_{\mathbf{p}}^S$  consists of two terms, of which the first one changes sign for antineutrinos whereas the second one remains unchanged. The trace expression in the first term implies that neutrinos in a bath of their own flavor experience twice the energy shift relative to a bath of another flavor.



## Neutrino in Cosmology and Astrophysics

In the standard Big-Bang cosmology, neutrinos as well as photons are the most abundant particles in the universe. The neutrino role during the early stages of the universe is significant since light neutrinos are essential ingredients in the universe density in the radiation-dominated stage, determining the dynamics of the universe. Neutrinos played an essential role in different processes in BBN, leptogenesis and baryogenesis as well as the CMB formation. At later stages of the universe ( $T \leq \text{eV}$ ) relic neutrinos contribute to the matter density because at least one of the neutrino species became non-relativistic affecting the formation of galaxies and their structures as well as the CMB anisotropies. This implies that neutrinos play an important role in the evolution of the universe from the very beginnings to the current state and consequently their properties within and beyond the standard model are strongly bounded by modern high precision cosmological observations. In this chapter, we will present an overview of the consequences and related constraints associated with the presence of sterile species along with the active ones in the early stages of universe and supernovae environments.

### 4.1 Early Universe

Relic neutrinos are an important product of the standard hot Big Bang model. The three left-handed neutrinos  $\nu_\alpha$  and their CP conjugated states are thermally excited in the hot plasma which filled the early universe and are maintained in kinetic and chemical equilibrium with charged leptons, baryons and photons through weak interactions. In this regime, neutrinos distribution is a Fermi-Dirac, with a negligible contribution of the mass to the energy and physical momentum  $p$ :

$$f_{\nu_\alpha}(p) = \frac{1}{e^{\frac{p-\mu_\alpha}{T}} + 1} \quad (4.1)$$

$$f_{\bar{\nu}_\alpha}(p) = \frac{1}{e^{\frac{p+\mu_\alpha}{T}} + 1}, \quad (4.2)$$

with  $T$ , the photon temperature. As long as the active neutrinos are in thermal equilibrium with the thermal bath, they have the same temperature  $T$ . As the universe expands and cools, the rates of weak interaction processes decrease and neutrinos decouple when these rates become smaller than the expansion rate of the universe. Since for the three active light neutrinos with masses smaller than about 1 eV the decoupling occurs when they are still relativistic, these neutrinos are hot relics.

The photon temperature, given by the conservation of entropy in the baryon–lepton–neutrino–photon fluid, decreases as the inverse of the scale factor,  $1/a$ , except near the time when particles disappear from the thermal bath and release their entropy to lighter particles. Since neutrinos have already decoupled at the time when electrons/positrons annihilate, only the photons are heated. Using the conservation of entropy density, one can obtain the temperature ratio after  $e^- e^+$  annihilation,

$$\frac{T_{\nu_\alpha}}{T} = \left( \frac{4}{11} \right)^{\frac{1}{3}}, \quad (4.3)$$

afterwards the ratio  $T_{\nu_\alpha}/T$  remains constant in the standard cosmology.

Defining  $\xi_\alpha \equiv \mu_\alpha$ , the neutrino–antineutrino asymmetry, energy density, pressure and entropy density can be written in the form:

$$n_{\nu_\alpha} - n_{\bar{\nu}_\alpha} = \frac{T^3}{6} \xi_\alpha \left( 1 + \frac{\xi_\alpha^2}{\pi^2} \right) \quad (4.4)$$

$$\rho_{\nu_\alpha} + \rho_{\bar{\nu}_\alpha} = \frac{7\pi^2}{120} T^4 \left( 1 + \frac{30\xi_\alpha^2}{7\pi^2} + \frac{15\xi_\alpha^4}{7\pi^4} \right) = 3(P_{\nu_\alpha} + P_{\bar{\nu}_\alpha}) \quad (4.5)$$

$$s_{\nu_\alpha} + s_{\bar{\nu}_\alpha} = \frac{7\pi^2}{90} T^3 \left( 1 + \frac{15\xi_\alpha^2}{7\pi^2} \right), \quad (4.6)$$

where the neutrino and antineutrino number density are given by:

$$n_{\nu_\alpha, \bar{\nu}_\alpha} = \frac{3\zeta(3)}{4\pi^2} T^3 \pm \frac{\xi_\alpha}{12} T^3 + O(\xi_\alpha^2), \quad (4.7)$$

with  $\zeta(3) = 1.202$ , the Riemann zeta function  $\zeta(n)$ . The above equations have been written for chiral neutrinos, for which the number of the internal degrees of freedom  $g$  is equal to 1, whereas in general for massive 1/2-spin fermions  $g = 2$ .

Neutrino decoupling occurs over an extended period of time. As neutrinos have different momenta and weak cross sections grow with the squared total energy in the two-particle center of mass of the system,  $s = E_{CM}^2$ , more energetic neutrinos will remain in equilibrium longer than low-energy neutrinos. Consequently, when  $e^-$  and  $e^+$  annihilate, some thermal distortions will affect neutrino distribution with respect to a standard Fermi–Dirac function. Using the instantaneous decoupling approximation, that is, the limit in which we consider neutrino decoupling as an instantaneous event happening at temperature  $T_{\nu d}$ , after decoupling neutrinos propagate freely and their distribution remains unchanged except for the effect of redshift of the physical momentum. In this approximation we can assume the distribution at  $T_{\nu d}$  to be a Fermi–Dirac one, which can be conveniently written in terms of the comoving momentum as:

$$f_{\nu_\alpha}(p) = \frac{1}{e^{\frac{p a_d}{T_{\nu d} a_d}} + 1}, \quad (4.8)$$

where  $a_d$  is the scale factor at the decoupling time  $T_{\nu d}$ . In the above equation (4.8),  $\xi_\alpha$  has been neglected, since the neutrino chemical potentials are expected to be very small and their values can be experimentally constrained using primordial nucleosynthesis. However, the same result still holds even if the constant chemical-potential-to-temperature ratio  $\xi_\alpha$  is included.

Regarding the decoupling temperature,  $T_{\nu d}$  can be estimated by comparing the weak interactions rate with the expansion rate  $H(T)$ . Taking into account that the leading processes contributing to equilibrium are scattering over electrons/positrons and pair conversions,  $e^+ e^- \leftrightarrow \nu_\alpha \bar{\nu}_\alpha$ , and that as long as the temperature  $T$  is smaller than the  $W$  and  $Z$  boson masses, the corresponding cross section times velocity for charged and neutral current interactions is of the order  $\langle \sigma v \rangle \sim G_F^2 T^2$ , the weak interaction rate for neutrinos is given by:

$$\Gamma_\nu = \langle \sigma v \rangle \sim G_F^2 T^2 n_e(T) \sim G_F^2 T^5, \quad (4.9)$$

where  $n_e \sim T^3$  is the target density corresponding to temperatures at which the electron/positron are still relativistic.

This rate in equation (4.9) has to be compared with the Hubble expansion parameter in the radiation-dominated era:

$$H(T) = \sqrt{\frac{8\pi G_N}{3} \rho_R} \quad (4.10)$$

with  $G_N$ , the Newton gravitational coupling constant and  $\rho_R$  the energy density in radiation:

$$\rho_R = g^* \frac{\pi^2}{30} T^4 \quad (4.11)$$

and  $g^*$  is the effective number of degrees of freedom contributing to  $\rho_R$ :

$$g^* = \sum_{i, \text{bosons}} g_i \left(\frac{T_i}{T}\right)^4 + \frac{7}{8} \sum_{j, \text{fermions}} g_j \left(\frac{T_j}{T}\right)^4. \quad (4.12)$$

The decoupling temperature is then given by  $\Gamma_\nu(T_{\nu d}) = H(T_{\nu d})$ :

$$T_{\nu d} = \left(\frac{\sqrt{g^*}}{G_F^2 m_{Pl}}\right)^{\frac{1}{3}} \sim g^{*\frac{1}{6}} \text{ MeV}, \quad (4.13)$$

where  $m_{Pl} = G_N^{-1/2} = 1.22 \times 10^{19}$  GeV is the Planck mass scale.

$T_{\nu d}$  is of the order of MeV, as it can be seen from the very weak dependence on the number of relativistic degrees of freedom  $g^*$ . Indeed at such temperatures, the thermal bath consists only of electrons/positrons, photons and neutrinos themselves, hence

$$g^* = 2 + \frac{7}{8} 4 + \frac{7}{8} 6 = \frac{43}{4} = 10.75. \quad (4.14)$$

Using the value of the CMB temperature at present time,  $T_0 = 2.725$  K, equation (4.3) provides neutrinos temperature today,  $T_{\nu 0} = 1.945$  K =  $1.676 \times 10^{-4}$  eV. Thus, the relic neutrinos that pervade space have temperature extremely small. This implies that their weak interaction cross-section with matter is also extremely small. For chiral neutrino this is given by:

$$\sigma \sim G_F^2 T_{\nu 0}^2 \sim 10^{-64} \text{ cm}^2. \quad (4.15)$$

For massive and nonrelativistic neutrinos, the cross section is larger but still very small:

$$\sigma \sim G_F^2 m_\nu^2 \sim 10^{-56} \left( \frac{m_\nu}{1 \text{ eV}} \right)^2 \text{ cm}^2. \quad (4.16)$$

This means that although the number density of cosmic neutrinos, given for each flavor by equation (4.7) assuming negligible chemical potentials, provides a rather large flux with respect to any astrophysical neutrino sources, including solar neutrinos:

$$n_{\nu 0} = n_{\bar{\nu} 0} \sim 56 \text{ cm}^{-3}, \quad (4.17)$$

the direct detection of such a large number of relic neutrinos still remains a difficult task with present experimental techniques.

From the value of  $T_{\nu 0}$  it follows that two of the three neutrino mass eigenstates are nonrelativistic today, being  $T_{\nu 0} < (\delta m^2)^{1/2}$ , with  $\delta m^2 \sim 10^{-5} \text{ eV}^2$ , the squared mass difference involved in the solar neutrino problem. Their contribution to the energy density today can be derived using the present value of the critical density  $\rho_c \equiv 3H^2/(8\pi G_N)$  and equation (4.17). Summing only over neutrinos which are nonrelativistic today and assuming standard Fermi-Dirac distributions with zero chemical potential,  $\Omega_\nu$  is given by:

$$\Omega_\nu = \frac{\sum_i m_{\nu i} n_{\nu 0}}{\rho_{c 0}} = \frac{\sum_i m_{\nu i}}{\text{eV}} \frac{1}{94.1(93.1)h^2}, \quad (4.18)$$

where the number in round brackets accounts for the effects of non instantaneous neutrino decoupling. The above formula (4.18) can be used as a good approximation for the sum over all three species, since if the lightest neutrino eigenstate is still relativistic today, its contribution to  $\Omega_\nu$  will be marginal. Since the current constraint on light neutrino masses is  $\sim 1 \text{ eV}$ , they can only contribute a small fraction of the total energy density of the universe, although their effect at late times, during structure formation, is expected to be very significant.

After the electron/positron annihilation, the only relativistic degrees of freedom present in the universe correspond to photons and neutrinos. Hence, the energy density in radiation is given by:

$$\rho_R = \rho_\gamma \left[ 1 + \frac{7}{8} \left( \frac{4}{11} \right)^{\frac{4}{3}} N_{eff} \right], \quad (4.19)$$

where, the effective number of neutrino species  $N_{eff}$  parametrizes any deviation from the assumptions of no other relativistic species than the three light neutrinos, instantaneous decoupling and standard Fermi-Dirac distributions with zero chemical potentials for neutrinos.

Note that, after LEP precision electroweak measurements on the Z resonance and its invisible width, the number of active neutrino generations is known to be three (Beringer et al. 2012). Even before these experimental results some bounds on  $N_{eff}$  had already been set by cosmology, mainly from primordial nucleosynthesis (Shvartsman 1969; Steigman et al. 1977). Besides nucleosynthesis, the spectra of CMB anisotropies and of matter fluctuations can actually provide further powerful constraints on  $\rho_R$  and therefore on  $N_{eff}$ . Now the question is no longer the assessment of the number of light-flavor neutrino species, but seeking for any evidence of other as yet unidentified light particles contributing to  $\rho_R$ , or nontrivial features such as chemical potentials in the neutrino distributions in phase space. In other words, the present concern is whether  $N_{eff} \neq 3$  may be due to fermionic or bosonic degrees of freedom which have nothing to do with neutrinos or to the assumption of a simple Fermi-Dirac distribution for the three neutrinos.

So far we have only considered the left-handed light neutrino component in the primordial plasma. If neutrinos are Majorana particles, right-handed sterile partners might either not exist at all or be very massive particles already disappeared from the thermal bath by the primordial nucleosynthesis epoch. If neutrinos have a Dirac mass term, right-handed neutrinos can be excited through the mass term which mixes chirality states but owing to the left-handed chiral character of the SM charged-current interaction, the production rate of right-handed states is suppressed with respect to that of the left-handed ones by a factor  $(m_\nu/E)^2$  in the relativistic limit. This leads to:

$$\Gamma_s = G_F^2 T^5 \frac{m_\nu^2}{T^2}, \quad (4.20)$$

which, imposing the condition  $\Gamma_s \geq H(T)$ , shows that these processes are at equilibrium only for  $T > MeV^3/m_\nu^2$ , that is,  $T > 10^9$  GeV for  $m_\nu \sim 1$  eV. As a matter of fact, for such temperatures, much higher than the W and Z boson masses, the weak cross section has different behavior and decreases as the inverse squared center of mass energy,  $\sigma \sim G_F^2 m_{W,Z}^4/T^2$ . It follows that the equilibrium condition leads to a temperature  $T \leq 10^2 MeV (m_\nu^2/eV)^{2/3} \ll$

$m_{W,Z}$ , which is far below the range where that  $\sigma$  can be applied. Therefore it is always  $\Gamma_s < H(T)$ . An hypothetical right-handed neutrino production in the primordial plasma by means of a Dirac mass term is then excluded by the smallness of neutrino masses, being the typical interaction rates suppressed by the factor  $(m_\nu/T)^2$ .

A further possibility of right-handed neutrino production could be the existence of weak right-handed currents mediated by  $W_R$  bosons, for instance in extensions of the Standard Model to gauge symmetries also having an  $SU(2)_R$  factor. In this case they would contribute to  $N_{eff}$  by an amount comparable to that for left-handed neutrinos, unless the right-handed gauge bosons are sufficiently massive, given that the cross sections scale as  $M_{W_R}^{-4}$ . The primordial nucleosynthesis sensitivity to the value of  $N_{eff}$  provides lower bounds on  $M_{W_R}$ . Assuming that the right-handed interaction has the same form as the left-handed one but with heavier intermediate bosons, the lower limit on their mass coming from BBN is  $M_{W_R} \gtrsim 75 m_W$ , which can depend on the particle spectrum of the physics beyond the SM (Lesgourgues et al. 2013 and references therein).

The left-right (LR) symmetric models of weak interaction are an interesting extension of the SM which may manifest itself in the TeV (maybe higher) range of energies. In these models, the left and right chiralities of fermions are assumed to play an identical role prior to symmetry breaking (or at energies higher than all symmetry breaking scales), so that in the symmetric phase weak interactions conserve parity, as it happens in strong and gravitational interactions. Lepton number violation occurs through the production of the heavy right-handed neutrinos and their subsequent decay. The main achievement of LR symmetric models based on the gauge group  $SU(2)_L \times SU(2)_R \times U(1)_{B-L}$  is a prediction of non-vanishing neutrino mass, whose smallness gets naturally tied to the maximal parity violation of weak interactions through the seesaw mechanism. The lightest right-handed neutrino with a mass around keV turns out to be the only viable candidate consistent with a TeV scale of left-right symmetry. A keV mass scale of one of the right-handed neutrinos could also make it a long-lived warm dark matter (DM) candidate (Senjanovic & Mohapatra 1975; Heeck & Patra 2015 and reference therein; Adhikari et al. 2016). Thus, possible sterile neutrinos, related to ordinary ones through a small mixing angle, in various extensions of the SM are expected to be relatively light, with masses in eV region (maybe smaller) or with keV masses. Besides this, another possibility is related to the production of much heavier sterile neutrinos, with masses in the MeV range. For such heavy sterile neutrinos, suggested by the KARMEN anomaly in the time distribution of the charged and neutral current events induced by neutrinos from pion decay, mass and mixing angle can be constrained on the

basis of cosmological and astrophysical arguments as well as by experiments (Dolgov et al. 2000; Ruchayskiya & Ivashko 2012).

In summary, sterile neutrino, in addition to providing neutrino mass generation, depending on its mass scale, may have many important cosmological implications. eV sterile neutrinos may explain the dark radiation (DR) problem (additional relativistic density quantified by  $N_{eff}$ ) and the experimental data of SBL experiments, a KeV sterile neutrino may be a warm DM candidate and furthermore sterile neutrinos provide the possibility of baryogenesis through leptogenesis (Fukugita & Yanagida 1986). The main way of obtaining a significant abundance of sterile neutrinos is through their mixing and oscillations with the active neutrinos. In the early universe neutrino oscillations are expected to be effective when the vacuum oscillation term becomes larger than the leading matter-induced potential term from charged leptons, respectively given by:

$$-\frac{\Delta m^2}{2p} \cos 2\theta, \quad -\frac{8\pi\sqrt{2}G_F p}{3m_W^2} (\rho_{l^-} + \rho_{l^+}), \quad (4.21)$$

where, because of the  $1/p$  dependence, the vacuum term grows with the cosmological expansion. With good approximation, this exceeds the matter term when the temperature drops below a certain value  $T_c$ , given by:

$$T_c \approx 150 \left( \frac{|\Delta m^2|}{keV^2} \right)^{\frac{1}{6}} \text{ MeV}, \quad (4.22)$$

where the approximation consists in the fact that the above expression (4.22) does not account for the proper evolution of other particle species at temperatures much higher than  $T \gtrsim 30$  MeV, and in particular close to the QCD transition phase at  $T \sim 200$  MeV.

Active-sterile neutrino oscillations may have considerable effects in the early universe. They may excite additional light particles into equilibrium, thus affecting the expansion rate of the universe. They may generate neutrino-antineutrino asymmetry and distort neutrino energy spectrum. In fact, fast active-sterile neutrino oscillations effective before the epoch of neutrino decoupling, only slightly affects active neutrino distributions, because the active neutrino states can be refilled through interactions with the plasma. However, active-sterile neutrino oscillations proceeding after  $\nu_e$  decoupling, if  $\nu_s$  was not in equilibrium before the start of oscillations,  $N_s = \rho_{\nu_s}/\rho_{\nu_e} < 1$ , may strongly distort neutrino energy spectrum and deplete neutrino number



density (Kirilova 2015). In particular  $\nu_e - \nu_s$  oscillations can affect the weak interaction rates of  $\nu_e$  and hence the Big-Bang Nucleosynthesis (BBN).

It being understood that in constraining cosmology in general, the BBN presents a limiting factor consisting of the systematic uncertainties in the astrophysical measurements of all primordial abundances. In this sense, the helium-4 mass fraction  $Y_p$  and the deuterium abundance D/H are the only effective probes. Nevertheless, the BBN remains the most powerful cosmological probe of sterile neutrinos effects as it reflects both kinetic and dynamical effects of a non-zero population of sterile neutrinos and active-sterile oscillations. This provides significant constraints on the number of thermalized neutrinos present at temperatures  $T \sim 0.1$  MeV, as it will be shown in the next chapter. Here, we first consider the effects of a population of thermal light sterile neutrinos, with eV-range masses as suggested by reactor and SBL oscillation data, produced in the early universe.

#### 4.1.1 Sterile Neutrino Thermalization

The evolution of an active-sterile neutrino system depends on the sign of  $\Delta m^2$ . For negative values of the squared-mass difference there could be a cancellation of the two terms in equation (4.21) for both helicity states, leading to resonant production, whereas,  $\Delta m^2 > 0$  leads to a nonresonant production of sterile neutrinos. In both cases, for  $\Delta m^2$  higher than  $\sim 10^{-7} eV^2$ , sterile neutrino population depends on the interplay between oscillations and interactions. If the mean free path of the active neutrinos is much shorter than the in-medium oscillation length, the probability for conversion of an active neutrino into a sterile state becomes very small.

In the non resonant production case, the production probability of sterile neutrinos can be written as (Barbieri and Dolgov, 1990):

$$\Gamma_s = \langle \sin^2 \theta_m \sin^2(\omega_m t) \Gamma_\alpha \rangle, \quad (4.23)$$

where  $\theta_m$  and  $\omega_m$  are the in-medium mixing angle and oscillation frequency, respectively;  $\Gamma_\alpha$  is the production rate of active neutrinos in the plasma and the averaging is done over the thermal background.

For high values of the oscillation frequency and small values of  $\theta_m$ ,  $\Gamma_s$  becomes:

$$\Gamma_s \approx \theta_m^2 \Gamma_\alpha, \quad (4.24)$$

for a small number density of sterile neutrinos and active neutrinos close

to equilibrium. Therefore, if the production rate of  $\nu_s$  is higher than the expansion rate of the universe (this condition holds for values of  $\Delta m^2$  or  $\theta_m$  not very small), one can expect a thermal or close-to-thermal population of sterile neutrinos. As regards resonant production of sterile neutrinos, at temperatures below  $T_c$  the resonance propagates over the whole momentum distribution while the active neutrinos are repopulated by interactions, leading to a significant enhancement of the  $\nu_s$  thermalization even for quite small values of the mixing angle. In particular, for the active-sterile parameters needed to explain the SBL oscillation anomalies the thermalization of sterile neutrinos is achieved, which means  $N_{eff} = 4$ .

Furthermore, all the active-sterile schemes with  $\nu_s$  mass on the eV scale are still in tension with the cosmological constraints on the sum of neutrino masses. This tension may be relieved if there exists some mechanism that suppresses the production of  $\nu_s$  in the early universe, such as a lepton asymmetry. This can lead to different outcome for resonant production (blocking of  $\nu_s$  production until  $\nu_\alpha$  decoupling) and for nonresonant production (delayed thermalization) but the final contribution of sterile neutrinos to  $N_{eff}$  can be significantly suppressed.

The existence of sterile neutrinos not fully thermalized with the active species in the early universe in principle is compatible with Big-Bang Nucleosynthesis (BBN) data, even if models with more than one sterile neutrino seem to be disfavored by BBN analysis based on current astrophysical data. It is also compatible with cosmological measurements of the Cosmic Microwave Background (CMB) and Large-Scale Structures (LSS) if the neutrino masses do not exceed 1 eV. Analysis based on a technique which exploits the full information contained in the one-dimensional Lyman- $\alpha$  forest flux power spectrum, complemented by additional cosmological probes, such as CMB data and in particular adding baryon acoustic oscillations, lead to rule out any possibility of thermalized sterile neutrinos or more generally any decoupled relativistic relic with  $\Delta N_{eff} \simeq 1$  at a significance of over  $5\sigma$ . Therefore, one or more than one sterile neutrino may exist avoiding the cosmological constraints only by suppressing the thermalization of sterile neutrinos in the early universe and/or by considering non-standard cosmological theories.

As mentioned above, neutrino thermalization can be suppressed by assuming a primordial asymmetry  $L_\nu$  between active neutrinos and antineutrinos (Bell et al. 1999; Chu & Cirelli 2006). This produces an additional matter-induced potential term in the active-sterile neutrino equations of motion, which is able to inhibit the active-sterile flavor conversions via suppression of the in-medium mixing angle, providing that this term be sufficiently large. The required asymmetry for achieving a sufficient suppression of the sterile neutrino abundance is  $L_\nu > 10^{-2}$  (Hannestad et al. 2012; Mirizzi

et al. 2012). Apart from considerations on the non-naturalness of such a high value of  $L_\nu$ , the distortions induced on the active energy spectra can have appreciable effects on the neutron-to-proton ratio and primordial nucleosynthesis (Saviano et al. 2013). An alternative mechanism for suppressing sterile neutrino thermalization is based on the introduction of new “secret” self-interactions among sterile neutrinos, mediated by a massive gauge boson, with mass less than  $m_W$  (Dasgupta & Kopp 2014; Hannestad et al. 2014), or by a light pseudoscalar (Archidiacono et al. 2014). As in the case of neutrino asymmetries, in the secret self-interaction scheme the suppression of the sterile neutrino production before decoupling occurs by means of a matter-induced potential term in the flavor evolution equations.

The outcome of these models will be discussed in some more detail in the next chapter.

## 4.2 Cosmological Constraints on Sterile Neutrinos

Big Bang Nucleosynthesis provides one of the most sensitive probes of the physical conditions in the early universe. The uncertainties on the observed values of the primordial abundances, although small, still leave some room to physics beyond the standard model. BBN is therefore often used to constrain new physics such as neutrino oscillations between active and sterile species. For this reason we will devote a separate chapter (Chapter 5) to sterile neutrino effects on the BBN and the related constraints. Here we will focus on sterile neutrino effects on the CMB radiation and LSS and the ensuing constraints.

Unlike the BBN, probes of the late-time inhomogeneities of the universe, such as the CMB anisotropies and the LSS distribution, are not sensitive to the flavor content of the neutrino sector but only to its contribution to the stress-energy tensor. If neutrinos are massless, the  $N_{eff}$  parameter as defined through the total neutrino energy density in radiation-dominated era,  $\rho_\nu = N_{eff}(7\pi^2/120)T_\nu^4$ , alone accounts for their effects on the universe evolution. If neutrinos are massive, in order to solve the evolution equations for the inhomogeneities exactly, in principle one should know the exact form of the neutrino phase space distribution. However, since the current generation of late-time cosmological probes are not sensitive to deviations of the neutrino phase space distribution from the relativistic Fermi-Dirac distribution (Cuoco et al. 2005), the neutrino sector can be safely treated in terms of the neutrino masses  $m_{\nu_i}$  and the  $N_{eff}$  parameter solely.

Additional relativistic energy density, due to a thermal population of light sterile neutrinos, affects the CMB anisotropies primarily for its effects

on the age around matter-radiation equality. If the particle has a rest mass significantly below the temperature of the thermal population around matter-radiation equality (approximately  $m_{\nu_i} \ll 0.1$  eV), the equality redshift  $z_{eq}$  will be altered in the following way:

$$1 + z_{eq} = \frac{\omega_M}{\omega_\gamma \left[ 1 + \frac{7}{8} \left( \frac{4}{11} \right)^{\frac{4}{3}} N_{eff} \right]} = \frac{\omega_M}{\omega_\gamma [1 + 0.227 N_{eff}]}, \quad (4.25)$$

where  $\omega_M$  and  $\omega_\gamma$  are the present-day matter and photon energy densities, respectively. The equality redshift  $z_{eq}$  is strongly constrained by observations of the CMB temperature anisotropies through the ratio of the first and the third acoustic peaks. Hence, measuring  $z_{eq}$  amounts to fixing the ratio of the matter energy density to the radiation energy density. On the other hand, equation (4.25) also implies that  $N_{eff}$  and the matter energy density  $\omega_M$  are degenerate parameters. For a fixed value of  $\omega_M$ , increasing  $N_{eff}$  leads to a shorter stage between equality and decoupling and then to higher acoustic peaks. If the rest mass of the particle is such that (for neutrinos  $m_{\nu_i}$  is estimated approximately in the range  $(0.1 - 1)$  eV) the transition of the thermal population from an ultra-relativistic to a nonrelativistic distribution occurs around matter-radiation equality, then  $z_{eq}$  will also depend on the particle mass to temperature ratio. This means that there can be some degeneracy of  $N_{eff}$  with the rest mass of the particle.

Regarding possible a population of heavier and/or colder particles ( $m_{\nu_i} \gg 10$  eV) that have become fully nonrelativistic before the epoch of matter-radiation equality, this would be a nonrelativistic matter component in the context of CMB and LSS. For this reason the  $N_{eff}$  parameter does not cover keV-mass sterile neutrinos when considering CMB and LSS.

A value other than the standard  $N_{eff} = 3.046$  also affects the sound horizon  $r_s$  at the time of CMB decoupling,

$$r_s = \int_0^{t^*} dt \frac{c_s(t)}{a(t)} \quad \text{with} \quad c_s(t) = \frac{1}{\sqrt{3} \left( \frac{3}{4} \frac{\omega_B a}{\omega_\gamma} \right)} \quad (4.26)$$

which in turn affects the angular position of the acoustic peaks:

$$\theta_s = \frac{r_s}{D_A} \propto \frac{\Omega_M^{-1/2}}{\int_{a^*}^1 \frac{da}{a^2 \sqrt{\Omega_M a^{-3} + (1 - \Omega_M)}}}, \quad (4.27)$$

where  $D_A$  is the angular diameter distance to the last scattering surface. The sound horizon at decoupling depends on the time of equality. A later

equality implies a smaller sound horizon at decoupling and then a shifting of all peaks to higher values of  $\ell$ .

The above equation (4.26) implies that  $\theta_s$  only constrains the parameter combination  $\Omega_M = \omega_M/h^2$ , not  $\omega_M$  and  $h$  singularly, from which it follow a correlation between  $N_{eff}$  and the present-time Hubble parameter  $H_0$ . Because of the aforementioned degeneracies,  $N_{eff} - \omega_M$  and  $N_{eff} - H_0$ ,  $N_{eff}$  cannot be completely constrained by measurements of the CMB acoustic peaks alone. However, as non-interacting, free-streaming relativistic particles, neutrinos may have another important effect on the CMB anisotropies through their anisotropic stress, which can suppress the amplitude of higher harmonics in the temperature anisotropy spectrum ( $\ell > 200$ ) and structure formation growth (Bashinsky & Seljak 2004; Hannestad 2013).

Measurements of the CMB damping tail ( $\ell \gtrsim 1000$ ) by ACT (Atacama Cosmology Telescope) and SPT (South Pole Telescope) have provided an additional route to  $N_{eff}$  through the effect of  $z_{eq}$  on diffusion damping (Silk damping). The measured quantity is the angular diffusion scale  $\theta_d = r_d/D_A$ , which, for fixed values of  $z_{eq}$ , baryon energy density  $\omega_B$  and using  $\theta_s$  can be written as:

$$\theta_d \propto (\Omega_M H_0^2)^{\frac{1}{4}} \theta_s. \quad (4.28)$$

Thus, measuring  $\theta_d$  in the CMB damping tail allows to determine the physical matter density  $\omega_M$  and hence  $N_{eff}$  through the  $N_{eff} - \omega_M$  degeneracy, independently of  $D_A$  (i.e., its defining parameters such as spatial curvature, dark energy equation of state). This allows to place constraints on  $N_{eff}$  also using CMB data alone (Dunkley et al. 2011; Keisler et al. 2011).

Consider now the effects of light sterile neutrinos on the LSS. The LSS matter power spectrum  $P(k)$  is determined by two quantities: the comoving wavenumber at matter-radiation equality  $k_{eq}$  and the baryon-to-matter ratio  $r_B$ , respectively given by:

$$k_{eq} \equiv a_{eq} H(a_{eq}) \simeq 4.7 \times 10^{-4} \sqrt{\Omega_M (1 + z_{eq})} h \text{ Mpc}^{-1} \quad r_B \equiv \frac{\omega_B}{\omega_M}. \quad (4.29)$$

The former determines the position of the turning point of the power spectrum  $P(k)$ , whereas the latter controls the power suppression due to baryon acoustic oscillations at  $k > k_{eq}$ .

Massless neutrinos are always part of the radiation content and  $k_{eq}$  is unaffected by species that are still relativistic today. Whereas, massive neu-

trinos contribute to radiation at early times but also to matter after becoming nonrelativistic. If some of the neutrinos, sterile or active, are massive enough to be nonrelativistic today, a third parameter  $r_\nu \equiv \omega_\nu/\omega_M$  (where  $\omega_\nu = \Omega_\nu h^2$  is defined by equation (4.18)) controls the power suppression, at  $k > k_{eq}$ , due to the neutrino thermal velocity dispersion. Thus, massive neutrinos also contribute to the present-time  $\omega_M$ , reducing the values of the cold dark matter and baryon density today,  $\omega_{CDM}$  and  $\omega_B$ . If massive neutrinos have not yet become nonrelativistic at the time of radiation/matter equality, this transition will be delayed, with the following consequence for the LSS matter power spectrum: since on sub-Hubble scales the matter density contrast  $\delta = \delta\rho/\rho$  grows more efficiently during matter domination than during radiation domination, the matter power spectrum is suppressed on small scales with respect to large scales.

The physical matter density  $\omega_M$  today is higher while  $\omega_B$  is unchanged, leading to a lower baryon-to-matter ratio. It follows a higher matter fluctuation amplitude today at  $k > k_B$ , where  $k_B$  corresponds approximately to the comoving Hubble rate at the epoch when baryons decouple from photons. Therefore, measurements of the LSS matter power spectrum can be used to solve the  $N_{eff} - \omega_M$  degeneracy problem in the CMB data.

On the other hand, the above mentioned suppression of the matter fluctuation amplitude at  $k > k_\nu$ , (where  $k_\nu$  is the neutrino free-streaming scale at the time when neutrinos become nonrelativistic) dependent on the ratio  $r_\nu$ , avoids some of the enhancement due to the extra relativistic energy density near CMB decoupling, leading to some persisting degeneracy between  $N_{eff} - r_\nu$  in combined analyses of CMB and LSS data.

### 4.3 Supernovae Environment

The formation of the elements in the universe is closely related to the weak interactions between neutrinos and matter. Neutrino interactions can interchange protons and neutrons (free or inside the nucleus), so that they contribute in determining the neutron abundance of the baryonic matter. Hence, from the light elements formation in the BBN to the heavy elements generated by neutron-capture processes in explosive astrophysical environments, neutrinos play a relevant role. As neutrinos with different flavors interact differently with matter, any mechanism that alters the flavor of neutrinos after their production may affect the prediction of the matter property and the outcome of the nucleosynthesis. In the explosive astrophysical events such as core-collapse supernovae and mergers of binary neutron stars as well as of a neutron star with a black hole, the neutrino influence on the property

of the ejected matter and the outcome of the associated nucleosynthesis has been studied in Refs. (Martinez-Pinedo et al. 2014; Wu et al. 2015).

During supernova explosion, almost 99% of the energy released comes out in the form of neutrinos, with only the remaining small percentage coming out as light. These neutrinos carry in their spectrum relevant information not only about the detailed nature of supernova collapse but also about properties of neutrino that cannot yet be explored in the laboratory. The neutrino flux consists essentially of two components. The first one arises during the first few milliseconds of stellar collapse, when electrons get absorbed into protons producing neutrinos via the inverse  $\beta$ -decay process:

$$e^- + p \rightarrow n + \nu_e. \quad (4.30)$$

These very energetic neutrinos are known as the *deleptonization neutrinos*. This burst lasts for about a hundred milliseconds. As the core collapse proceeds, a second stage of neutrino emission begins, which consists of a flux of  $\nu_e$ ,  $\bar{\nu}_e$ ,  $\nu_\mu$ ,  $\bar{\nu}_\mu$ ,  $\nu_\tau$  and  $\bar{\nu}_\tau$ , with energy in the range (15 – 20) MeV, corresponding to an emission temperature of about (5 – 6) MeV, if a thermal distribution with zero chemical potential is assumed. Such neutrinos originate from reactions of the type  $e^+ + e^- \rightarrow \nu_l + \bar{\nu}_l$ ,  $n + p \rightarrow n + p + \nu_l + \bar{\nu}_l$ . These processes lead to the thermalization of neutrinos, before they are finally emitted, within a sphere named *neutrino sphere*, whose size is much larger than the collapsed core radius. The temperature in the neutrino sphere depends on the distance from the core. Since neutrino interactions increase with energy, the extension from the core of the effective neutrino sphere increases with energy. Even if in their neutrino sphere neutrinos are in thermal equilibrium with matter, the spectrum becomes depleted at higher and lower energies with respect to a thermal spectrum, as a consequence of the fact that the temperature decreases with increasing radius while the density decreases faster than  $1/r$ . The emission temperature corresponds to the surface temperature, so that the neutrinos having stronger interaction emerge with lower energy. Since  $\nu_e e$  scattering gets a contribution from the charged current interactions while  $\nu_\mu e$  and  $\nu_\tau e$  scatterings do not, the  $\nu_e$  and  $\bar{\nu}_e$  are expected to leave the neutrino sphere at lower energy than the  $\nu_\mu$  and  $\nu_\tau$ .

In a supernova the matter density grows from zero up to nuclear density,  $\rho \simeq 10^{14} \text{ g cm}^{-3}$ , in the inner core. Matter effects are then important for all the neutrino (active and sterile) mass range ( $\lesssim 10^2 \text{ eV}$ ). For such values of the masses and given the typical supernovae neutrino energy of  $\sim 10 \text{ MeV}$ , active/sterile MSW resonances can take place outside the neutrino

sphere (usually identified as the regions after which neutrinos freely stream,  $\rho \ll 10^{12} \text{ g cm}^{-3}$ ).

Unlike the sun where only  $\nu_e$  are produced, supernovae produce all active  $\nu_\alpha$  and  $\bar{\nu}_\alpha$ , approximately in similar amounts. They mix and convert among themselves and with eventual sterile neutrinos (Mikheev & Smirnov 1986; Shi & Sigl 1994; Fetter et al. 2002).

The free-streaming stage of the neutrino evolution is influenced by matter effects due to coherent forward scattering of the neutrinos on the background matter (electrons and nucleons). Furthermore, in a supernova, forward scattering on the neutrinos themselves also play an important role in the flavor evolution of both neutrinos and antineutrinos (Duan et al. 2010), inducing large flavor conversions depending on the ratio among the fluxes of different-flavor neutrinos and the mass hierarchy. Self-induced neutrino oscillations dominate the neutrino propagation at a radius far deeper than the conventional matter-induced MSW effect among active flavors and give rise to r-process nucleosynthesis. For sterile neutrinos, the active-sterile MSW resonance location depends on the sterile neutrino mass, covering the possibility of coupling active-sterile MSW conversion with collective oscillations among the active states.

The analysis of supernovae neutrinos can be carried on in a way similar to that of solar neutrinos, following the evolution of the emitted neutrino from neutrino spheres along their travel through the star matter, the vacuum and the earth. The density matrix formalism is suitable for describing the supernova initial neutrino flux, which has a mixed flavor composition. This amounts to following the evolution of a  $4 \times 4$  density matrices  $\rho(E)$  (and the analogous for antineutrinos) for each neutrino mode with energy  $E$ . MSW resonances, that affect the neutrino density matrix, may introduce off-diagonal elements. However, these are averaged to zero by large oscillation phases.

The radial flavor evolution of the quasi-stationary neutrino flux, in the flavor space, is given by:

$$i \partial_r \rho(E) = [H_E, \rho(E)] \quad (4.31)$$

and an analogous equation for the antineutrinos  $\bar{\rho}(E)$ . The Hamiltonian matrix includes a vacuum term and in-medium interaction and self-interaction terms:

$$H_E = H_E^{Vac} + H_E^{\nu m} + H_E^{\nu\nu}, \quad (4.32)$$



where  $H_E^{\nu m}$ , accounts for neutrino interactions with other matter components and  $H_E^{\nu\nu}$  for neutrino-neutrino interactions. The vacuum term in the flavor basis reads:

$$H_E^{Vac} = U \frac{M^2}{2E} U^\dagger, \quad (4.33)$$

with  $M^2$  the diagonal matrix of the squared mass differences between the mass eigenstates,  $U$  the unitary matrix of the mixing angles that encode the transformation between the mass and the weak interaction bases.

$H_E^{\nu m}$  comprises both CC and NC contributions:

$$H_E^{\nu m} = \sqrt{2} G_F \text{diag} \left( n_e - \frac{n_n}{2}, -\frac{n_n}{2}, 0 \right). \quad (4.34)$$

Note that one can define a linear combination  $\nu_x$  of  $\nu_\mu$  and  $\nu_\tau$ , since in a supernova environment they are indistinguishable, so that the above matter term  $H_E^{\nu m}$  can be thought of as expressed in the flavor basis spanned by  $(\nu_e, \nu_x, \nu_s)$ . Regarding the last term in the Hamiltonian (4.32) corresponding to neutrino-neutrino interactions, only the elements involving the active flavors are nonzero, while all elements involving the sterile neutrino flavor eigenstate vanish,  $H_{es}^{\nu\nu} = H_{xs}^{\nu\nu} = H_{ss}^{\nu\nu} = 0$ .

If sterile neutrinos have a rest mass in the preferred mass range of the SBL anomalies (from about 0.1 eV to few eV), two MSW resonances are expected to occur close to the neutrino sphere, one for neutrinos and one for antineutrinos. These resonances are not adiabatic because the matter potential is very steep as a result of a rapidly changing electron fraction  $Y_e$  at small radii. At larger radii, a second and almost adiabatic resonance occurs in the neutrino sector only. As a result a large fraction of  $\nu_e$  is converted to  $\nu_s$  while the conversion of the  $\bar{\nu}_e$  flux to  $\bar{\nu}_s$  is only partial.

The equilibrium of the neutrino capture processes:

$$\nu_e + n \rightarrow p + e^-, \quad (4.35)$$

$$\bar{\nu}_e + p \rightarrow n + e^+ \quad (4.36)$$

and their reverse processes reduces the electron abundance  $Y_e$ , thus creating a neutron-rich environment that enables the formation of elements via the r-process. However, collective oscillations in the active sector due to neutrino

self-interactions are expected to become dominant especially in the late cooling phase. This may contribute to repopulate the  $\nu_e$  flux, so that the resulting  $Y_e$  is always lower than in the case with no active-sterile oscillations, but not necessarily as low as without considering the neutrino-neutrino matter effects. Therefore, the presence of light sterile neutrinos can alter the conditions for the elements formation, although active-sterile oscillations alone probably cannot activate the r-process.

As regards heavy sterile neutrinos in supernovae,  $\nu_s$  with rest masses in the keV region and mixing angles with active species such that they can be DM candidates can also affect fundamental aspects of energy transport in the proto-neutron star core. In fact, as a consequence of the high matter density and large electron lepton number in the core as well as typical active neutrino energies of order 10 MeV, keV-mass sterile neutrinos can be resonant. If the flavor evolution through the resonance is sufficiently adiabatic, then the  $\nu_e$  will be turned into a sterile neutrino, which is likely to stream out of the core at near the speed of light, unless it encounters another MSW resonance that re-converts it to an active neutrino (Abazajian et al. 2001). In fact, the dependence of the potential on  $Y_e$  can produce such an effect: at first as the core collapses  $\nu_e$ s are converted, the unbalanced electron capture lowers  $Y_e$ , eventually until leading it below 1/3 so that the matter potential becomes negative, thereby causing the conversion of  $\bar{\nu}_e$  to sterile species. This can bring the potential up again if the collapse/expansion rate of the material in the core is slow enough, producing a double resonance scenario where  $\nu_e$ s are regenerated from the sterile neutrinos but closer to the neutrino sphere. As a result the effective transport time for  $\nu_e$ s can be drastically reduced, bringing up the  $\nu_e$  luminosity at the neutrino sphere, thereby affecting nearly every aspect of downstream supernova evolution, for example increasing the material heating rate behind the shock. Active-to-sterile conversions have also been considered as a way to produce large space motions of pulsar/neutron star remnants following core collapse (Fryer & Kusenko 2005).

Note that assuming sterile neutrinos with rest mass in the keV region and active-to-sterile neutrino flavor conversion to produce shock re-heating can lead to a loss of energy from the core. This could prove to be in conflict with the SN 1987A neutrino burst observations (Raffelt & Sigl 1993). However, the total kinetic energy of bulk motion plus optical energy in a core collapse supernova explosion is only  $10^{51}$  ergs, about 1% of the energy residing in the active neutrino energy in the core. Therefore, much energy could be transferred in sterile states escaping from the core and there would be active neutrino energy still sufficient to power an explosion, especially if the

transport of this energy to the shock is enhanced by efficient hydrodynamic motion.

Even heavier sterile neutrinos, with rest masses in the 100 MeV region, have been considered for supernova shock re-heating, although these may conflict with cosmological constraints on nucleosynthesis or measurements of  $N_{eff}$  derived from the CMB anisotropies (Fuller et al 2011).

## The Effective Number of Neutrino Species

The Standard Model of Particle Physics predicts the existence of exactly three active neutrinos, one for each flavor of the three charged leptons, and that neutrinos are all massless and left-handed. Experimental results on flavor neutrino oscillations have shown that neutrinos are massive particles and at least two species have a large enough mass for being nonrelativistic today, so that they contribute a small fraction of the dark matter of the universe (Mangano et al. 2005; Lesgourgues & Pastor 2006). Since the distinctness of the three flavors is strictly connected with the condition of being massless, the experimental evidence that neutrinos have nonzero mass opens also the question of the number of neutrino species. Although the measurement of the absolute neutrino mass scale remains a challenge, particle physics experiments are capable of determining two of the squared mass differences, along with the number of active neutrino families, their mixing angles, and one of the complex phases. On the other hand, a combination of cosmological data sets also allows to put more accurate upper bounds on the total neutrino mass (summed over all species) and on the number of effective neutrino species  $N_{eff}$  (Mangano & Serpico 2011; Rossi et al. 2015; Palanque-Delabrouille et al. 2015).

When the universe was a fraction of a second old, neutrinos experienced decoupling from electromagnetic plasma while flavor neutrino oscillations became effective. Afterwards they witnessed electron-positron annihilations and in the meantime were involved in the processes that fixed the initial conditions for the primordial production of light nuclei. All these processes depend upon the values of some unrelated parameters such as the Fermi constant, the neutrino mixing angles and squared mass differences, the electron mass and the binding energy of nuclei, in particular that of deuterium. The

shape of relic neutrino spectra and their contribution to radiation are parameterized in terms of the effective number of neutrino species  $N_{eff}$ . Any process that alters the thermal abundance of neutrinos can mimic a non-standard  $N_{eff}$  value. In this chapter we will focus on the case of additional sterile species and their oscillations with active species, which in the most part of the analyses of active-sterile oscillations has been considered in the two-neutrino limit.

## 5.1 From Neutrino Decoupling to Big-Bang Nucleosynthesis

Energy density and particle number densities, defined through the Fermi–Dirac distribution, are referred to a state where all the particles are in thermal equilibrium. In general, the condition for thermal equilibrium in a gaseous ensemble of particles, is attained when the state of the system (number of particles at a given energy level) does not change with time. Since in an expanding universe, the temperature is constantly changing, to be in equilibrium particles must adjust their energy faster than the time it takes to change the temperature. For this to be achievable, the interaction rate of the particles must be faster than the expansion rate of the universe  $H(T)$ , that is,

$$\Gamma_{int}(T) > H(T). \quad (5.1)$$

The decoupling of a particular species of particles occurs when at some point in the evolution of the universe the above condition fails to hold for such particles. In the early universe, active neutrinos are maintained in thermal equilibrium with charged leptons, baryons and photons by weak interactions and decouple from the electromagnetic plasma when they are still relativistic, which, as already mentioned, means that their Fermi-Dirac phase space distribution, parametrized by temperature and chemical potential, remains almost unaltered. In equation (4.13) we derived the decoupling temperature  $T_{\nu d}$  which is about 1 MeV, with a slight dependence on the neutrino flavor. Namely, since  $\nu_e$  has both CC and NC interactions with  $e^\pm$ ,  $T_d(\nu_e) \sim 2$  MeV while  $T_d(\nu_{\mu,\tau}) \sim 3$  MeV.

Shortly after neutrino decoupling the temperature drops below the electron mass, favoring electron/positron annihilations that heat the photons. The processes of neutrino decoupling and  $e^\pm$  annihilations are sufficiently close in time so that some relic interactions between  $e^\pm$  and neutrinos still

take place, leading to non-thermal distortions in the neutrino spectra at the per cent level (Mangano & Serpico 2004). The larger the energy of neutrinos, the more these relic processes are efficient. Thus, due to non-instantaneous decoupling and flavor oscillations, neutrinos shared a small part of the released entropy so that neutrinos were slightly heated. As already mentioned, such effects are accounted for by the effective number of neutrino species  $N_{eff}$ .

After electron-positron annihilation at  $t \sim 1$  second, the constituents of the universe are photons, neutrinos and, at an abundance smaller by a factor  $\eta^{-1} \sim 10^9$ , protons, neutrons and electrons. The amount of nucleosynthesis depends on the number of neutrons present in the thermal plasma. When the weak interaction processes were in equilibrium, the number densities of protons and neutrons were given by:

$$n_B \simeq g_B \left( \frac{m_B T}{2\pi} \right)^{3/2} e^{\frac{\mu_B - m_B}{T}}, \quad (5.2)$$

which, neglecting the small factor in front of the exponential, leads to the ratio:

$$\frac{n_n}{n_p} \simeq e^{-\frac{m_n - m_p - (\mu_n - \mu_p)}{T}}, \quad (5.3)$$

with  $m_n - m_p \simeq 1.293$  MeV.

At the moment of neutrino decoupling, the densities of all nuclei are set by nuclear statistical equilibrium. Fast nuclear and electromagnetic interactions keep nuclear species in chemical equilibrium. Due to chemical equilibrium and assuming negligible electron neutrino chemical potential, the neutron-to-proton ratio in thermal equilibrium before BBN becomes:

$$\frac{n_n}{n_p} \simeq e^{-\frac{m_n - m_p}{T}}. \quad (5.4)$$

The weak interaction processes  $n + e^+ \leftrightarrow p + \bar{\nu}_e$ ,  $p + e^- \leftrightarrow n + \nu_e$ ,  $n \leftrightarrow p + e^- + \bar{\nu}_e$  go out of equilibrium at the freeze-out temperature, which in the standard BBN is given by:

$$T_{fr} \simeq 0.7 \left( \frac{g^*}{10.75} \right)^{1/6} \text{ MeV} = 0.7 \text{ MeV}. \quad (5.5)$$

At freeze-out, the neutron-to-proton ratio is given by:

$$\left(\frac{n_n}{n_p}\right)_{fr} \simeq e^{-\frac{m_n - m_p}{T_{fr}}} \simeq \frac{1}{6}, \quad (5.6)$$

After freeze-out, the only process affecting the neutron-to-proton ratio is the neutron decay:

$$n \rightarrow p + e^- + \bar{\nu}_e. \quad (5.7)$$

At this stage, the photon temperature is already below the deuterium binding energy, however, since the large number of photons in the high-energy tail of the distribution break up nuclei as soon as they are formed, deuterium synthesis starts only when the photo-dissociation process becomes ineffective. Although  ${}^4\text{He}$  becomes thermodynamically favored before  ${}^2\text{H}$ , it cannot be produced in large quantities before  $T_{2H} \simeq 0.7$  MeV is reached because its production occurs through a chain of reactions which require a previous formation of  ${}^2\text{H}$ . This circumstance, denoted as *deuterium bottleneck*, leads to the effective BBN temperature  $T_{BBN} \simeq 0.07$  MeV, which corresponds to the BBN time  $t_{BBN} \simeq 150$  s. The neutron decay in the time interval from freeze-out to nucleosynthesis, lowers the neutron-to-proton ratio at the nucleosynthesis. Using the theoretical estimate of the neutron lifetime (Salvati et al. 2015)  $\tau_n \sim 883$  s, one gets the value:

$$\left(\frac{n_n}{n_p}\right)_{BBN} \simeq \frac{1}{7}. \quad (5.8)$$

Almost all neutrons end up by forming  ${}^4\text{He}$ , which is the most tightly bound stable light nucleus, with the resulting mass fraction of  ${}^4\text{He}$ :

$$Y_p \simeq \left(\frac{2n_n}{n_p + n_n}\right)_{BBN} = \frac{2(n_n/n_p)_{BBN}}{1 + (n_n/n_p)_{BBN}} \simeq 0.25. \quad (5.9)$$

The values of  $Y_p$  inferred from astrophysical data (which require the subtraction of  ${}^4\text{He}$  produced in stars and other astrophysical corrections) are in agreement with the approximate estimation in equation (5.9), confirming the basics of the standard BBN.

Note that positive chemical potential of electron neutrinos decreases the neutron-to-proton ratio at freeze-out, leading to a smaller abundance of  ${}^4\text{He}$  than in the standard BBN.

After the deuterium bottleneck is overcome at  $T_{BBN}$ , a large fraction of the available neutrons get bound in deuterium nuclei. This affects the subsequent nuclear processes in two ways. Firstly, the delayed population of deuterium results in BBN taking place at relatively low temperatures, with consequences for the efficiency of all the reactions which follow. Secondly, neutrons continue to decay until  $T_{BBN}$ , changing the neutron-to-proton ratio at the time of the effective  ${}^2\text{H}$  production. Deuterium production marks the beginning of the nuclear phase of BBN. The formation of heavier elements such as  ${}^3\text{H}$ ,  ${}^3\text{He}$ ,  ${}^4\text{He}$  proceeds through the interaction of deuterium nuclei with nucleons and other  ${}^2\text{H}$  nuclei, followed by  ${}^3\text{H}$  and  ${}^3\text{He}$  nucleon and deuterium capture processes.  ${}^7\text{Li}$  is produced via tritium and, for a sufficiently high baryon density, through  ${}^3\text{He}$  radiative capture on  ${}^4\text{He}$ . Thus, as a result of BBN, within just a few minutes, about a quarter of the baryonic matter of the universe is converted to  ${}^4\text{He}$ , while the rest remains as hydrogen H with tiny traces of deuterium and  ${}^7\text{Li}$ .

### 5.1.1 Neutron Decay

A basic parameter for estimating the nucleosynthesis effect is the baryon-to-photon ratio  $\eta = n_B/n_\gamma$ . The number of baryons per photon is related to the temperature and density of the early universe. In this sense, it allows to determine the conditions in which nucleosynthesis occurs and then the initial abundance of elements. Along with the parameter  $\eta$ , the nucleosynthesis of light elements is also based on other fundamental quantities, such as the rate of weak reactions, the rate of expansion of the universe and the neutron lifetime  $\tau_n$ .

The neutron decay process (5.7) is particularly important because it affects the n/p ratio at the onset of primordial nucleosynthesis as well as the light elements abundances produced in the standard BBN. The neutron lifetime determines the rate of weak-interaction processes. Indeed, the shorter the neutron lifetime, the faster weak reactions proceed and the earlier the neutrinos go out of thermodynamic equilibrium. A shorter neutron lifetime also leads to fewer neutrons in the period when weak interactions become frozen and nucleosynthesis begins. For instance, for a fixed value of  $\eta$ , a variation in the neutron lifetime by 1% changes the value of the initial abundance of  ${}^4\text{He}$  by 0.75% which is larger than the accuracy of measurement of the helium-4 abundance. Similarly, a variation in the neutron lifetime by 1% changes  $\eta$  by 17%, which is again larger than the accuracy of estimation of this quantity (Serebrov 2006 and references therein). Thus, the use of an accurate estimate of the neutron lifetime improves the agreement between the data on the initial abundances of deuterium and helium as well as those



on baryon asymmetry.

A theoretical estimate of  $\tau_n$ , when accuracy of the order of one percent is required, must include QED *outer* corrections (that is, nucleons are treated as a whole), and *inner* corrections which depend on the details of the nucleon structure. Perturbative QCD corrections, weak magnetism and finite nucleon mass effects, related to proton recoil, as well as the Fermi function describing the electron rescattering in the proton Coulomb field, must also be included. Taking into account all these corrections, the expression of the neutron lifetime takes the form:

$$\tau_n^{-1} = \frac{G_F^2 (C_V^2 + 3C_A^2)}{2\pi^3} \int_{m_e}^{\Delta} dp'_0 p'_0 |\mathbf{p}'| (p'_0 - \Delta)^2 \mathcal{G}(p'_0, q_0) \mathcal{F}(p'_0) \mathcal{L}(p'_0), \quad (5.10)$$

where the radiative corrections,  $\mathcal{G}(p'_0, q_0)$ , are given by:

$$\mathcal{G}(p'_0, q_0) = \left[ 1 + \frac{\alpha}{2\pi} \left( \ln \left( \frac{m_p}{M_A} \right) + 2C \right) + \frac{\alpha(m_p)}{2\pi} (g(p'_0, q_0) + A_g) \right] S(m_p, m_Z), \quad (5.11)$$

with  $\alpha(\mu)$ , the QED running coupling constant.  $g(p'_0, q_0)$  is a function of electron and neutrino energy, whose explicit expression can be found in Ref. (Sirlin 1967), and  $S(m_p, m_Z)$  is the short-distance enhancement factor:

$$S(m_p, m_Z) = \left( \frac{\alpha(m_c)}{m_p} \right)^{\frac{3}{4}} \left( \frac{\alpha(m_\tau)}{m_c} \right)^{\frac{9}{16}} \left( \frac{\alpha(m_b)}{m_\tau} \right)^{\frac{9}{16}} \left( \frac{\alpha(m_W)}{m_b} \right)^{\frac{9}{20}} \left( \frac{\alpha(m_Z)}{m_W} \right)^{\frac{36}{17}}. \quad (5.12)$$

The correction factor  $\mathcal{F}(p'_0) \mathcal{L}(p'_0)$ , due to the distortion of the outgoing electron wave function by the Coulomb field of the proton, is given by:

$$\mathcal{F}(p'_0) \mathcal{L}(p'_0) \simeq \left( 1 + \alpha\pi \frac{p'_0}{|\mathbf{p}'|} \right) \left[ 1 - \alpha R p'_0 \left( 1 + \frac{m_e^2}{2p_0'^2} \right) \right] \approx 1 + \alpha\pi \frac{p'_0}{|\mathbf{p}'|} = \mathcal{F}(p'_0), \quad (5.13)$$

with  $R \simeq 1$  fm, the radius of the proton charge distribution.

The value of parameters entering the above expression (5.10), such as vector and axial coupling  $C_V$  and  $C_A$ , fine structure constant, particle masses, strong coupling constant etc. has been updated to the most recent results reported in (Olive et al. 2014). Finally, the low energy cutoff applied to the short-distance part of the  $\gamma - W$  box diagram is chosen in the range  $M_A = (1 - 1.5)$  GeV.

The resulting value of our theoretical estimate for the neutron lifetime is:

$$\tau_n = (883 \pm 3)\text{s}, \quad (5.14)$$

where the theoretical error is obtained by propagating the uncertainties on all parameters to the value of  $\tau_n$  and is largely dominated by the present error on  $C_A/C_V$ .

Note that the theoretical estimate of  $\tau_n$  is still affected by smaller effects, such as higher order terms in  $\alpha$ , sub-leading corrections and residual average proton polarization due to parity non-conservation, however all these further corrections are expected to be quite sub-dominant (Esposito et al. 1999; Salvati et al. 2015 and references therein).

## 5.2 The Big Bang Nucleosynthesis and $N_{eff}$

Neutrinos play a relevant role in different processes in BBN. In particular, electron neutrino takes part in the pre-BBN neutron-proton transitions and nucleons freezing, thus affecting significantly the primordial production of the light elements. Hence, BBN is very sensitive to neutrino characteristics: number density of different neutrino types, neutrino-antineutrino asymmetries, presence of light sterile neutrino, deviations from thermal equilibrium of neutrino, neutrino decays, etc.

Primordial element abundances depend primarily on the neutron-to-proton ratio at the weak freeze out,  $(n/p)_{fr}$ , of the reactions that interchange neutrons and protons. Hence, the produced helium essentially depends on  $N_{eff}$ , since it depends on the competition between the weak interaction rate and the expansion rate  $H(T)$ , which determines the freezing temperature  $T_{fr}$ . It also depends on the baryon abundance (i.e. baryon asymmetry) and neutrino degeneracy (i.e. lepton asymmetry). After nucleon-antinucleon annihilation, the excess (i.e. nucleons, by definition,  $n_B - \bar{n}_B \rightarrow n_B \equiv n_N$ ) survives and the number of nucleons in a comoving volume is preserved until the present time.

After  $e^\pm$  annihilation, the ratio baryon-to-photon density  $\eta$  remains unchanged as the universe expands and cools. The present value of the baryon density is often measured by comparing the nucleon mass density to the critical mass density ( $\Omega_B \equiv \rho_B/\rho_c$ ). An asymmetry in the neutrino sector is strongly constrained by BBN. In particular, an asymmetry between electron neutrinos and electron antineutrinos has a direct effect on BBN through the charged current weak interactions which regulate the neutron-to-proton ratio. Since the relic abundance of  ${}^4\text{He}$  depends directly on the neutron-to-proton ratio when BBN begins and during BBN, it provides a strong bound on lepton asymmetry.

Flavor neutrino oscillations, with parameters favored by the atmospheric and solar neutrino data, lead to an equilibrium among active neutrino species before BBN epoch, so that the tight BBN bound on  $\nu_e$  degeneracy applies to all flavors. However, a lepton asymmetry  $L$  may possibly exist in the post-BBN. In the standard theories  $L$  is assumed to be of the same order of the baryon one  $\eta$ , whose value is given by independent and precise measurements (BBN, CMB). As a matter of fact, a value of  $L$  larger or even much larger than the baryon number  $\eta$  cannot be excluded on the basis of any theoretical principle. Charge neutrality indeed implies that the asymmetry in the electron sector must be of the same order of  $\eta$ . Since  $L$  is the sum of the asymmetries in the different neutrino sectors,  $L$  might be many orders of magnitude larger than  $\eta$ . A relic lepton asymmetry has been considered for overcoming the BBN constraints on neutrino oscillations involving eV sterile neutrino by preventing its thermalization, providing that this relic lepton asymmetry is large enough to suppress neutrino oscillations (Kirilova 2013 and references therein).

The presence of neutrino–antineutrino asymmetry when neutrinos are still interacting implies that their spectrum is described by a Fermi–Dirac distribution (4.1), characterized by neutrino degeneracy parameters  $\xi_\alpha \equiv \mu_{\nu_\alpha}/T_\nu$ , and the neutrino energy density, pressure and entropy density take the form in equations (4.4) - (4.6). Since the neutrino energy density (4.5) only contains even powers of  $\xi_\alpha$ , additional terms from nonzero asymmetries are always positive, thus enhancing the contribution of the radiation content. Expressing this contribution to  $\rho_R$  in terms of the effective number of neutrinos  $N_{eff}$ , one gets (neglecting the small effect of non-thermal neutrino distortions):

$$N_{eff} = 3 + \sum_{\alpha=e,\mu,\tau} \left[ \frac{30}{7} \left( \frac{\xi_\alpha}{\pi} \right)^2 + \frac{15}{7} \left( \frac{\xi_\alpha}{\pi} \right)^4 \right], \quad (5.15)$$

which means that any nonzero flavor neutrino asymmetry leads to  $N_{eff} > 3$ , without introducing additional relativistic species. Present cosmological observations are not sensitive to neutrino asymmetry if  $|L_\nu| \lesssim 10^{-2}$ . Higher values are required for a significant enhancement of  $N_{eff}$  or changings in the production of light elements during Big Bang nucleosynthesis. In particular, the primordial abundance of  ${}^4\text{He}$  is highly sensitive to the presence of an electron neutrino asymmetry leading to a stringent BBN bound on  $L_{\nu_e}$  which does not apply to the other flavors, as long as the effects of oscillations are not included.

As already mentioned, neutrino oscillations follow an MSW-like conversion when the vacuum term overcomes the matter potential. The amplitude of this effect depends upon the values of the parameter  $\Delta m^2$  as well as  $\theta_{13}$ , being larger as they grow.

Oscillations redistribute the asymmetries among the flavors, but only if they occur early enough the interactions would preserve Fermi–Dirac spectra for neutrinos, thereby leaving a chemical potential well defined for each  $L_{\nu_\alpha}$  and the relations (4.1) and (5.15) still valid. If the initial values of the flavor asymmetries have opposite signs, neutrino conversions will tend to reduce the asymmetries which in turn will decrease  $N_{eff}$ . However, if flavor oscillations take place at temperatures close to neutrino decoupling this would not happen, instead there would be an extra contribution of neutrinos to radiation with respect to the value in equation (5.15) (see Pastor et al., 2009).

Since, the BBN outcome depends on the expansion rate of the universe below MeV temperatures, when the universe is still radiation-dominated, this in turn means that it depends on  $N_{eff}$  as defined in equation (4.19). The effect of a variation of  $N_{eff}$  on the primordial production of light nuclei is that all abundances are modified, but especially the value of  $Y_p$ , because a larger  $N_{eff}$  produces a speed-up of the universe expansion, which in turn leads to an earlier n/p freeze-out, leading to a larger relic neutron abundance, and thus, to a higher production of  ${}^4\text{He}$ . A non-standard  $N_{eff}$  can be also caused by a population of light sterile neutrinos. Active-sterile oscillations can take place in two possible stages of the universe evolution, before or after the decoupling of the active neutrinos. If oscillations become effective before thermal decoupling, the abundance of sterile neutrinos grows via the conversion of the active states, kept in equilibrium by weak interactions. In this case, the sterile neutrinos contribution to  $\rho_R$  adds to that of the active states, increasing  $N_{eff}$  by a factor within 0 and 1 (for each sterile state), depending on the effectiveness of the sterile neutrinos thermalization. If, instead, active-sterile oscillations become effective after decoupling ( $T < 1$  MeV), the total number

of neutrinos is conserved and the main outcome is that large distortions may appear on the spectra of both the sterile and active states, which again has consequences on BBN, in particular when the active neutrinos are  $\nu_e$ .

The contribution from possible dark radiation (that is, sterile neutrinos) in  $\rho_R$  can be expressed in terms of an equivalent number of SM neutrinos,  $\Delta N_{eff}$ , which has the effect of increasing neutrinos contribution to the total radiation density. Namely, after  $e^\pm$  annihilation  $N_{eff}$  can be written as:

$$N_{eff} = 3.046 + \Delta N_{eff}. \quad (5.16)$$

A BBN determination of a nonzero  $\Delta N_{eff}$ , at a significant level of confidence, can provide evidence for new physics, that is, dark radiation such as one or more sterile neutrinos (thermally populated) or a modification of the equations describing the expansion rate of the early Universe (Steigman 2012).

### 5.3 Sterile Neutrino and Primordial Nucleosynthesis

As discussed in the previous sections, neutrinos are important in the BBN for two main reasons: electron neutrinos participate in the CC weak interactions that determine the neutron-to-proton ratio; neutrinos of all flavors affect the expansion rate of the universe before and during BBN, altering the neutron-to-proton ratio and hence the light element abundances, notably  $Y_p$ . The presence of sterile neutrinos therefore may affect BBN in two ways: distorting the  $\nu_e$  phase space distribution via flavor oscillations and increasing the Hubble expansion rate by modifying  $N_{eff}$ .

For sterile neutrinos with parameters according to terrestrial experiments, the first effect, is not expected to occur. In fact, the experimentally favored large mass-squared difference  $\Delta m^2 \sim 1 \text{ eV}^2$  and mixing  $\sin^2 2\theta \sim 10^{-3}$  between sterile and active states lead to full thermalization of the sterile species before the active neutrino decoupling. Consequently, the phase space distribution of the sterile states, as well as the active species, will follow a relativistic Fermi-Dirac distribution, thereby contributing an additional  $\Delta N_{eff} = 1$  for each sterile species. If active-sterile flavor oscillations take place after decoupling, the  $\nu_e$  phase space distribution will not deviate from a relativistic Fermi-Dirac distribution. Hence, under this assumption, the standard BBN scenario may account for the effects of sterile neutrinos by introducing just one extra parameter  $\Delta N_{eff}$  to  $N_{eff}$  (note that this may not hold in more complicated scenarios, such as models with a nonzero lepton asymmetry).

Since  $Y_p$  is the most sensitive probe of  $N_{eff}$ , whereas deuterium abundance  $D/H$ , is mainly sensitive to  $\eta$ , by combining the two one can constrain the two free parameters of the standard BBN with sterile neutrinos.

However, within the standard BBN scenario, models with more than one fully thermalized sterile species appears to be disfavored by current BBN data (Hamann et al. 2011). Furthermore, a thermal population of sterile neutrinos seems to be incompatible also with other cosmological observables. As already mentioned in Section 4.1.1, in order to relieve this tension, different mechanisms to suppress the sterile neutrino thermalization and their eventual large production have been studied. In particular, the existence of neutrino asymmetries (Mirizzi et al. 2012; Saviano et al. 2013) or the introduction of secret interactions among sterile neutrinos. Several models of secret self-interactions have been proposed, where the mediator can be a heavy gauge boson (Hannestad et al. 2014), a light “dark photon” (Dasgupta & Kopp 2014), a light scalar or pseudoscalar (Archidiacono et al. 2014). Let us see now, with some more details, the implications of the introduction of secret interactions on  $N_{eff}$ .

It has been shown that secret interactions also generate strong collisional terms in the sterile neutrino sector that induce an efficient sterile neutrino production after a resonance in matter is encountered, which increases their contribution to the number of relativistic particle species  $N_{eff}$  (Saviano et al. 2014). Moreover, for values of the parameters of the  $\nu_s - \nu_s$  interactions such that the resonance takes place at temperature  $T \lesssim$  few MeV, significant distortions can be expected in the electron (anti)neutrino spectra, which would alter the abundance of light elements in the BBN.

When the matter potential induced by the secret interactions in the sterile sector becomes of the order of the active-sterile vacuum oscillation frequency, a resonance is encountered which enhances the in-medium mixing angle, leading to a resonant flavor conversion among active and sterile neutrinos similar to the MSW effect. Moreover, the presence of strong collisional effects in the sterile sector due to  $\nu_s - \nu_s$  secret interactions, on one hand would damp the MSW conversions, on the other would increase the sterile neutrino production via non-resonant processes (Kainulainen 1990). In particular, the latter can redistribute momenta among sterile neutrinos bringing the active-sterile neutrino ensemble towards the flavor equilibrium (see Saviano et al. 2014 and references therein). In fact, as long as the scattering rate of the secret self-interactions is larger than the Hubble parameter sterile neutrinos will soon reach the Fermi-Dirac distribution, with  $n_s = n_\alpha$ .

For a quite large range of the model parameters (i.e. coupling constants  $\gtrsim 10^{-2}$  and masses of the gauge boson  $> 10$  MeV), resonances may take

place in a range of temperatures relevant for BBN, which leads to a shift of  $N_{eff}$  to larger values by a  $\Delta N_{eff}$  dependent on the model parameters. For a fixed baryon density an increase of  $\Delta N_{eff}$  implies an increase in the freezing temperature, which in turn leads to a higher number of neutrons available at the onset of deuterium formation and this translates into a larger value of  $Y_p$ . This effect could be compensated if electron neutrino number density is larger, since in this case weak rates get increased. However, models of secret interaction in the sterile sector typically lead to a smaller electron neutrino density  $\rho_{ee} < 1$ . A positive  $\Delta N_{eff}$  and less electron neutrinos both lead to a larger  $Y_p$ . As regards deuterium, as a result of a larger  $N_{eff}$ ,  ${}^2\text{H}/\text{H}$  density ratio excludes much of the parameter space of this kind of models, if one assume a baryon density at the best fit value of Planck experiment,  $\Omega_B h^2 = 0.02207$  (these bounds become weaker for a higher baryon density, taken as the upper bound of Planck).

In the case of light bosons (Dasgupta & Kopp 2014), the advantage is a matter-induced potential sufficiently strong as to inhibit any sterile neutrino production during BBN, thus evading the related constraints. Moreover, if the new interaction mediator couples to both sterile neutrinos and dark matter particles, for the considered small masses there also exists the possibility of relieving some of the small-scale structure problems of the cold dark matter scenario. The case of secret interactions among sterile neutrinos mediated by very light pseudoscalars and a possible connection with dark matter has been also explored in (Archidiacono et al. 2014). The outcome of this type of studies is that also for small masses a large sterile neutrino production is unavoidable at  $T \ll 0.1$  MeV, when the matter potential becomes smaller than the vacuum oscillation term. As the small vacuum oscillations can trigger a scattering-induced decoherent production of sterile neutrinos, this process leads to a flavor equilibration among the active and the sterile neutrino species after the active neutrino decoupling. Besides, since the rate of sterile neutrino re-thermalization is extremely fast, the process is almost instantaneous. This means that, if the initial state is described by a density matrix  $\rho = \text{diag}(\rho_{ee}, \rho_{\mu\mu}, \rho_{\tau\tau}, \rho_{ss}) = (1, 1, 1, 0)$ , for all the parameter space favored by the eV sterile neutrino anomalies, the final state that is quickly reached will be described by (Mirizzi et al. 2015):

$$\rho = \text{diag}(\rho_{ee}, \rho_{\mu\mu}, \rho_{\tau\tau}, \rho_{ss}) = (3/4, 3/4, 3/4, 3/4). \quad (5.17)$$

The above result is independent of the particular values of the coupling and the boson mass. Furthermore, the final equilibrium value is also independent

of the values of the active-sterile neutrino mixing angles. Also assuming that the sterile species mixes only with an active one, the equilibrium will involve all flavors, due to the active mixing angles connecting the different species. It only depends on the realization of the condition of strong damping. The same equilibrium value still holds true for a wide range of masses of the mediator boson, as long as  $T_\nu$  is larger than the boson mass. In fact, for large enough values of the coupling ( $\gtrsim 10^{-2}$ ) and masses of the mediator  $\gtrsim 10$  MeV, the sterile neutrino production would occur at  $T \gtrsim 0.1$  MeV, which would have significant effects on the BBN. Moreover, resonances occurring at  $T \lesssim$  few MeV happen late enough to produce significant distortions in the electron (anti)neutrino spectra, which also would affect the abundance of light elements BBN. Conversely, models with couplings in the same range and gauge boson mediators with masses  $\lesssim 10$  MeV succeed in suppressing the sterile neutrino production before the neutrino decoupling, leaving unaffected the BBN, but the subsequent large sterile neutrino production and flavor equilibration has consequences on  $N_{eff}$  at matter radiation equality and recombination. After the sterile states produced via oscillations have reached kinetic equilibrium through secret interactions, in a 3+1 scheme one has four species sharing a common temperature  $T_\nu = (4/11)^{1/3} (3/4)^{1/3} T_\gamma$ . Correspondingly, as long as all neutrinos are fully relativistic the effective number of neutrino species reduces to a value:

$$N_{eff} \sim 2.7. \tag{5.18}$$

Moreover, for a boson mass larger than the coupling, sterile neutrinos would be free-streaming at the matter-radiation equality epoch.  $\nu_s$  free streaming until the epoch when they become nonrelativistic would affect the large-scale structure power spectrum, suppressing the growth of perturbations on small scales. As a consequence, for this range of parameters the large sterile neutrino production of eV mass scale would be in tension with the current cosmological mass bounds on sterile neutrinos. On the other hand, if sterile states experience secret interactions, the free-streaming regime is delayed until the scattering rate becomes smaller than the Hubble parameter. This means that for some values of the model parameters such that this condition holds at the non relativistic transition, sterile neutrinos would diffuse, without ever having a free streaming phase.

Regarding secret interactions in the sterile sector mediated by a light pseudoscalar (Archidiacono et al. 2014), the mechanism of sterile neutrino production and flavor equilibration would apply similarly, at least to all



cases where the coupling is  $\gtrsim 10^{-6}$ , which implies a  $\nu_s$ -pseudoscalar plasma strongly interacting until sterile neutrinos become nonrelativistic.

This leads to the conclusion that the scenarios of secret self-interactions studied so far are not sufficient to reconcile sterile neutrinos with cosmology. The new picture, that we will introduce in Chapter 6, consists in assuming the same secret interactions with a light pseudoscalar as the source of sterile neutrino production by oscillations (when they involve active species) and in addition, along with the self-interactions  $\nu_s - \nu_s$  we will also consider  $\nu_s - \phi$  interactions in the sterile sector.

## Neutrino Interactions with a Light Pseudoscalar

Spin-0 particles light and weakly interacting are predicted by many extensions of the Standard Model of Particle Physics. Assuming the existence of a light scalar particle in the background medium, it has been shown (Sawyer 2011) that sterile neutrino production can occur through a collective effect induced by a minimal Yukawa coupling of a Dirac neutrino to such a light scalar particle. Starting with an initial thermalized state of active neutrinos and anti-neutrinos, sterile states may arise through a sudden reversal of their helicities as a consequence of the instability experienced.

A similar study will be applied in the following sections to the case of a light pseudoscalar particle as a mediator of Yukawa interactions. Such a field might arise as pseudo-Nambu-Goldstone boson of a spontaneously broken chiral symmetry, first introduced by Peccei and Quinn (Peccei & Quinn 1977) to address the problem of strong CP violation.

### 6.1 Active-Sterile Neutrino Interactions

Possible additional interactions of active neutrinos with a light pseudoscalar can be described by the interaction Hamiltonian:

$$\mathcal{H}^Y = ig_\phi \bar{\nu}_s \gamma_5 P_L \nu_\alpha \phi + h.c. \quad (6.1)$$

where  $\nu$  and  $\phi$  are the neutrino and pseudoscalar fields respectively,  $g_\phi$  is a dimensionless hermitian matrix of coupling constants, assumed for simplicity to be diagonal,  $g_\phi = \text{diag}(g_{e\phi}, g_{\mu\phi}, g_{\tau\phi}, 0)$ .

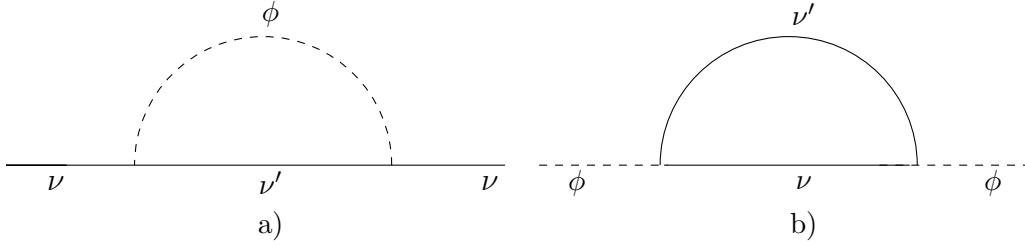


Figure 6.1: Bubble contributions to neutrino and pseudoscalar self-energy.

The refractive energy shifts due to neutrino interactions is generally given by the bubble and tadpole contributions to neutrino self-energy. Since the Hamiltonian (6.1) mixes active and sterile states, the tadpole term is not present. Thus the only contributions come from the bubble terms. In particular, considering a test neutrino  $\nu_\alpha$ , with  $\alpha = e, \mu, \tau$ , interacting with a sterile neutrino background,  $\nu_s$  ( $\nu'$  in Figure 6.1a):

$$i\Sigma_{bubble}(p) = -(ig_\phi)^2 \int \frac{d^4q}{(2\pi)^4} P_R \gamma_5 i S_T(q) \gamma_5 P_L i D_T^\phi(\Delta), \quad (6.2)$$

where,  $D_T^\phi$  and  $S_T$  are the thermal propagators of the pseudoscalar particle and neutrino, respectively defined as:

$$iD_T^\phi(k) = \left[ \frac{i}{k^2 - m_\phi^2 + i\epsilon} + \Gamma_B(k) \right] \quad (6.3)$$

with,

$$\Gamma_B(k) = 2\pi\delta(k^2 - m_\phi^2)\eta_B(k, \mu, \beta) \quad (6.4)$$

and

$$\eta_B(k, \mu, \beta) = \Theta(k \cdot u) f_B(k, \mu, \beta) + \Theta(-k \cdot u) \bar{f}_B(k, -\mu, \beta), \quad (6.5)$$

where  $k \cdot u = \mathcal{E}_k$  is the energy of the neutrino in the rest frame of the medium, and

$$f_B(k, \mu, \beta) = \frac{1}{e^{\beta(|k \cdot u| - \mu)} - 1} \quad (6.6)$$

is the Bose-Einstein distribution function. The pseudoscalar particle will be assumed as a real singlet field, so that  $f_B = \bar{f}_B$ .

$$iS_T(k) = (k + m) \left[ \frac{i}{k^2 - m^2 + i\epsilon} - \Gamma_F(k) \right] \quad (6.7)$$

with,

$$\Gamma_F(k) = 2\pi\delta(k^2 - m^2)\eta_F(k, \mu, \beta) \quad (6.8)$$

$$\eta_F(k, \mu, \beta) = \Theta(k \cdot u)f_F(k, \mu, \beta) + \Theta(-k \cdot u)\bar{f}_F(k, -\mu, \beta) \quad (6.9)$$

$$f_F(k, \mu, \beta) = \frac{1}{e^{\beta(|k \cdot u| - \mu)} + 1} \quad (6.10)$$

and an analogous expression for the Fermi-Dirac distribution function  $\bar{f}_F$  of the anti-particle, with opposite sign for the chemical potential.

By substitution of the propagator expressions, the expression (6.2) becomes:

$$\begin{aligned} \Sigma_{bubble}(p) = & -ig_\phi^2 \int \frac{d^4q}{(2\pi)^4} P_R \gamma_5 \left( \frac{i(\not{q} + m)}{q^2 - m^2} - (\not{q} + m) \Gamma_F(q) \right) \\ & \times \gamma_5 P_L \left( \frac{i}{\Delta^2 - m_\phi^2} + \Gamma_B(\Delta) \right), \end{aligned} \quad (6.11)$$

which provides the following matter-induced potential:

$$V_{\alpha s}(\mathbf{p}) = \frac{g_\phi^2}{8\pi^2 |\mathbf{p}|} \int_0^\infty d|\mathbf{q}| |\mathbf{q}| [(\rho_{\mathbf{q}} + \bar{\rho}_{\mathbf{q}} + f_\phi(\mathbf{q})\mathbb{1})]_{\alpha s}, \quad (6.12)$$

which, because of the dependence on the inverse momentum, grows with the cosmological expansion.

In the above equation (6.12) a logarithmic term proportional to  $m_\phi/(4|\mathbf{p}||\mathbf{q}|) \ll 1$  has been neglected. Note that  $V_{\alpha s}$  does not change sign for anti-neutrino test particle, since one has to replace both  $g_\phi^2 \rightarrow -g_\phi^2$  and  $p_0 \simeq |\mathbf{p}| \rightarrow p_0 \simeq$

–  $|\mathbf{p}|$ .

Consider now the analogous contribution to the neutrino potential due to sterile neutrinos interactions with a background of active neutrinos. For a sterile neutrino,  $\nu_s$ , forward scattering on a background active neutrino,  $\nu_\alpha$ , the bubble term,

$$i\Sigma_{bubble}(p) = -(ig_\phi)^2 \int \frac{d^4q}{(2\pi)^4} \gamma_5 P_L i S_T(q) P_R \gamma_5 i D_T^\phi(\Delta), \quad (6.13)$$

provides the additional contribution to the neutrino potential energy:

$$V_{s\alpha}(\mathbf{p}) = \frac{g_\phi^2}{8\pi^2 |\mathbf{p}|} \int_0^\infty d|\mathbf{q}| |\mathbf{q}| [(\rho_{\mathbf{q}} + \bar{\rho}_{\mathbf{q}} + f_\phi(\mathbf{q})\mathbb{1})]_{s\alpha}. \quad (6.14)$$

The above results have been obtained considering a single sterile species and in the limit of massless neutrinos for all species. This is a reasonable approximation for nearly ultra-relativistic neutrinos in the early universe. Taking  $m \neq 0$  would provide an additional term to the neutrino potential  $\sim m/|E_{\mathbf{q}}|$ , where  $m$  in eq. (6.12) is the sterile neutrino mass, while in eq. (6.14) is the mass of the background active neutrino, and a further logarithmic term, as it will be shown for a model 1 + 1 with a single species for both active and sterile species.

As regards the corrections to the pseudoscalar propagator (figure 6.1b), the leading order thermal contribution to the bubble diagram is given by:

$$\begin{aligned} \Sigma_{bubble}(q) = & -g_\phi^2 \int \frac{d^4p}{(2\pi)^4} Tr \left[ \frac{(\not{q} - \not{p} + m_s)}{(q-p)^2 - m_s^2} P_R (\not{p} + m_\alpha) P_L 2\pi\delta(p^2 - m_\alpha^2) \eta_F^\alpha + \right. \\ & \left. (\not{q} - \not{p} + m_s) \frac{P_R (\not{p} + m_\alpha) P_L}{p^2 - m_\alpha^2} 2\pi\delta((q-p)^2 - m_s^2) \eta_F^s \right]. \end{aligned} \quad (6.15)$$

Neglecting the active neutrino mass and logarithmic terms of order  $\mathcal{M}^2/|\mathbf{q}|$ , where  $\mathcal{M}^2$  can be the mass squared difference or the sum, we find:

$$V_\phi(\mathbf{p}) = \frac{g_\phi^2}{2\pi^2} \int_0^\infty d|\mathbf{p}| |\mathbf{p}| [f_\alpha(\mathbf{p}) + \bar{f}_\alpha(\mathbf{p}) + f_s(\mathbf{p}) + \bar{f}_s(\mathbf{p})]. \quad (6.16)$$

## 6.2 Matter Potential in the Sterile Sector

Consider the Yukawa interaction in the sterile sector, described by the Hamiltonian:

$$\mathcal{H}^Y = iG_\phi \bar{\nu}_{s_i} \gamma_5 \nu_{s_j} \phi + h.c. \quad (6.17)$$

In the case under examination there is also a tadpole term to be taken into account:

$$i\Sigma_{tadpole}(p) = (iG_\phi)^2 \gamma_5 iD_T^\phi(\Delta) \int \frac{d^4q}{(2\pi)^4} Tr [\gamma_5 i S_F(q)]. \quad (6.18)$$

Since the momentum conservation implies zero momentum transfer,  $\Delta = p - q = 0$ , equation (6.18) becomes:

$$i\Sigma_{tadpole}(p) = -(iG_\phi)^2 \gamma_5 \left( \frac{-i}{m_\phi^2} \right) \int \frac{d^4q}{(2\pi)^4} Tr [\gamma_5 (\not{q} + m_s)]. \quad (6.19)$$

For antineutrinos as test particles the above contribution changes sign.

However, the tadpole term (6.19) does not contribute to the neutrino self-energy, since the product of  $n$   $\gamma$  matrices containing  $\gamma_5$  for  $n < 5$  has zero trace as well as the product of an odd number of  $\gamma$  matrices:

$$\Sigma_{tadpole}(p) = -\frac{G_\phi^2}{m_\phi^2} \gamma_5 \int \frac{d^3q}{(2\pi)^3} Tr [\gamma_5 (\not{q} + m_s) (\rho_{\mathbf{q}} - \bar{\rho}_{\mathbf{q}})] \frac{1}{2|E_{\mathbf{q}}|} = 0. \quad (6.20)$$

Note that the tadpole term would not be zero if instead of a pseudoscalar we consider a scalar mediator:

$$\Sigma_{tadpole}(p) = -\frac{G_\phi^2}{2m_\phi^2} \int \frac{d^3q}{(2\pi)^3} Tr [(\rho_{\mathbf{q}} - \bar{\rho}_{\mathbf{q}})] \frac{m_s}{|E_{\mathbf{q}}|}. \quad (6.21)$$

As for the bubble term, generalizing to the case of sterile species of different flavor and assuming that the coupling constant matrix in the above interaction Hamiltonian is  $G_\phi = \text{diag}(g_{ee}^s, g_{\mu\mu}^s, g_{\tau\tau}^s, 0)$ , the effective matter produced by the bubble contribution has the form:

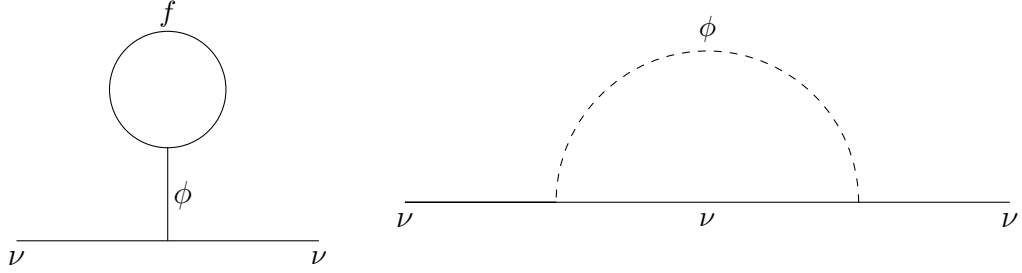


Figure 6.2: Tadpole and bubble contributions to sterile neutrino self-energy.

$$V_{ij}(\mathbf{p}) = \frac{G_\phi^2}{8\pi^2 |\mathbf{p}|} \int_0^\infty d|\mathbf{q}| |\mathbf{q}| [(\rho_{\mathbf{q}} + \bar{\rho}_{\mathbf{q}} + f_\phi(\mathbf{q})\mathbb{1})]_{ij}. \quad (6.22)$$

Sterile neutrinos compatible with the experimental data should have masses heavier than the active species, of the order of eV. Furthermore, since BBN considerations (Esposito et al. 1999) seem to disfavor a model with more than one additional sterile species, let's assume that only a single sterile neutrino is present and consider the effects of non negligible mass at temperatures around the eV.

The boson part in equation (6.22) including all contributions becomes:

$$V^{(\phi)} = \frac{g_\phi^2}{16\pi^2 |\mathbf{p}|} \int_0^\infty d|\mathbf{q}| |\mathbf{q}| f_\phi(E_\phi) \left\{ \frac{m}{E_\phi} \ln \left( \frac{2E_{\mathbf{p}}E_\phi(1 + v_{\mathbf{p}}v_\phi) - m_\phi^2}{2E_{\mathbf{p}}E_\phi(1 - v_{\mathbf{p}}v_\phi) - m_\phi^2} \right) + \left( \frac{m_\phi^2 E_{\mathbf{p}}}{2|\mathbf{p}|^2 E_\phi} - \frac{m^2}{|\mathbf{p}|^2} \right) \ln \left( \frac{2E_{\mathbf{p}}E_\phi(1 + v_{\mathbf{p}}v_\phi) - m_\phi^2}{2E_{\mathbf{p}}E_\phi(1 - v_{\mathbf{p}}v_\phi) - m_\phi^2} \right) + \frac{2v_\phi}{v_{\mathbf{p}}} \right\}, \quad (6.23)$$

whereas the part related to the neutrino distribution becomes:

$$V^{(\nu)} = \frac{g_\phi^2}{16\pi^2 |\mathbf{p}|} \int_0^\infty d|\mathbf{q}| |\mathbf{q}| \left\{ \frac{m}{E_{\mathbf{q}}} (f_\nu(E_{\mathbf{q}}) - \bar{f}_\nu(E_{\mathbf{q}})) \ln \mathcal{E} + (f_\nu(E_{\mathbf{q}}) + \bar{f}_\nu(E_{\mathbf{q}})) \kappa \left( \frac{m_\phi^2 E_{\mathbf{p}}}{2|\mathbf{p}|^2 E_{\mathbf{q}}} - \frac{m^2(E_{\mathbf{p}} - E_{\mathbf{q}})}{|\mathbf{p}|^2 E_{\mathbf{q}}} \right) \ln \mathcal{E} + \frac{2v_{\mathbf{q}}}{v_{\mathbf{p}}} \right\} \quad (6.24)$$

with,

$$\mathcal{E} = \frac{2E_{\mathbf{p}}E_{\mathbf{q}}(1 + v_{\mathbf{p}}v_{\mathbf{q}}) + \kappa(m_{\phi}^2 - 2m^2)}{2E_{\mathbf{p}}E_{\mathbf{q}}(1 - v_{\mathbf{p}}v_{\mathbf{q}}) + \kappa(m_{\phi}^2 - 2m^2)} \quad (6.25)$$

and  $\kappa = \pm 1$  takes into account of the sign associated to the background neutrino and antineutrino respectively,  $q_0 = \pm |E_{\mathbf{q}}|$ , in the shorthand notation of the above equation (6.24).

### 6.3 The Collision Integrals

The kinetic equations which describe the time evolution of the density matrices  $\rho_{\mathbf{q}}$  and  $\bar{\rho}_{\mathbf{q}}$  also include a Boltzmann collision integral accounting for non-forward collisions:

$$\dot{\rho}_{\mathbf{p}} = -i[\Omega_{\mathbf{p}}, \rho_{\mathbf{p}}] + C[\rho_{\mathbf{p}}] \quad (6.26)$$

$$\dot{\bar{\rho}}_{\mathbf{p}} = i[\Omega_{\mathbf{p}}, \bar{\rho}_{\mathbf{p}}] + C[\bar{\rho}_{\mathbf{p}}], \quad (6.27)$$

where  $\Omega_{\mathbf{p}}$  comprises all the relevant contributions to the refractive energy shifts due to different medium components and the collision operator  $C[\cdot]$  represents the rate of change of the particle distribution due to the different types of neutrino interactions, depending on the cases under consideration. Namely, in the active neutrino sector,  $\Omega_{\mathbf{p}}$  takes the form:

$$\Omega_{\mathbf{p}} = \Omega_{\mathbf{p}}^{Vac} + \Omega_{\mathbf{p}}^{Weak} + \Omega_{\mathbf{p}}^Y, \quad (6.28)$$

where  $\Omega_{\mathbf{p}}^{Vac}$  describes oscillations in vacuum,  $\Omega_{\mathbf{p}}^{Weak}$ , includes all weak interactions in charged and neutral currents with other leptons and neutrino self-interactions, and  $\Omega_{\mathbf{p}}^Y$  are the above calculated matter potential terms, (6.12) and (6.14), due to the additional neutrino interactions with the pseudoscalar particle.

Since sterile neutrinos have no weak interactions, in the sterile sector  $\Omega_{\mathbf{p}}$  is given by the Yukawa term (6.22).

Similarly, the collision integral is given by:

$$C[\rho_{\mathbf{p}}] = (C[\rho_{\mathbf{p}}])^{Weak} + (C[\rho_{\mathbf{p}}])^Y, \quad (6.29)$$



where  $(C[\rho_{\mathbf{p}}])^{Weak}$  consists of all possible second order weak processes involving neutrinos and other leptons and  $(C[\rho_{\mathbf{p}}])^Y$  is related to the Yukawa interactions with the pseudoscalar  $\phi$ .

Different approximate forms for the collision terms can be used, such as the Relaxation Time Approximation (RTA), introduced for small deviations of the distribution function from its equilibrium state (Lundstrom 2000). This approximation well describes realistic situations, when the scattering is isotropic or elastic. The relaxation time  $\tau = 1/\Gamma$ , depends only on the nature of the scattering process. For isotropic scattering it is the average time between collisions. For elastic scattering there will be a weighting factor.

By means of the RTA, the collision term can be expressed as:

$$\dot{\rho}_{\mathbf{p}}^{coll} = -\Gamma (\rho_{\mathbf{p}} - \rho_{\mathbf{p}}^{eq}) \quad (6.30)$$

and an analogue equation for  $\bar{\rho}$ , where  $\Gamma = n \langle \sigma |v| \rangle = 1/\tau$  is the interaction rate,  $\langle \sigma |v| \rangle$  is the thermally averaged product of cross section and relative speed of the colliding particles, and  $\rho^{eq}$  (or  $\bar{\rho}^{eq}$ ) is essentially the unit matrix with coefficient the equilibrium distribution function  $f^{eq}$  (or  $\bar{f}^{eq}$ ).

Using an alternative approximation procedure (Chu & Cirelli 2006) based on a second quantized formalism (Raffelt & Sigl 1993), the collision term takes the form:

$$\dot{\rho}_{\mathbf{p}}^{coll} = -\frac{\Gamma}{2} (\{G_s^2, \rho - \rho^{eq}\} - 2G_s (\rho - \rho^{eq}) G_s + \{G_a^2, (\rho - \rho^{eq})\} + 2G_a (\rho - \rho^{eq}) G_a) \quad (6.31)$$

$$\dot{\bar{\rho}}_{\mathbf{p}}^{coll} = -\frac{\Gamma}{2} (\{G_s^2, \bar{\rho} - \bar{\rho}^{eq}\} - 2G_s (\bar{\rho} - \bar{\rho}^{eq}) G_s + \{G_a^2, (\bar{\rho} - \bar{\rho}^{eq})\} + 2G_a (\bar{\rho} - \bar{\rho}^{eq}) G_a) \quad (6.32)$$

where  $G_s$  and  $G_a$  are diagonal matrices formed by the numerical coefficients for the scattering and annihilation processes for the different flavors; the neutrino and antineutrino distributions,  $\rho_{\mathbf{p}}(t)$  and  $\bar{\rho}_{\mathbf{p}}(t)$ , are approximated as Fermi-Dirac functions with a negligibly small chemical potential, multiplied by an overall normalization factor, meant as an average of the available phase space,

$$\rho_{\mathbf{p}}(t) = \rho(t) f_F(\mathbf{p}), \quad \bar{\rho}_{\mathbf{p}}(t) = \bar{\rho}(t) f_F(\mathbf{p}). \quad (6.33)$$

Pointing out that in the Chu & Cirelli approximation only the annihilation processes contribute to the repopulation term (reasonable for the momentum-averaged quantum rate equations but not rigorously correct in the momentum-dependent quantum kinetic equations where elastic scattering processes is also expected to contribute to the momentum equilibration) a different repopulation approximation scheme has been developed by Hannestad and colleagues, called the A/S approximation, where the annihilation and scattering terms are kept separate (Hannestad et al. 2015).

The total reaction rate  $\Gamma$ , associated with the new interaction involving active and sterile species, which enters the collision integrals is given by:

$$\Gamma_{ij} = \langle \sigma_{ij} v_{ij} \rangle n_j = \frac{1}{n_i} \int d^3 p_i d^3 p_j f(p_i) f(p_j) \sigma_{ij} v_{ij}, \quad (6.34)$$

where

$$n_{i,j} = g_{i,j} \int \frac{d^3 p_{i,j}}{(2\pi)^3} f(p_{i,j}) \quad (6.35)$$

is the number density of the colliding particles.

The cross section  $\sigma_{ij}$  for the various processes under consideration is estimated for the case of active neutrinos with negligible mass, whereas the sterile neutrino masses are kept everywhere non-vanishing, for different values of the mass of the light particle  $\phi$ , ranging from the value of the active neutrino mass (therefore negligible) to that of the sterile.

Consider first the interactions between active and sterile neutrinos related to the Hamiltonian (6.1). For all the allowed processes, the cross section is calculated in the center of mass frame.

The various reactions mediated by the pseudoscalar  $\phi$  provide the following cross sections times relative velocity:

$$\begin{aligned} \text{a)} \quad & \nu_\alpha \nu_s \longleftrightarrow \nu_\alpha \nu_s \\ \sigma |v| = & \frac{g_\phi^4 (1 - v_p \cos \theta)}{64\pi s} \left\{ 1 - \frac{4\Delta^2 s^2}{(s - m_s^2)^4 - [m_s^4 - s(s - 2\Delta)]^2} \right. \\ & \left. + \frac{2s\Delta}{(s - m_s^2)^2} \ln \left| \frac{s(s + m_\phi^2 - 2m_s^2)}{(m_\phi^2 s - m_s^4)} \right| \right\} \end{aligned} \quad (6.36)$$

where  $\Delta = m_s^2 - m_\phi^2$ .

And for the processes related to the above by crossing symmetry the cross sections are given by:

$$\sigma |v| = \frac{g_\phi^4 (1 - v_p \cos \theta)}{64\pi s} \left\{ 1 + \frac{2\Delta}{(s - m_s^2)} \ln \left| \frac{m_\phi^2 s + (s - m_s^2)^2}{m_\phi^2 s} \right| + \frac{s (m_\phi^2 - 2m_s^2)}{m_\phi^2 s + (s - m_s^2)^2} \right\} \quad (6.37)$$

and

$$\sigma |v| = \frac{g_\phi^4 (1 - v_p \cos \theta)}{64\pi s} \left\{ \frac{(s - m_s^2)^2}{(s - m_\phi^2)^2 + \Gamma_D^2 m_\phi^2} \right\} \quad (6.38)$$

where  $\Gamma_D$  is the  $\phi$  particle decay rate:

$$\Gamma_D = \frac{g_\phi^2}{16\pi} \frac{(m_\phi^2 - m_s^2)^2}{m_\phi^3} \quad (6.39)$$

For  $m_\phi \rightarrow 0$  equation (6.36) reduces to:

$$\sigma |v| \simeq \frac{g_\phi^4 (1 - \cos \theta)}{64\pi s} \left\{ 1 - \frac{s}{s - 2m_s^2} + \ln \left| \frac{s (s - 2m_s^2)}{m_s^4} \right| \right\} \quad (6.40)$$

Since in the limit of negligible mass,  $m_\phi \rightarrow 0$ , equation (6.37) has a divergent logarithmic term, keeping  $m_\phi$  non zero only in that term,

$$\sigma |v| \simeq \frac{g_\phi^4 (1 - \cos \theta)}{64\pi s} \left\{ 1 + \left( \frac{2m_s^2}{s - m_s^2} \right) \ln \left| \frac{m_\phi^2 s + (s - m_s^2)^2}{m_\phi^2 s} \right| + \frac{2m_s^2}{(s - m_s^2)} \right\} \quad (6.41)$$

Further allowed processes yield:

$$\sigma |v| = \frac{g_\phi^4 (1 - v_q \cos \theta)}{64\pi s} \left\{ \frac{(s - m_s^2)^2}{(s - m_\phi^2)^2 + \Gamma_D^2 m_\phi^2} + \frac{\Delta^2 s}{m_s^2 (s - m_s^2)^2 + \Delta (m_s^4 - s^2 + s\Delta)} + 1 - \frac{(s - m_s^2)}{(s - m_\phi^2)} + \ln \left| \frac{s (s + m_\phi^2 - 2m_s^2)}{(m_\phi^2 s - m_s^4)} \right| \left[ \frac{2\Delta s}{(s - m_s^2)^2} + \frac{2s (m_\phi s - m_s^4)}{(s - m_s^2)^2 (s - m_\phi^2)} \right] \right\} \quad (6.42)$$

and

$$\sigma |v| = \frac{g_\phi^4 (1 - \cos \theta)}{64\pi s} \left\{ \frac{2\Delta^2 s}{m_\phi^2 [m_\phi^2 s + (s - m_s^2)^2]} - \frac{\Delta^2 s}{(2m_s^2 - m_\phi^2) (m_\phi^2 s - m_s^4)} + \right. \\ \left. \ln \left| \frac{m_\phi^2 s + (s - m_s^2)^2}{m_\phi^2 s} \right| \left[ \frac{2\Delta s}{(s - m_s^2)^2} + \frac{(2\Delta s - s^2 - m_s^4) (2\Delta s - s^2 + m_s^4)}{4s (2\Delta - s) (s - m_s^2)^2} + \right. \right. \\ \left. \frac{s (2Ms - s^2 - m_s^4 + 2\Delta^2)}{2 (2\Delta - s) (s - m_s^2)^2} \right] + \ln \left| \frac{s (2m_s^2 - m_\phi^2 - s)}{\Delta s - m_s^2 (s - m_s^2)} \right| \left[ \frac{2\Delta s}{(s - m_s^2)^2} - \right. \\ \left. \frac{(2\Delta s - s^2 - m_s^4) (2\Delta s - s^2 + m_s^4)}{4s (2\Delta - s) (s - m_s^2)^2} - \frac{s (2Ms - s^2 - m_s^4 + 2\Delta^2)}{2 (2\Delta - s) (s - m_s^2)^2} \right] \left. \right\}, \quad (6.43)$$

where  $M = m_s^2 + m_\phi^2$ .

Now consider neutrino interactions with a background of pseudoscalar particles. The allowed processes involve an active or sterile neutrino propagator.

$$b) \quad \nu_\alpha \phi \longleftrightarrow \nu_\alpha \phi$$

The cross section for active neutrino interactions with a background of pseudoscalar particles yields:

$$\sigma |v| = \frac{g_\phi^4 (1 - v_q \cos \theta)}{64\pi s} \left\{ \frac{m_\phi^4 - s^2 + 2\Delta s}{2 (s - m_s^2)^2} + \frac{2s}{s + m_s^2 - 2m_\phi^2} + \right. \\ \left. \frac{s^2 (s + 2\Delta + m_s^2) + 2m_\phi^2 s (m_\phi^2 - 2s)}{(s - m_\phi^2)^2 (s + m_s^2 - 2m_\phi^2)} \ln \left| \frac{s (m_s^2 - s)}{\Delta s + m_\phi^2 (m_\phi^2 - s)} \right| \right\}, \quad (6.44)$$

and for the cross symmetric process  $\nu_\alpha \bar{\nu}_\alpha \longleftrightarrow \phi \phi$ :

$$\begin{aligned}
\sigma |v| = & \frac{g_\phi^4 (1 - \cos \theta)}{64\pi s} \left\{ 4 + \frac{s (\Delta^2 + m_s^2 s)}{2m_s^2 [m_s^2 s + (s - m_\phi^2)^2]} + \frac{s [\Delta^2 - m_s^2 s]}{(m_s^2 - s) [m_\phi^4 + s (m_s^2 - 2m_\phi^2)]} + \right. \\
& \ln \left| \frac{m_s^2 s + (s - m_\phi^2)^2}{m_s^2 s} \right| \left[ \frac{m_s^4 + 2m_\phi^2 \Delta}{(s - m_\phi^2)^2} - \frac{s (s + 2\Delta)}{(s - m_\phi^2)^2} - \frac{m_s^2 (s + 2m_\phi^2)}{2s (s - m_\phi^2)} \right] + \\
& \ln \left| \frac{s (m_s^2 - s)}{\Delta s + m_\phi^2 (m_\phi^2 - s)} \right| \left[ \frac{s (2\Delta - s)}{(s - m_\phi^2)^2} + \frac{m_\phi^2 (\Delta - 2s) + \Delta s}{(s - m_\phi^2)^2} - \frac{1}{2} + \right. \\
& \left. \left. \frac{(s + m_\phi^2) (s - m_s^2)}{2s (s - m_\phi^2)} \right] \right\}. \tag{6.45}
\end{aligned}$$

As for the interactions of the sterile neutrino with a background of  $\phi$ :

$$c) \quad \nu_s \phi \longleftrightarrow \nu_s \phi$$

for this process the cross section times relative velocity is given by:

$$\begin{aligned}
\sigma |v| = & \frac{g_\phi^4 (1 - v_p v_q \cos \theta)}{64\pi s} \frac{\sqrt{s^2 - 2sM + \Delta^2}}{s - M} \left\{ \frac{(s + \Delta)^2}{2s^2} + \frac{s}{(2M - s)} + 2 + \right. \\
& \left. \frac{s (s + 2m_s^2) + 2\Delta (\Delta - 2m_s^2) - 2s (s - 2m_\phi^2)}{s^2 - 2sM + \Delta^2} \ln \left| \frac{s (2M - s)}{\Delta^2} \right| \right\}. \tag{6.46}
\end{aligned}$$

Lastly, the cross section for the cross symmetric process  $\nu_s \bar{\nu}_s \longleftrightarrow \phi \phi$  yields:

$$\begin{aligned}
\sigma |v| = & \frac{g_\phi^4 (1 - v_p v_q \cos \theta)}{64\pi s} \frac{\sqrt{s (s - 4m_s^2)}}{s - 2m_s^2} \left\{ \frac{s}{2M - s} - \frac{\Delta s^2 (3m_s^2 - m_\phi^2)}{(s^2 - 2sM + \Delta^2)^2} \left( \frac{1 + \cos \theta_0}{1 - \cos \theta_0} \right) + \right. \\
& 1 - \frac{s [(s - 4m_\phi^2) (2M - s) - 2\Delta M]}{(s^2 - 2sM + \Delta^2) (2M - s)} \ln \left| \frac{s (2M - s)}{\Delta^2} \right| + \\
& \left. \frac{s [2\Delta^2 + (4m_\phi^2 - s) (s - 2M)]}{(s^2 - 2sM + \Delta^2) (2M - s)} \ln \left( \sin^2 \frac{\theta_0}{2} \right) \right\}, \tag{6.47}
\end{aligned}$$

where  $\theta_0$  is related to the Debye shielding that should be used as the maximum value of the impact parameter in a medium. The divergence of the cross section for small angles in the forward direction is removed integrating the differential cross section over all angles such that  $\theta_0 \leq \theta_{CM} \leq \pi$ .

## 6.4 Collisions in the Sterile Sector

The Hamiltonian (6.17) also allows processes involving only sterile species. The cross section for the process  $\nu_s \nu_s \longleftrightarrow \nu_s \nu_s$  provides:

$$\sigma |v| = \frac{G_\phi^4 (1 - v_p v_q \cos \theta)}{16\pi s} \frac{\sqrt{s(s - 4m_s^2)}}{s - 2m_s^2} \left\{ \frac{s^2}{(s - m_\phi^2)^2 + \Gamma_D^2 m_\phi^2} + 1 + \ln \left| \frac{m_\phi^2}{m_\phi^2 + s - 4m_s^2} \right| \left[ \frac{2(2m_\phi^2 + 4m_s^2 - s)}{s - 4m_s^2} - \frac{4m_\phi^2 (s + m_\phi^2 - 4m_s^2)}{(s - 4m_s^2)(s + 2m_\phi^2 - 4m_s^2)} \right] \right\}, \quad (6.48)$$

where

$$\Gamma_D = \frac{G_\phi^2}{8\pi} m_\phi \left( 1 - \frac{4m_s^2}{m_\phi^2} \right)^{3/2}, \quad (6.49)$$

whereas for the process  $\nu_s \phi \longleftrightarrow \nu_s \phi$  the cross section times relative velocity is given by:

$$\sigma |v| = \frac{G_\phi^4 (1 - v_p v_q \cos \theta)}{16\pi s} \frac{\sqrt{s^2 - 2sM + \Delta^2}}{s - M} \left\{ \frac{s [\Delta (s - M) + 2m_\phi^2 (s - m_s^2)]}{4(s - M)(m_s^2 s - \Delta^2)} + 1 - \frac{[\Delta^2 (s - m_s^2) + s(s - 2M)(m_\phi^2 + M - s)]}{4s(s - m_s^2)^2} + \ln \left| \frac{s(m_\phi^2 + M - s)}{\Delta^2 - m_s^2} \right| \left[ \frac{s(s - m_s^2)}{2(s^2 - 2sM + \Delta^2)} + \frac{(s + \Delta)^2}{8s(s - m_s^2)} + \frac{s[m_s^2(s - 2m_s^2) + m_\phi^2(s - m_s^2)]}{(s^2 - 2sM + \Delta^2)(s - m_s^2)} \right] \right\}. \quad (6.50)$$

## 6.5 Quantum Kinetic Equations for a $\nu_\alpha - \nu_s$ System

The evolution of the neutrino ensemble in the early universe is in the first place affected by the expansion of the universe. Furthermore, neutrinos are

subjected to decoherent collision processes with the background medium and to the coherent process of oscillations governed by a matter-dependent Hamiltonian. The effect of both collisions and oscillations is quantified by means of the Quantum Kinetic Equations (QKEs), which generalize the Pauli-Boltzmann Equations to include quantum coherence between the particle species involved.

We start by considering a two-flavor system, comprising a single species of active and sterile neutrinos. The extension to the multi-flavor case is deferred to a subsequent stage of our study. We will assume that at very high temperature number densities of sterile neutrinos are zero until they are produced by oscillations with the active species as they undergo reversal of helicity through Yukawa interactions with the pseudoscalar particle.

Sterile neutrinos do not have electroweak or strong interactions with the background plasma which at the epoch of interest, ranging from  $T \sim 100$  MeV to BBN temperatures ( $T \sim 0.1 - 1$  MeV), consists essentially of photons, electrons, positrons, neutrinos and antineutrinos. However, they can have secret interactions, that is, interactions not shared by particles charged under  $SU(3)$  or  $SU(2) \times U(1)$ .

Assuming that there exist such secret interactions and a sterile neutrino production is induced by oscillations, we consider all possible interactions that can take place in a medium that includes pseudoscalar particles and sterile neutrinos, once they have been produced, along with the above mentioned typical background of the era. We aim at verifying, in a future work, to what extent such interactions are able to prevent full thermalization of the sterile neutrino with the active species at the considered epoch, and analyzing all cosmological implications stemming from our model in detail.

For this purpose, we start by describing oscillations between an active neutrino state  $\nu_\alpha$ , where  $\alpha = e, \mu, \tau$ , and a sterile neutrino state  $\nu_s$  in the early universe background medium, in terms of a two-state system characterized by  $2 \times 2$  density matrices  $\rho(p, t)$  and  $\bar{\rho}(p, t)$ , for neutrino and antineutrino respectively, for each momentum  $p$ , which are conveniently expanded in terms of the Pauli matrices  $\sigma_i$  and polarisation vector components  $P^i(p, t)$  as  $1/2\sigma_\mu P^\mu$ , where  $\sigma_\mu = (\sigma_0, \sigma_i)$ , with  $\sigma_0 \equiv \mathbb{1}$ :

$$\rho(p, t) = \begin{pmatrix} \rho_{\alpha\alpha} & \rho_{\alpha s} \\ \rho_{s\alpha} & \rho_{ss} \end{pmatrix} = \frac{1}{2} [P_0(p, t) + \boldsymbol{\sigma} \cdot \mathbf{P}(p, t)] \quad (6.51)$$

and for antineutrinos

$$\bar{\rho}(p, t) = \begin{pmatrix} \bar{\rho}_{\alpha\alpha} & \bar{\rho}_{\alpha s} \\ \bar{\rho}_{s\alpha} & \bar{\rho}_{ss} \end{pmatrix} = \frac{1}{2} [\bar{P}_0(p, t) + \boldsymbol{\sigma} \cdot \bar{\mathbf{P}}(p, t)], \quad (6.52)$$

where  $\rho$  and  $\bar{\rho}$  are normalized to a Fermi-Dirac distribution with zero chemical potential, such that  $f_i(p, t) = \rho_{ii}(p, t)f(p)$ , with  $i = \alpha, s$  and:

$$f(p) = \frac{1}{e^{p/T} + 1}. \quad (6.53)$$

The density matrices express the flavor content and coherence of the ensemble; the diagonal entries are the particle and antiparticle distribution functions, namely the occupation numbers of the involved neutrino species, while the off-diagonal (correlation) entries carry information of neutrino flavor mixing. Using (6.51) and (6.52) the equations of motion for the density matrices (6.26) and (6.27) become equations of motion for the polarization vector:

$$\dot{P}_0(p) = R(p) \quad (6.54)$$

$$\dot{\mathbf{P}} = \mathbf{V}(p) \times \mathbf{P}(p) + R(p)\hat{z} - D(p)\mathbf{P}_T \quad (6.55)$$

and analogous equations for the antineutrinos.

In the above equation (6.55), the general expression of the repopulation function  $R(p)$  and decoherence function  $D(p)$  can be found in Refs. (McKellar & Thomson 1994; Hannestad et al. 2015).  $\mathbf{V}(p) \equiv V_x(p)\hat{x} + V_z(p)\hat{z}$  consists of the vacuum oscillation term and the medium induced potential from forward scattering,  $V^{Vac} + V^{Med}$ , where  $V^{Med}$  comprises all contributions from weak interactions and the additional contribution due to secret interactions.  $R(p)$  is the repopulation function controlling the evolution of  $P_0(p)$ . The evolution of  $P_0(p)$  is governed by processes that reduce or increase the abundance of active neutrinos with momentum  $p$ . The rate of change of  $P_0$  receives no contribution from coherent  $\nu_\alpha - \nu_s$  oscillations, because the two flavors simply swap. Therefore it is essentially equal to the difference between the rate at which active neutrinos of momentum  $p$  are generated by scattering processes and the rate at which they are scattered out of that momentum value.  $\mathbf{P}_T$  is the transverse part of  $\mathbf{P}$  i.e. its x-y-projection, and  $D$  is a damping parameter associated with the rate of loss of coherence of the ensemble. It can be thought of as a rate parameter measuring the effectiveness of the collisions in interrupting the mixing of the two states (Stodolsky 1987).

Defining (see Dolgov et al. 2002 for the case active-active oscillations):

$$x = ma \quad y = pa, \quad (6.56)$$



where  $a \equiv a(t)$  is the cosmic scale factor which represent the relative expansion of the universe and  $m$  an arbitrary mass scale chosen to be 1 MeV. For the oscillations between a doublet active neutrino state and an initially unpopulated sterile neutrino state, the equations (6.54) and (6.55) for the components of the neutrino polarization vector yield:

$$\frac{dP_0(x, y)}{dx} = R_\alpha(x, y) \quad (6.57)$$

$$\frac{dP_x(x, y)}{dx} = -\frac{V_z}{Hx}P_y(x, y) - \frac{D}{Hx}P_x(x, y) \quad (6.58)$$

$$\frac{dP_y(x, y)}{dx} = \frac{V_z}{Hx}P_x(x, y) - \frac{V_x}{Hx}P_z(x, y) - \frac{D}{Hx}P_y(x, y) \quad (6.59)$$

$$\frac{dP_z(x, y)}{dx} = \frac{V_x}{Hx}P_y(x, y) + R_\alpha(x, y) \quad (6.60)$$

where:

$$R_\alpha(x, y) = \frac{2D}{Hx} \left[ \frac{f_{eq}(y, \xi_\alpha)}{f_{eq}(y)} - \frac{P_0(x, y) + P_z(x, y)}{2} \right] \quad (6.61)$$

with  $\xi_\alpha = \mu_\alpha/T$  the degeneracy parameter of the corresponding active neutrino species.

As for the antineutrino, equations (6.57) - (6.61) take an analogous form, with the following substitutions:

$$P^\mu \rightarrow \bar{P}^\mu \quad \mathbf{V} \rightarrow \bar{\mathbf{V}} \quad D \rightarrow \bar{D} \quad R \rightarrow \bar{R} \quad (6.62)$$

and  $\xi_\alpha \rightarrow -\xi_\alpha$  in (6.61).

The component of the polarization vector are:

$$P_0(x, y) = \frac{f_\alpha(x, y) + f_s(x, y)}{f(y)} \quad (6.63)$$

$$P_z(x, y) = \frac{f_\alpha(x, y) - f_s(x, y)}{f(y)} \quad (6.64)$$

Thus, equation (6.61) can be written as:

$$R_\alpha(x, y) = \frac{2D}{Hx} \left[ \frac{f_{eq}(y, \xi_\alpha)}{f_{eq}(y)} - \frac{f_\alpha(x, y)}{f_{eq}(y)} \right] \quad (6.65)$$

Now consider the component of the vector  $\mathbf{V}(p)$ . The vacuum oscillation term  $V^{Vac}$  provides:

$$V^{Vac}(p) = \left( 0, \frac{\Delta m^2}{2p} \sin 2\theta, 0, -\frac{\Delta m^2}{2p} \cos 2\theta \right). \quad (6.66)$$

The contribution of the medium-induced potential from forward scattering  $V^{Med}$  due to weak interactions is:

$$V^W(p) = \left( 0, 0, 0, -\frac{8}{3} \frac{\sqrt{2}G_F p}{m_W^2} (\rho_{l^+} + \rho_{l^-}) h_\alpha - \frac{8}{3} \frac{\sqrt{2}G_F p}{m_Z^2} (\rho_{\nu_\alpha} + \rho_{\bar{\nu}_\alpha}) \right) \quad (6.67)$$

where  $h_\alpha = 1$  if  $\alpha = e$  and 0 if  $\alpha = \mu, \tau$  and the refractive term proportional to neutrino asymmetry  $L$ ,  $\sqrt{2}G_F L$ , has been omitted since it is negligible at high temperatures compared to the terms coming from the second order contribution of  $\Sigma_{bubble}$  and at  $T \sim 1$  MeV compared to the vacuum oscillation term. In what follows we will neglect the chemical potential, which is a reasonable approximation as long as the asymmetries under consideration are small, as it is assumed.

The contributions  $V^Y$  coming from (6.12) and (6.14), expressed in terms of the components of the polarization vector are:

$$V_{\alpha s}^Y(p) = \frac{g_\phi^2}{16\pi^2 |\mathbf{p}_\alpha|} \int_0^\infty d|\mathbf{q}| |\mathbf{q}| (P_0 + \bar{P}_0 - P_z - \bar{P}_z) \quad (6.68)$$

$$V_{s\alpha}^Y(p) = \frac{g_\phi^2}{16\pi^2 |\mathbf{p}_s|} \int_0^\infty d|\mathbf{q}| |\mathbf{q}| (P_0 + \bar{P}_0 + P_z + \bar{P}_z) \quad (6.69)$$

In the above equations (6.68) and (6.69) we have neglected the part of  $V^Y$  proportional to the identity. Since

$$V^Y(p) = \begin{pmatrix} V_{\alpha s}(p) \\ V_{s\alpha}(p) \end{pmatrix} = \frac{1}{2} \begin{pmatrix} V_0^Y + V_z^Y & V_x^Y - iV_y^Y \\ V_x^Y + iV_y^Y & V_0^Y - V_z^Y \end{pmatrix}, \quad (6.70)$$

and  $\mathbf{p}_\alpha = \mathbf{p}_s \equiv \mathbf{p}$ , then we get:

$$V_{0,z}^Y = \frac{g_\phi^2}{16\pi^2 |\mathbf{p}|} \int_0^\infty d|\mathbf{q}| |\mathbf{q}| [(P_0 + \bar{P}_0 - P_z - \bar{P}_z) \pm (P_0 + \bar{P}_0 + P_z + \bar{P}_z)]. \quad (6.71)$$

This provides the additional term  $V_z^Y$  to the kinetic equations (6.57) - (6.60):

$$V_z^Y = -\frac{g_\phi^2}{16\pi^2 |\mathbf{p}|} \int_0^\infty d|\mathbf{q}||\mathbf{q}| (P_z + \bar{P}_z). \quad (6.72)$$

Note that  $V_0^Y$  gives no contribution to the equations of motion because it provides a diagonal term proportional to the identity matrix which cancels out when we take the commutator.

The different terms contributing to the kinetic equations can be conveniently rewritten as follows:

$$\frac{\Delta m^2}{2p H x} = \frac{10^{10} M_P}{2\sqrt{8\pi/3}} \left( \frac{\Delta m^2}{eV^2} \right) \frac{1}{\tilde{\rho}} \frac{x^2}{y} \quad (6.73)$$

is the contribution of the vacuum oscillation terms, where  $M_P \equiv 1.221$ ,  $\tilde{\rho} = (x/m)^4 \rho_{tot}$ , with  $\rho_{tot}$ , the total energy density of the universe.

The charged lepton contribution provides:

$$\frac{V_l}{H x} = -\frac{8\sqrt{2\tilde{G}_F}}{3\tilde{m}_W^2} \frac{10^5 M_P}{\sqrt{8\pi/3}} \frac{1}{\tilde{\rho}} \frac{y}{x^4} (\tilde{\rho}_l^+ + \tilde{\rho}_l^-), \quad (6.74)$$

where  $\tilde{G}_F \equiv 1.1664$  and  $\tilde{m}_W \equiv 80.385$ . Lastly, the additional term provided by equation (6.72):

$$\frac{V_z^Y}{H x} = -\frac{g_\phi^2}{8\pi^2 eV^2} \frac{10^{10} M_P}{\sqrt{8\pi/3}} \frac{1}{\tilde{\rho}} \frac{x^2}{y} \int_0^\infty d|\mathbf{q}||\mathbf{q}| (P_z + \bar{P}_z). \quad (6.75)$$

## Conclusions

The first introductory chapters of this thesis provide an overview of neutrino physics within the context of the SM of the elementary particles and beyond. The SM predicts massless left-handed neutrinos and no right-handed partner exists, making them essentially different from all other fermions. Many scenarios of physics beyond the SM are concerned with the aspect of masslessness of neutrinos, which appears in some way as an artifact in the SM, since there is no fundamental reason why one cannot introduce a right handed field  $\nu_R$  that could have paired with the  $\nu_L$  through the Higgs mechanism and produce a mass term for neutrinos the same way as any other fermion. The problem of neutrino masses is addressed within the context of the Standard Model and beyond in connection with neutrino static properties. In particular, mixing and oscillations, the nature of neutrinos as Dirac or Majorana particles and the possible existence of a right-handed component.

The existence of right-handed neutrinos is then shown as a well-motivated hypothesis from both theoretical and experimental point of view. In fact, so far there is no other experimental evidence of significant departures from the SM, except neutrino oscillation observations, which have shown that neutrinos are massive and mixed particles. Furthermore, the introduction of right-handed states is a still valid solution for explaining a few anomalies in experimental results that find no explanation in a three-flavor active neutrino pattern with nonzero mixing.

The origin of the small neutrino mass can find a possible explanation in the hypothesis that neutrino masses are a low-energy manifestation of physics beyond the SM and their smallness is due to a suppression generated by a new high-energy scale, possibly related to the unification of forces.

The right-handed neutrinos can explain in a natural way, through the see-saw mechanism, the observed extremely small masses of the active neutrinos compared with those of charged fermions in the standard model. All this seems a clear indication of the SM as an effective theory of the yet unknown theory beyond the SM.

The physics of neutrino oscillations in vacuum and in matter is then reviewed in order to introduce extended models, including active-sterile neutrino oscillations, and the related effects that can be expected in the hot and dense environments of the early universe and supernovae.

In particular, a fully thermalized population of sterile neutrinos may excite additional light particles into equilibrium, thus affecting the expansion rate of the universe. The BBN outcome depends on the expansion rate of the universe when the universe is still radiation-dominated and therefore it depends on the effective number of neutrino species  $N_{eff}$ . A larger  $N_{eff}$  produces a larger expansion rate of the universe, which in turn leads to an earlier n/p freeze-out, leading to a larger relic neutron abundance, and thus, to a higher production of  ${}^4\text{He}$ . Besides, the nucleosynthesis of light elements also depends on the rate of weak reactions. In particular, the  $\beta$  - *decay* process affects the n/p at the onset of primordial nucleosynthesis because. Hence, an accurate theoretical estimate of  $\tau_n$  has been performed, in Chapter 5, including QED *outer* corrections, where nucleons are treated as a whole, and *inner* corrections which depend on the details of the nucleon structure. Perturbative QCD corrections, weak magnetism and finite nucleon mass effects, related to proton recoil, as well as the Fermi function describing the electron rescattering in the proton Coulomb field, have also been included. Taking into account all these corrections, the value obtained for the neutron lifetime is compatible with the value quoted by PDG.

Since a fully thermalized population of sterile neutrinos appears to be in conflict with current BBN data and other cosmological observables, in Chapter 6 previous attempts to solve this tension are reviewed. Different mechanisms to suppress the sterile neutrino thermalization and their eventual large production have been considered, such as the existence of neutrino asymmetries or secret interactions among sterile neutrinos. However, so far none of these models succeeded in providing sterile neutrinos with the appropriate interactions to respond to the problem of the observed anomalies and evade all the cosmological constraints.

This has motivated the construction a new model of sterile neutrino production and secret interactions in order to explore the possibility of reconciling with cosmology the existence of sterile neutrinos with mass in the range favored by the observed anomalies. The model that has been introduced consists in assuming the same secret interactions with a light pseudoscalar

as the source of sterile neutrino production by oscillations with active species and, in addition, along with the self-interactions  $\nu_s - \nu_s$  further interactions  $\nu_s - \phi$  have been considered in the sterile sector.

The results presented in this dissertation are the first step of the analysis of the eventual compatibility of the introduced model with cosmology. In order to develop a first understanding of the active-sterile system with non-standard interactions in the early universe it has been considered first a two-flavor situation. This simplified scheme needs to be improved by considering a full multi-flavor density matrix calculation, which to date has not been performed.

## Bibliography

S. Bilenky, *Introduction to the Physics of Massive and Mixed Neutrinos*, Springer, Berlin Heidelberg, 2010.

Z.-Z. Xing, S. Zhou, *Neutrinos in Particle Physics, Astronomy and Cosmology*, Springer-Verlag Berlin Heidelberg, 2011.

B. Pontecorvo, *Mesonium and anti-mesonium*, Sov. Phys. JETP, 6, 429, 1957.

B. Pontecorvo, *Inverse beta processes and nonconservation of lepton charge*, Sov. Phys. JETP, 7, 172, 1958.

B. Pontecorvo, *Neutrino Experiments and the Problem of Conservation of Leptonic Charge*, Sov. Phys. JETP, 26, 984, 1968.

C. Giunti, C. W. Kim, *Fundamentals of Neutrino Physics and Astrophysics*, Oxford University Press, 2007.

L. Lesgourgues, G. Mangano, G. Miele, S. Pastor, *Neutrino Cosmology*, Cambridge University Press, New York, 2013.

R. N. Mohapatra, P. B. Pal, *Massive Neutrinos in Physics and Astrophysics*, World Scientific Lecture Notes in Physics, Vol. 72, Singapore, 2004.

P. W. Higgs, *Broken symmetries, massless particles and gauge fields*, Phy. Lett., 12, 132, 1964; *Broken Symmetries and the Masses of Gauge Bosons*, Phys. Rev. Lett., 13, 508, 1964.

- G. S. Guralnik, C. R. Hagen, T. W. B. Kibble, *Global Conservation Laws and Massless Particles*, Phys. Rev. Lett. 13, 585, 1964.
- F. Englert, R. Brout, *Broken Symmetry and the Mass of Gauge Vector Mesons*, Phys. Rev. Lett. 13, 321, 1964.
- T. W. B. Kibble, *Symmetry Breaking in Non-Abelian Gauge Theories*, Phys. Rev. 155, 1554, 1967.
- N. Cabibbo, *Unitary Symmetry and Leptonic Decays*, Phys. Rev. Lett., 10, 531, 1963.
- M. Kobayashi, T. Maskawa, *CP-Violation in the Renormalizable Theory of Weak Interaction*, Prog. Theor. Phys., 49, 652, 1973.  
<http://pdg.lbl.gov/2015/reviews/rpp2014-rev-ckm-matrix.pdf>
- G. 't Hooft, *Renormalization of massless Yang-Mills fields*, Nucl. Phys. B 33, 173, 1971; G. 't Hooft, *Renormalizable Lagrangians for massive Yang-Mills fields*, Nucl. Phys. B 35, 167, 1971.
- S. L. Adler, *Axial-Vector Vertex in Spinor Electrodynamics*, Phys. Rev. 177, 2426, 1969.
- J. S. Bell, R. Jackiw, *Nuovo Cimento*, A 60, 47, 1969.
- R. Barbieri, J. Ellis, M. K. Gaillard, *Neutrino Masses and Oscillations in SU(5)*, Phys. Lett. B 90, 249, 1980.
- E. Akhmedov, Z. Berezhiani, G. Senjanovic, *Planck-scale Physics and neutrino masses*, Phys. Rev. Lett. 69, 3013, 1992.
- K. S. Babu, R. N. Mohapatra *Is there a connection between quantization of electric charge and a Majorana neutrino?*, Phys. Rev. Lett. 63, 938, 1989.
- E. Majorana, *Teoria simmetrica dell'elettrone e del positrone*, Nuovo Cim., 14, 171, 1937.
- M. Gell-Mann, P. Ramond, R. Slansky, *Supergravity*, P. van Nieuwenhuizen et al. eds., North Holland, Amsterdam, 1979.
- T. Yanagida, *Horizontal Symmetry and Masses of Neutrinos*, Progress of Theoretical Physics 64, 1103, 1980.
- R. N. Mohapatra, G. Senjanovic, *Neutrino Mass and Spontaneous Parity Nonconservation*, Phys. Rev. Lett. 44, 912, 1980.



- H. Murayama, *Physics Beyond the Standard Model and Dark Matter*, arXiv:0704.2276 [hep-ph] 2007.
- S. Dodelson, L. M. Widrow, *Sterile neutrinos as dark matter*, Phys. Rev. Lett. 72, 17, arXiv:hep-ph/9303287, 1993.
- G. Senjanovic, *LHC and the origin of neutrino mass*, arXiv:0911.0029 [hep-ph], 2010.
- G. Senjanovic, *Probing the Origin of Neutrino Mass: from GUT to LHC*, arXiv:1107.5322 [hep-ph], 2011.
- G. Altarelli, *Lectures on Models of Neutrino Masses and Mixings*, arXiv:0711.0161 [hep-ph], 2007.
- W. Buchmüller, *Neutrinos, Grand Unification and Leptogenesis*, arXiv:hep-ph/0204288 [hep-ph], 2002.
- W. Buchmüller, M. Plümacher, *Baryon Asymmetry and Neutrino Mixing*, Phys. Lett. B 389, 73, arXiv:hep-ph/9608308, 1996.
- W. Buchmüller, R.D. Peccei, T. Yanagida, *Leptogenesis as the origin of matter*, Ann. Rev. Nucl. Part. Sci. 55, 311, arXiv:hep-ph/0502169, 2005.
- S. A. Bludman, D. C. Kennedy, P. G. Langacker, *Solutions of the solar neutrino problem*, Nucl. Phys. B 374, 373, 1992.
- C. Athanassopoulos et al., *Candidate Events in a Search for  $\bar{\nu}_\mu \rightarrow \bar{\nu}_e$  Oscillations*, Phys. Rev. Lett. 75, 2650-2653, arXiv:nucl-ex/9504002, 1995.
- C. Athanassopoulos et al., *Evidence for  $\nu_\mu \rightarrow \nu_e$  neutrino oscillations from LSND*, Phys. Rev. Lett. 81, 1774-1777, arXiv:nucl-ex/9706006 1998.
- A. Aguilar et al., *Evidence for neutrino oscillations from the observation of  $\bar{\nu}_e$  appearance in a  $\bar{\nu}_\mu$  beam*, Phys. Rev. D 64, 112007, arXiv:hep-ex/0104049, 2001.
- Schael S et al. (ALEPH, DELPHI, L3, OPAL, SLD, LEP Electroweak Working Group, SLD Electroweak Group, SLD Heavy Flavour Group), *Precision Electroweak Measurements on the Z Resonance*, Phys. Rept. 427, 257-454, arXiv:hep-ex/0509008 2006.
- A. Yu. Smirnov, R. Zukanovich Funchal, *Sterile neutrinos: direct mixing effects versus induced mass matrix of active neutrinos*, Phys. Rev. D 74, 013001, arXiv:hep-ph/0603009, 2006.

- A. Donini, P. Hernandez, J. Lopez-Pavon, M. Maltoni, *Minimal models with light sterile neutrinos*, JHEP 1107, 105, arXiv:1106.0064 [hep-ph], 2011.
- K. N. Abazajian et al., *Light Sterile Neutrinos: A White Paper*, arXiv:1204.5379 [hep-ph], 2012.
- S. M. Bilenky, B. Pontecorvo, *The Quark-Lepton Analogy and the Muonic Charge*, Sov. J. Nucl. Phys., 24, 316, 1976; *Again on Neutrino Oscillations*, Nuovo Cim. Lett., 17, 569, 1976.
- S. M. Bilenky, B. Pontecorvo, *Lepton Mixing and Neutrino Oscillations*, Phys. Rep., 41, 225, 1978.
- S. Eliezer, A. R. Swift, *Experimental Consequences of electron Neutrino-Muon-neutrino Mixing in Neutrino Beams*, Nucl. Phys., B 105, 45, 1976.
- H. Fritzsch, P. Minkowski, *Vector-Like Weak Currents, Massive Neutrinos, and Neutrino Beam Oscillations*, Phys. Lett., B 62, 72, 1976.
- L. Wolfenstein, *Neutrino oscillations in matter*, Phys. Rev. D 17, 2369, 1978.
- P. Langacker, S.T. Petcov, G. Steigman, S. Toshev, *On the Mikheev-Smirnov-Wolfenstein (MSW) Mechanism of Amplification of Neutrino Oscillations in Matter*, Nucl. Phys. B 282, 589, 1987.
- R. Davis, *Solar neutrinos. II: Experimental*, Phys. Rev. Lett. 12, 303, 1964.
- R. Davis, D. S. Harmer, K. C. Hoffman, *Search for neutrinos from the sun*, Phys. Rev. Lett. 20, 1205, 1968.
- Y. Fukuda et al. (Kamiokande Collaboration), *Solar Neutrino Data Covering Solar Cycle 22*, Phys. Rev. Lett. 77, 1683, 1996.
- W. Hampel et al. (GALLEX Collaboration) *GALLEX solar neutrino observations: results for GALLEX IV*, Phys. Lett. B 447, 127, 1999.
- J. N. Abdurashitov et al. (SAGE Collaboration), *Measurement of the solar neutrino capture rate with gallium metal*, Phys. Rev. C 60, 055801, 1999.
- S. Fukuda et al. (Super-Kamiokande Collaboration), *Evidence for Oscillation of Atmospheric Neutrinos*, Phys. Rev. Lett. 81, 1562, 1998; *Measurements of the Solar Neutrino Flux from Super-Kamiokande's First 300 Days*, Phys. Rev. Lett. 81, 1158, 1998; Erratum Phys. Rev. Lett. 81, 4279, 1998.

- Q. R. Ahmad et al. (SNO Collaboration), *Direct Evidence for Neutrino Flavor Transformation from Neutral-Current Interactions in the Sudbury Neutrino Observatory*, Phys. Rev. Lett. 89, 011301, 2002.
- K. Eguchi et al. (KamLAND Collaboration), *First results from KamLAND: evidence for reactor antineutrino disappearance*, Phys. Rev. Lett. 90, 021802, arXiv:hep-ex/0212021, 2003.
- G. Bellini, et al. (Borexino Collaboration), *Measurement of the solar 8B neutrino rate with a liquid scintillator target and 3 MeV energy threshold in the Borexino detector*, Phys. Rev. D 82, 033006, arXiv:0808.2868, 2010.
- K. Abe, et al. (T2K Collaboration), *Observation of Electron Neutrino Appearance in a Muon Neutrino Beam*, Phys. Rev. Lett. 112, 061802, arXiv:1311.4750, 2014.
- P. Adamson et al. (MINOS Collaboration), *First direct observation of muon antineutrino disappearance*, Phys. Rev. Lett. 107, 021801, arXiv:1104.0344 [hep-ex], 2011.
- E. D. Church, K. Eitel, G.B. Mills, M. Steidl, *Statistical Analysis of Different Muon-antineutrino  $\rightarrow$  Electron-antineutrino Searches*, Phys. Rev. D 66, 013001, arXiv:hep-ex/0203023, 2002.
- J. M. Conrad, W. C. Louis, M. H. Shaevitz, *The LSND and MiniBooNE Oscillation Searches at High  $\Delta m^2$* , Annu. Rev. Nucl. Part. Sci. 63, 45, arXiv:1306.6494 [hep-ex], 2013.
- M. C. Gonzalez-Garcia, M. Maltoni, T. Schwetz, *Global Analyses of Neutrino Oscillation Experiments*, arXiv:1512.06856 [hep-ph], 2015.
- B. Achkar et al. (Bugey Collaboration), *Search for neutrino oscillations at 15, 40 and 95 meters from a nuclear power reactor at Bugey*, Nucl. Phys. B 434, 503, 1995.
- J. Kopp, P. A. N. Machado, M. Maltoni, T. Schwetz, *Sterile Neutrino Oscillations: The Global Picture*, JHEP 05, 050, arXiv:1303.3011, 2013.
- J. M. Conrad, C. M. Ignarra, G. Karagiorgi, M. H. Shaevitz, J. Spitz, *Sterile Neutrino Fits to Short Baseline Neutrino Oscillation Measurements*, Adv. High Energy Phys., 2013, 163897. arXiv:1207.4765, 2013.
- C. Giunti, M. Laveder, *Statistical Significance of the Gallium Anomaly*, Phys. Rev. C 83, 065504. arXiv:1006.3244, 2011.

- T. A. Mueller, D. Lhuillier, M. Fallot, A. Letourneau, S. Cormon, M. Fechner, L. Giot, T. Lasserre, J. Martino, G. Mention, A. Porta, F. Yermia, *Improved Predictions of Reactor Antineutrino Spectra*, Phys. Rev. C 83, 05461, arXiv:1101.2663, 2011.
- G. Raffelt, G. Sigl, L. Stodolsky, *Non-Abelian Boltzmann equation for mixing and decoherence*, Phys. Rev. Lett. 70, 2363, 1993.
- G. Raffelt, G. Sigl, *General kinetic description of relativistic mixed neutrinos*, Nucl. Phys. B 406, 1993.
- J. Beringer et al. (Particle Data Group Collaboration), *Review of Particle Physics*, Phys. Rev. D 86, 010001, 2012.
- V. F. Shvartsman, *Density of relict particles with zero rest mass in the universe*, JETP Lett. 9, 184, 1969.
- G. Steigman, D. N. Schramm, J. E. Gunn, *Cosmological Limits to the Number of Massive Leptons*, Phys. Lett. B 66, 202, 1977.
- G. Senjanovic, R. N. Mohapatra, *Exact Left-Right Symmetry and Spontaneous Violation of Parity*, Phys. Rev. D 12, 1502, 1975.
- J. Heeck, S. Patra, *Minimal Left-Right Symmetric Dark Matter*, Phys. Rev. Lett. 115, 121804, arXiv:1507.01584 [hep-ph], 2015.
- R. Adhikari et al., *A White Paper on keV Sterile Neutrino Dark Matter*, arXiv:1602.04816 [hep-ph], 2016.
- A. D. Dolgov, S.H. Hansen, G. Raffelt, D. V. Semikoz, *Cosmological and astrophysical bounds on a heavy sterile neutrino and the KARMEN anomaly*, Nucl. Phys. B 580, 331, arXiv:hep-ph/0002223, 2000.
- O. Ruchayskiya, A. Ivashko, *Restrictions on the lifetime of sterile neutrinos from primordial nucleosynthesis*, JCAP 10, 014, arXiv:1202.2841 [hep-ph], 2012; O. Ruchayskiya, A. Ivashko, *Experimental bounds on sterile neutrino mixing angles*, JHEP 1206, 100, arXiv:1112.3319 [hep-ph], 2012.
- M. Fukugita, T. Yanagida, *Baryogenesis Without Grand Unification*, Phys. Lett. B 174, 45, 1986.
- D. Kirilova, *Neutrinos from the Early Universe and physics beyond standard models*, Open Phys. 13, 22, 2015.

- R. Barbieri, A. Dolgov, *Bounds on sterile neutrinos from nucleosynthesis*, Phys. Lett. B 237, 440, 1990
- N. F. Bell, R. R. Volkas, Y. Y. Y. Wong, *Relic neutrino asymmetry evolution from first principles*, Phys. Rev. D 59, 113001, arXiv:hep-h/9809363, 1999.
- Y.-Z. Chu, M. Cirelli, *Sterile neutrinos, lepton asymmetries, primordial elements: how much of each?*, Phys. Rev. D 74, 085015, [astro-ph/0608206], 2006.
- S. Hannestad, I. Tamborra, T. Tram, *Thermalisation of light sterile neutrinos in the early universe*, JCAP 1207, 025, arXiv:1204.5861 [astro-ph.CO], 2012.
- A. Mirizzi, N. Saviano, G. Miele, P. D. Serpico, *Light sterile neutrino production in the early universe with dynamical neutrino asymmetries*, Phys. Rev. D 86, 053009, arXiv:1206.1046 [hep-ph], 2012.
- N. Saviano, A. Mirizzi, O. Pisanti, P. D. Serpico, G. Mangano, G. Miele, *Multi-momentum and multi-flavour active-sterile neutrino oscillations in the early universe: role of neutrino asymmetries and effects on nucleosynthesis*, Phys. Rev. D 87, 073006, arXiv:1302.1200 [astro-ph.CO], 2013.
- B. Dasgupta, J. Kopp, *A menage a trois of eV-scale sterile neutrinos, cosmology, and structure formation*, Phys. Rev. Lett. 112, 031803, arXiv:1310.6337 [hep-ph], 2014.
- S. Hannestad, R. S. Hansen, T. Tram, *How secret interactions can reconcile sterile neutrinos with cosmology*, Phys. Rev. Lett. 112, 031802, arXiv:1310.5926 [astro-ph.CO], 2014.
- M. Archidiacono, S. Hannestad, R. Sloth Hansen, T. Tram, *Cosmology with self-interacting sterile neutrinos and dark matter - A pseudoscalar model*, Phys. Rev. D 91, 065021, arXiv:1404.5915 [astro-ph.CO], 2014.
- A. Cuoco, J. Lesgourgues, G. Mangano, S. Pastor, *Do observations prove that cosmological neutrinos are thermally distributed?*, Phys. Rev. D 71, 123501, arXiv:astro-ph/0502465, 2005.
- S. Bashinsky, U. Seljak, *Signatures of Relativistic Neutrinos in CMB Anisotropy and Matter Clustering*, Phys. Rev. D 69, 083002, arXiv:astro-ph/0310198, 2004.

- S. Hannestad, *Neutrino physics from Cosmology*, PoS EPS-HEP 2013, 519, 2013.
- J. Dunkley et al., *The Atacama Cosmology Telescope: cosmological parameters from the 2008 power spectra*, *Astrophys. J.* 739, 52, arXiv:1009.0866 [astro-ph.CO], 2011.
- R. Keisler et al., *A Measurement of the Damping Tail of the Cosmic Microwave Background Power Spectrum with the South Pole Telescope*, *Astrophys. J.* 743, 28, arXiv:1105.3182 [astro-ph.CO], 2011.
- G. Martinez-Pinedo, T. Fischer, L. Huther, *Supernova neutrinos and nucleosynthesis*, *J. Phys., G* 41, 044008, arXiv:1309.5477 [astro-ph.HE], 2014.
- M.-R. Wu, G. Martinez-Pinedo, Y.-Z. Qian, *Linking neutrino oscillations to the nucleosynthesis of elements*, *EPJ Web Conf.* 109, 06005, arXiv:1512.03630 [astro-ph.HE], 2016.
- S.P. Mikheev, A. Y. Smirnov, *Neutrino Oscillations in a Variable Density Medium and Neutrino Bursts Due to the Gravitational Collapse of Stars*, *Sov. Phys. JETP* 64, 4, 1986.
- X. Shi, G. Sigl, *A Type II Supernovae Constraint on  $\nu$ - $\nu_s$* , *Phys. Lett. B* 323, 360, 1994; ERRATUM-ibid.B 324, 516, 1994.
- J. Fetter, G. C. McLaughlin, A. B. Balantekin, G. M. Fuller, *Active-Sterile Neutrino Conversion: Consequences for the r-Process and Supernova Neutrino Detection*, *Astropart. Phys.* 18, 433, arXiv:hep-ph/0205029, 2003.
- H. Duan, G. M. Fuller, Y.-Z. Qian, *Collective Neutrino Oscillations*, *Ann. Rev. Nucl. Part. Sci.* 60, 569, arXiv:1001.2799 [hep-ph], 2010.
- K. Abazajian, G. M. Fuller, M. Patel, *Sterile Neutrino Hot, Warm, and Cold Dark Matter*, *Phys. Rev. D* 64, 023501, arXiv:astro-ph/0101524, 2001.
- C. L. Fryer, A. Kusenko, *Effects of neutrino-driven kicks on the supernova explosion mechanism*, *Astrophys. J. Suppl.* 163, 335, arXiv:astro-ph/0512033 [astro-ph], 2005.
- G. Raffelt, G. Sigl, *Neutrino Flavor Conversion in a Supernova Core*, *Astropart. Phys.* 1, 165, arXiv:astro-ph/9209005, 1993.
- G. M. Fuller, C. T. Kishimoto, A. Kusenko, *Heavy sterile neutrinos, entropy and relativistic energy production, and the relic neutrino background*, arXiv:1110.6479 [astro-ph.CO], 2011.

- G. Mangano, G. Miele, S. Pastor, T. Pinto, O. Pisanti, P. D. Serpico, *Relic neutrino decoupling including flavour oscillations*, Nucl. Phys. B 729, 221, arXiv:hep-ph/0506164, 2005.
- J. Lesgourgues, S. Pastor, *Massive neutrinos and cosmology*, Phys. Rept. 429, 307, arXiv:astro-ph/0603494, 2006.
- G. Mangano, P. D. Serpico, *A robust upper limit on  $N_{eff}$  from BBN, circa 2011*, Phys. Lett. B 701, 296, arXiv:1103.1261 [astro-ph.CO], 2011.
- G. Rossi, C. Yeche, N. Palanque-Delabrouille, J. Lesgourgues, *Constraints on dark radiation from cosmological probes*, Phys. Rev. D 92, 063505, arXiv:1412.6763 [astro-ph.CO], 2015.
- N. Palanque-Delabrouille, C. Yeche, J. Baur, C. Magneville, G. Rossi, J. Lesgourgues, A. Borde, E. Burtin, J.-M. LeGoff, J. Rich, M. Viel, D. Weinberg, *Neutrino masses and cosmology with Lyman-alpha forest power spectrum*, JCAP 11, 1011, arXiv:1506.05976 [astro-ph.CO], 2015.
- G. Mangano, P.D. Serpico, *Neutrinos and Primordial Nucleosynthesis*, Nucl. Phys. Proc. Suppl. 145, 351, astro-ph/0412255, 2005.
- L. Salvati, L. Pagano, R. Consiglio, A. Melchiorri, *Cosmological constraints on the neutron lifetime*, arXiv:1507.07243 [astro-ph.CO], 2015, forthcoming in JCAP.
- A. P. Serebrov, *Neutron  $\beta$ -decay, Standard Model and cosmology*, Phys. Lett. B 650 321, nucl-ex/0611038, 2007.
- S. Esposito, G. Mangano, G. Miele, O. Pisanti, *Precision rates for nucleon weak interactions in primordial nucleosynthesis and He-4 abundance*, Nucl. Phys. B 540, 3, arXiv:astro-ph/9808196, 1999.
- A. Sirlin, *General Properties of the Electromagnetic Corrections to the Beta Decay of a Physical Nucleon*, Phys. Rev. 164, 1767, 1967.
- D. Kirilova, *Lepton Asymmetry and Neutrino Oscillations Interplay*, Hyperfine Interact. 215, 111, arXiv:1302.2923 [astro-ph.CO], 2013.
- S. Pastor, T. Pinto, G. Raffelt, *Relic density of neutrinos with primordial asymmetries*, Phys. Rev. Lett. 102, 241302, arXiv:0808.3137 [astro-ph], 2009.
- G. Steigman, *Neutrinos And Big Bang Nucleosynthesis*, Adv. High Energy Phys. 2012, 268321, arXiv:1208.0032 [hep-ph], 2012.

- J. Hamann, S. Hannestad, G. G. Raffelt, Y. Y. Y. Wong, *Sterile neutrinos with eV masses in cosmology - how disfavoured exactly?*, JCAP 1109, 034, arXiv:1108.4136v2 [astro-ph.CO], 2011.
- N. Saviano, O. Pisanti, G. Mangano, A. Mirizzi, *Unveiling secret interactions among sterile neutrinos with big-bang nucleosynthesis*, Phys. Rev. D 90, 113009, arXiv:1409.1680 [astro-ph.CO], 2014.
- K. Kainulainen, *Light Singlet Neutrinos and the Primordial Nucleosynthesis*, Phys. Lett. B 244, 191, 1990.
- A. Mirizzi, G. Mangano, O. Pisanti, N. Saviano, *Collisional production of sterile neutrinos via secret interactions and cosmological implications*, Phys. Rev. D 91, 025019, arXiv:1410.1385 [hep-ph], 2015.
- R. F. Sawyer, *Instabilities in neutrino systems induced by interactions with scalars*, Phys. Rev. D 83, 065023, arXiv:1011.4585 [astro-ph.CO], 2011.
- R. D. Peccei, H. Quinn, *CP Conservation in the Presence of Pseudoparticles*, Phys. Rev. Lett. 38, 1440, 1977; R. D. Peccei, H. Quinn, *Constraints imposed by CP conservation in the presence of instantons*, Phys. Rev. D 16, 1791, 1977.
- M. Lundstrom, *Fundamentals of carrier transport*, Cambridge University Press, Cambridge, 2000.
- Y.-Z. Chu, M. Cirelli, *Sterile neutrinos, lepton asymmetries, primordial elements: how much of each?*, Phys. Rev. D 74, 085015, 2006.
- S. Hannestad, R. Sloth Hansen, T. Tram, Y. Y. Y. Wong, *Active-sterile neutrino oscillations in the early Universe with full collision terms*, arXiv:1506.05266, [hep-ph], 2015.
- L. Stodolsky, *Treatment of neutrino oscillations in a thermal environment*, Phys. Rev. D 36, 2273, 1987.
- B. H. J. McKellar, M. J. Thomson, *Oscillating doublet neutrinos in the early universe*, Phys. Rev. D 49, 2710, 1994.
- A. Dolgov, S. Hansen, S. Pastor, S. Petcov, G. Raffelt, D.V. Semikoz, *Cosmological bounds on neutrino degeneracy improved by flavor oscillations*, Nucl. Phys. B 632, 363, arXiv:hep-ph/0201287 [hep-ph], 2002.